Effects of Rotor Tip Blade Loading Variation on Compressor Stage Performance

by

Aniwat Tiralap

B.E., Chulalongkorn University (2010)

Submitted to the Department of Mechanical Engineering
in partial fulfillment of the requirements for the degree of

Master of Science in Mechanical Engineering

at the

MASSACHUSETTS INSTITUTE OF TECHNOLOGY

Febuary 2015

Signature redacted

Author .....
Department of Mechanical Engineering
January 15, 2015

Signature redacted

Certified by...
Choon S. Tan
Senior Research Engineer, Department of Aeronautics and Astronautics
Thesis Supervisor

Signature redacted

Certified by...
John G. Brisson
Professor of Mechanical Engineering
Thesis Reader

Signature redacted

Accepted by .....
David E. Hardt
Professor of Mechanical Engineering
Chair, Graduate Program Committee

Effects of Rotor Tip Blade Loading Variation on Compressor Stage Performance

by

Aniwat Tiralap

Submitted to the Department of Mechanical Engineering
on January 15, 2015, in partial fulfillment of the
requirements for the degree of
Master of Science in Mechanical Engineering

Abstract

Changes in loss generation associated with altering the rotor tip loading of an embedded compressor stage is assessed. Steady and unsteady three-dimensional computations, complemented by control volume analyses, for varying rotor tip loading distributions provided results for determining if aft-loading rotor tip would yield a stage performance benefit in terms of a reduction in loss generation. Aft-loading rotor blade tip yields a relatively less-mixed-out tip leakage flow at the rotor exit and a reduction in overall tip leakage mass flow hence a lower loss generation; however, the attendant changes in tip flow angle distribution are such that there is an overall increase in the flow angle mismatch between tip flow and main flow leading to higher loss generation. The latter outweighs the former so that rotor passage loss from aft-loading rotor tip is marginally higher unless a constraint is imposed on tip flow angle distribution so that associated induced loss is negligible; a potential strategy for achieving this is proposed. In the course of assessing the benefit from unsteady tip leakage flow recovery in the downstream stator, it was determined that tip clearance flow is inherently unsteady with a time-scale distinctly different from the blade passing time. The disparity between the two timescales: (i) defines the periodicity of the unsteady rotor-stator flow, which is an integral multiple of blade passing time; and (ii) causes tip leakage vortex to enter the downstream stator at specific pitchwise locations for different blade passing cycles, which is a tip leakage flow phasing effect. Because of an inadequate grid resolution defining the unsteady interaction of tip flow with downstream stator, the benefit from unsteady tip flow recovery is the lower bound of its actual benefit. A revised design hypothesis is thus as follows: "rotor should be tip-aft-loaded and hub-fore-loaded while stator should be hub-aft-loaded and tip-fore-loaded with tip/hub leakage flow angle distribution such that it results in no additional loss". For the compressor stage being assessed here, an estimated 0.15% enhancement in stage efficiency is possible from aft-loading rotor tip only.

Thesis Supervisor: Choon S. Tan
Title: Senior Research Engineer, Department of Aeronautics and Astronautics

Acknowledgments

First, I would like to express my deep gratitude to my advisor, Dr. Choon Tan. His advice has guided me through numerous challenges over two years of the research. He has been supportive and made me to think more critically when I face new challenges while giving me opportunity to learn from my mistakes. This work would not be possible without his support. Moreover, I would like to thank Professor John Brisson for being my thesis reader and his constructive comments on my work.

Furthermore, I am indebted to several engineers at Siemens Energy for their continuous help. First, Dr. Matt Montgomery, who coordinated the collaboration between MIT and Siemens Energy. His expertise in the field always brings in insightful perspectives and interesting questions to remind me the overall view of the research. I also appreciate support from Dr. Christian Cornelius, whose experience provides invaluable guidance related to computational setup and compressor blade designing process. Especially, I have to thank Dr. Eric Donahoo for not only a number of computational meshes but also his countless advice, a lesson on compressor blade design process, and most importantly his warm friendship during my internship at Siemens Energy. Also, I would like to thank Mr. Elliot Griffin for being my host during the internship at Siemens Energy.

Many labmates at Gas Turbine Laboratory have provided me a great support and made time at MIT enjoyable experience. A special thank would go to Jinwook Lee for countless insightful and entertaining discussions. I am also grateful to Dr. Timothy Palmer, George Christou, and Sitanun Sakulkaew for their advice on CFD, CFX, and turbomachinery.

I would like to thank many friends at MIT for their warm friendship throughout my studies here, especially for those from TSMIT. Last but not least, I am totally indebted to my family for their encouragement and love, motivating me through endless obstacles toward my goal.

This research has been supported by MITEI Sustaining Member Siemens CKI, agreement dated 09/30/2008.

Contents

List of Figures

List of Tables

Nomenclature

A = Area

F_c^+ = Reduced frequency

H = Enthalpy

P = Pressure

S = Entropy

T = Temperature

V = Volume

W = Work

c = Chord

f = Frequency

g = Tip clearance

h = Specific enthalpy

k = Thermal conductivity

p = Pressure

u = Velocity

t = Time

x_i = Coordinate i

β = Relative flow angle

γ = Specific heat ratio

η = Efficiency

ρ = Density

τ = Shear stress

ξ = Non-dimensinonal loss

$\mathcal{L}$ = Relative non-dimensional loss

Subscripts

aft = aft-loaded

$blade\ ss$ = blade suction side

$fore$ = fore-loaded

gen = generation

inj = injected

ori = original

t = stagnation conditions

$rotor\ in$ = rotor inlet

$rotor\ out$ = rotor out

$stator\ in$ = stator inlet

$stator\ out$ = stator outlet

$stage$ = across stage

∞ = upstream conditions

Supercripts

ta = time-averaged

wa = work-averaged

$()'''$ = per unit volume

$(\dot{})$ = per unit time

Abbreviation

BPF = Blade passing frequency

CFD = Computational fluid dynamics

LE = Leading edge

PS = Pressure side

RANS = Reynolds-averaged Navier-Stokes

SS = Suction side

TE =Trailing edge

TLF = Tip leakage flow

Chapter 1

Introduction

Gas turbines for power generation have been an industrial focus due to increasing use of natural gas with its lower pollution emission and operating cost. A small improvement in gas turbine efficiency would thus result in a substantial reduction of global fuel consumption, emission, and operating costs. In addition, there is a need for industrial gas turbines to operate with a broader operating range to accommodate rapid changes in electricity demand and electricity supply from several energy sources. Therefore, performance improvement for the next generation of industrial gas turbines would require research and development that serves to increase efficiency as well as to broaden the operable range while retaining high efficiency; this invariably involves reducing the opportunity for losses and flow blockage generation associated with flow through a multistage axial compressor.

Rotor tip leakage flow is known to have strong detrimental effects on compressor performance in terms of efficiency, pressure rise capability, and operating range. Tip clearance exists in unshrouded axial compressor rotors as a finite clearance is required to prevent rubbing between the tip of rotor blades and the stationary casing. Tip leakage flow is driven through tip clearance by the pressure difference between the pressure side and the suction side of a rotor blade. Shear layer forms between the leakage flow and the main flow, and the leakage fluid leaving tip clearance rolls up and becomes a tip leakage vortex as shown in Figure 1-1. The detrimental effects

are considerable especially for rear-stage industrial axial compressors, where non-dimensional tip clearance size is relatively large. The overall goal of this research is to utilize and assess a hypothesized compressor design strategy available in literature to minimize the opportunity for tip leakage flow to generate loss and flow blockage, thus improving compressor performance in a multistage environment.

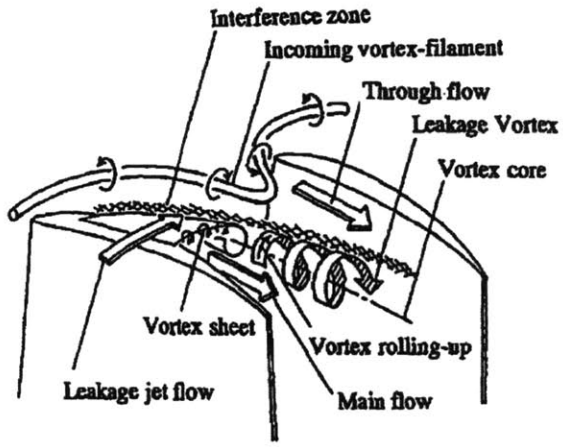

Figure 1-1: Flow structure of tip leakage flow during its formation in the endwall region [1]

1.1 A Suggested Design Guideline for Multistage Axial Compressors

A design guideline for multistage axial compressors has been proposed by Sakulkaew [2] to reduce losses and flow blockage induced by tip leakage flow. The required attributes of rotor and stator blade rows are such that the rotor should be tip-aft-loaded and hub-fore-loaded while the stator should be hub-aft-loaded and tip-fore-loaded as shown in Figure 1-2. Such attributes create an environment that prevents tip/hub leakage flow from mixing out so as to enhance the benefit of an unsteady tip/hub leakage flow recovery process in the downstream blade row. In other words, a tip-aft-loaded rotor and a hub-aft-loaded stator would generate relatively less mixed-out leakage flow while a hub-fore-loaded rotor and a tip-fore-loaded stator would enhance

the leakage flow attenuation/recovery process. The design philosophy was hypothesized to improve overall compressor performance, including efficiency, pressure ratio, and stall margin. The design hypothesis is applicable for a multistage compressor as well as an embedded single stage compressor. We first focus on utilizing the design hypothesis for an embedded compressor stage with an upstream rotor and a downstream stator.

The first mechanism utilized in the hypothesis is a reduction of tip leakage mixing loss through delaying the tip leakage flow formation towards the rotor trailing edge (TE). As tip leakage flow in an aft-loaded blade has less time to mix out, it can be inferred that viscous mixing loss in the rotor generated from tip leakage flow in an aft-loaded blade would be lower. An implicit assumption underlying the hypothesis is that tip leakage flow must not be mixed-out when it enters a downstream stator. For relatively small tip clearances less than approximately 2% span, tip leakage flow tends to mix out in a rotor; if so, all potential loss in the tip leakage flow has been realized and loss reduction from the hypothesis may not be achievable. Hence, the hypothesis is applicable for a rotor with tip clearance size large enough that tip leakage flow does not mix out before it arrives in a downstream stator. This geometrical characteristic is generally found in rear-stage compressors.

The second key mechanism of the proposed design philosophy is a reversible unsteady recovery process for tip leakage flow in a downstream stator blade row. The recovery process in a stator blade row will convert the potential loss in tip leakage flow to useful kinetic energy without additional entropy generation. According to the proposed design guideline, the relatively less mixed-out tip leakage flow would thus have higher loss potential downstream of the rotor. This potential loss is continuously realized by viscous mixing as tip leakage flow proceeds downstream in a compressor. If potential loss in tip leakage flow can be reduced before it has opportunity to convert itself into actual loss, tip leakage flow will generate lower overall loss than its full loss potential. Because of the relatively less-mixed-out tip leakage flow, tip leakage recovery process would be able to reduce the opportunity for the higher potential loss to be realized in an aft-loaded blade. If the recovery process is not adequately

effective, then the subsequent viscous mixing would realize the tip leakage loss potential. For preventing the mixing out of tip leakage flow in a stator passage, the recovery process in a stator should occur as soon as possible; thus, the stator tip (i.e. the shroud/casing of a stator blade), which interacts with tip leakage flow, should be fore-loaded to improve the effectiveness of the recovery process. It has to be noted that the two delineated mechanisms are of equal importance and must be effective in order to achieve an overall compressor stage performance improvement.

There has been some research conducted on each of the two mechanisms separately. However, there is a lack of research that quantifies the achievable overall improvement from the proposed design concept and elucidates the effects of each mechanism on the overall improvement. Therefore, this thesis will first focus on quantifying the effects of the two mechanisms separately and then synthesize the overall effects from each of the mechanisms to assess the utility of the proposed design guideline.

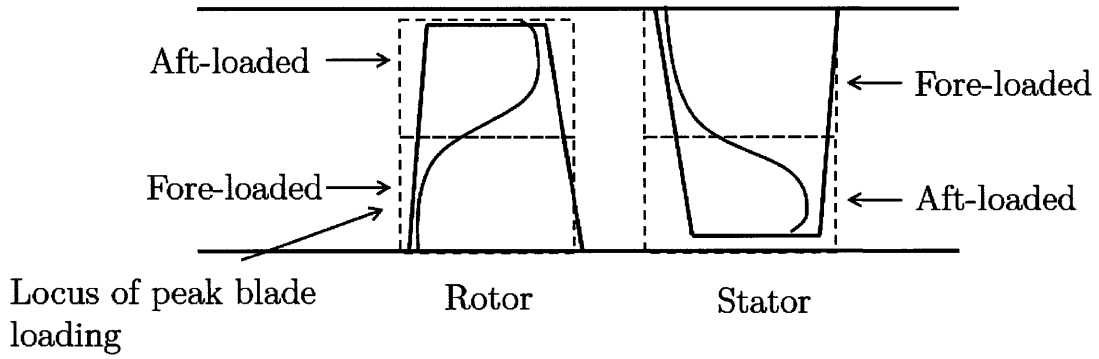

Figure 1-2: Locus of peak blade loading on a rotor and a stator blade designed according to the proposed design guideline

1.2 Literature Review

As noted above, there is a lack of research that shows both the quantitative and the qualitative benefits of the proposed design strategy. Nevertheless, there has been research that addresses each of the followings on an individual basis: (i) the effects of aft-loading rotor blades (delay of tip leakage flow formation), (ii) the inherent

unsteadiness in tip leakage flow, and (iii) the benefit and the mechanisms of the reversible unsteady tip leakage recovery process.

A preliminary study for an aft-loaded blade design was carried out by Sakulkaew [2]. However, the original blade design was inadvertently modified so that a consistent back-to-back assessment on the effects cannot be made and this set of results cannot be used for quantifying the merits of the new design philosophy. Nevertheless, the computed results have shed some light on the qualitative nature of steady flow fields of the aft-loaded blade. The aft-loaded blade was aft-loaded approximately 20% span from the blade tip and the peak blade loading was shifted approximately 20% chord toward the TE as shown in Figure 1-3. As the formation of tip leakage flow induces relatively high local entropy generation rate, local entropy generation rate can be used to track the formation of tip leakage flow. If the formation of tip leakage flow is delayed, local entropy generation rate in the aft-loaded blade is expected to be lower (relative to the original blade) near the leading edge (LE) and higher in the midchord region. The delay in tip leakage flow formation visualized from local entropy generation rate is shown in Figure 1-4; higher entropy generation rate on the second plane from the LE can be seen in the original blade while the aft-loaded blade has higher entropy generation rate on the third plane. Therefore, the steady flow fields suggested that the aft-loaded blade has the desired aft-loaded rotor blade loading and the formation of tip leakage flow is successfully delayed toward the trailing edge.

Due to flow changes accompanying aft-shifting rotor tip peak loading, the adverse streamwise pressure gradient at the blade tip TE was stronger in the aft-loaded blade, which led to flow separation at the blade tip TE. Although aft-loading a rotor blade could prevent the mixing out of the tip leakage flow, it also inevitably causes flow separation thus generating additional loss in the rotor. This flow separation has been hypothesized to be one of the two competing effects that set the optimum location of the peak blade loading. However, the amount of loss generated from flow separation has not been quantified.

In the 1980s, Wisler conducted experiments in a low-speed 4-stage compressor with the goal to reduce endwall loss in axial compressors by improving designs of ro-

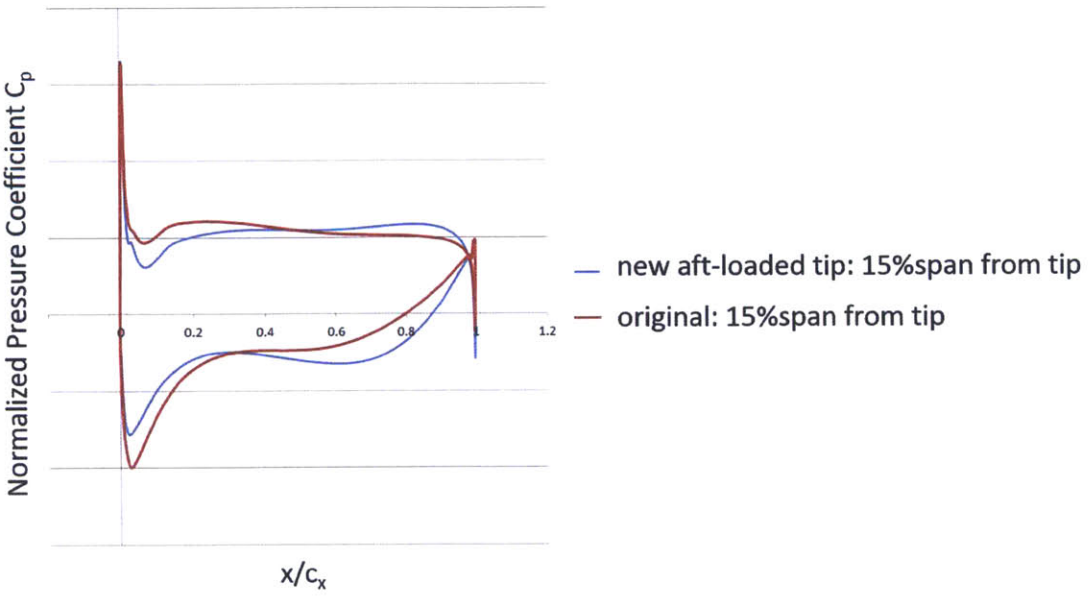

Figure 1-3: Comparison of rotor blade surface pressure coefficient distribution of the original and aft-loaded blade at 15% span from the blade tip (adapted from [2])

tor and stator blades [3]. Several rotor and stator blade designs were tested through a series of experiments and the effects of aft-loading tip section of the rotor blade on compressor performance were assessed. Rotor B was tip-aft-loaded approximately 40% span from the blade tip and the peak blade loading in the tip region was shifted approximately 10% chord toward the TE as shown in Figure 1-5. The tip clearance size is approximately 1.4% span. As shown in Figure 1-6, the results showed that Rotor B (aft-loaded rotor) has 0.3% higher efficiency at design point and at operating points toward choke, and higher pressure rise capability for the operating range compared with Rotor A (baseline rotor). However, detailed measurements of rotor loss in the tip region were not carried out and it was hypothesized that efficiency improvement was a result of changes of flow field in the tip region.

Tip leakage flow is known to be inherently unsteady and have its own periodic timescale, which scales with the rotor flow-through time [6]. This timescale of tip leakage flow is different from that of blade passing and has been identified in both experiments and computational simulations [6–9]. Hwang et al. found that the upstream effect from a downstream stator blade row could affect the behavior of tip

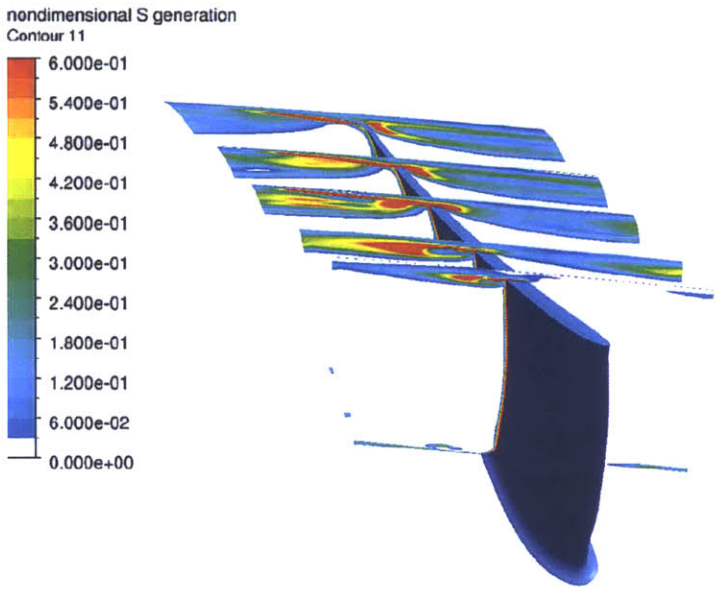

(a) Original rotor blade

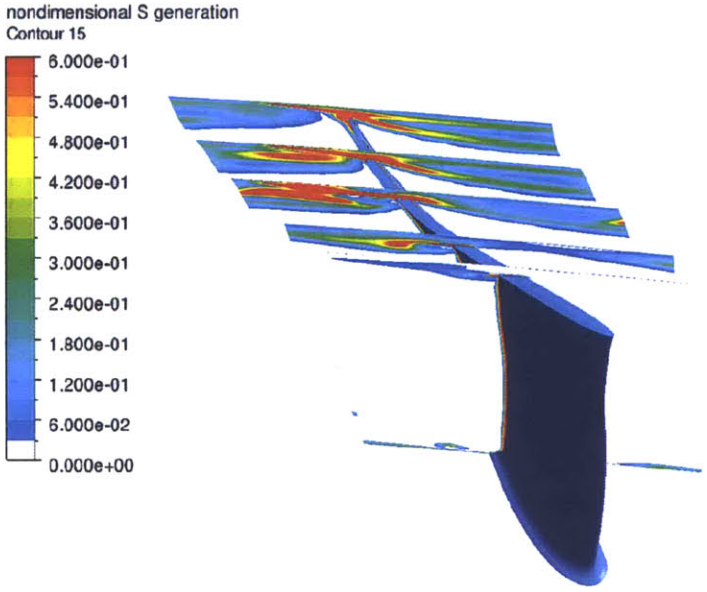

(b) Aft-loaded 20% chord rotor blade

Figure 1-4: Contours of local entropy generation rate showing delay of tip leakage flow formation in the aft-loaded blade; corresponding blade-to-blade planes are at identical chordwise location [2]

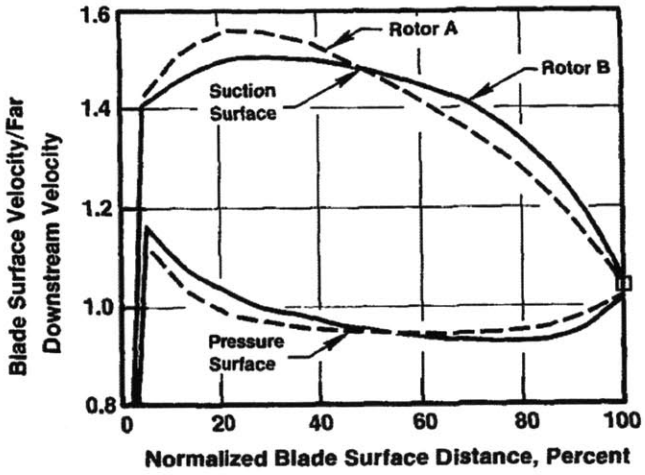

Figure 1-5: Comparison of surface velocity distribution of the baseline airfoil (Rotor A) and the aft-loaded blade (Rotor B) [3]

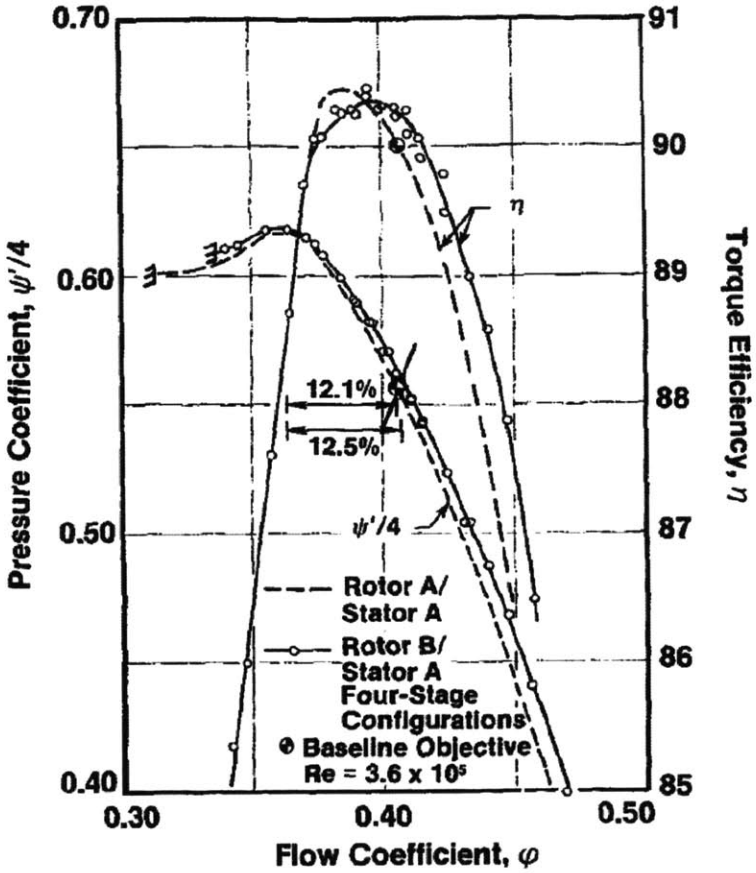

Figure 1-6: Efficiency and pressure rise capability improvement from the aft-loaded blade (Rotor B) compared with the baseline airfoil (Rotor A) [3]

leakage flow in an upstream rotor blade row [10]. Their computational results show that the structure of tip leakage flow is not identical in adjacent rotor flow passages when a downstream stator blade row is present while the structure is identical in an isolated rotor case .

Reversible unsteady attenuation/recovery process occurs to both rotor/stator wake and tip/hub leakage flow. Wake recovery process, which was first proposed by Smith [5], was investigated and demonstrated to be beneficial by Van Zante et al. [11]. Van Zante et al. have demonstrated that wake recovery process is primarily inviscid and viscous mixing plays a small role in the process. Valkov proposed that tip leakage recovery process occurs in a similar manner to wake recovery process as tip leakage flow has a wake-like structure [12]. As such, one would expect inviscid-dominated flow behavior to apply for the situation of tip leakage flow recovery. In Valkov's study, the inlet boundary condition of the stator was based on the steady computational results of Khalid [13] for an isolated rotor with a tip clearance of 2.5% span. Thus, Valkov's assessment of recovery process involving tip leakage flow neglects the effects associated with the inherent unsteadiness in rotor tip leakage flow as well as the impact of rotor-stator interactions on formation and evolution of tip leakage flow. Despite these shortcomings, the attenuation process has been clearly described and the effects of tip leakage recovery process have been quantified to be beneficial. Furthermore, he performed a sensitivity study and found that a reduction in axial rotor-stator gap by 30% chord yields additional 0.11% efficiency recovery benefit due to relatively less mixed-out tip leakage flow at the stator inlet.

Although tip and hub leakage recovery process could be explained similarly with Kelvin's theorem, the unsteady mechanism of the processes is slightly different. The stagnation pressure defect in the tip/hub leakage flow in an incompressible and inviscid flow can be changed from an unsteady mechanism shown in Equation 1.1 [14]. For hub leakage flow in a rotor, the $\partial p/\partial t$ term is positive from the motion of a rotor and a circumferential pressure gradient from the SS and the PS of a rotor blade. Hub leakage flow, which has longer convection time from its lower velocity compared with the main flow, can experience larger $\partial p/\partial t$ effect than the main flow, resulting in a

smaller stagnation pressure defect at the rotor exit. On the other hand, for tip leakage flow in a stator, the stator is stationary and the $\partial p/\partial t$ term might be generated from other flow processes and differ from that in hub leakage flow in a rotor; thus, the recovery effect could be different from that of hub leakage flow.

$$\frac{Dp_t}{Dt} = \frac{\partial p}{\partial t} \tag{1.1}$$

In summary, the effects of aft-loading the tip section of rotor blades have been found to be beneficial by Wisler [3]; however, his work did not provide a detailed explanation for the cause of the performance improvement. Sakulkaew, on the other hand, delineated the changes of the flow field in the tip region but has not demonstrated performance improvement conclusively [2]. Furthermore, the unsteady reversible tip leakage recovery process has been shown to be beneficial by Valkov [12]. Thus, it can be stated that there is a need to quantify the effects of aft-loading a rotor blade tip followed by subsequent tip leakage recovery process in a downstream stator with the presence of unsteady tip leakage flow and the rotor-stator interaction (and vice versa i.e. aft-loading a stator hub followed by hub leakage flow recovery in a downstream rotor).

1.3 Research Questions

The overall goal of the research is to assess the compressor design strategy proposed by Sakulkaew [2] and to determine if the design guideline can indeed yield a compressor performance improvement as postulated; and if it does not, what additional constraints or attributes need be incorporated. The proposed design strategy suggests that rotor should be tip-aft-loaded and hub-fore-loaded while stator should be hub-aft-loaded and tip-fore-loaded. The research presented in this thesis will focus on varying a rotor blade tip loading and employing a representative downstream stator blade row to leverage on the benefit of tip leakage recovery process.

The key research questions to be addressed for accomplishing the stated goal are as follows:

1. What are the flow processes setting up the optimum aft-loaded blade tip profile that is conducive to effective management of tip flow to minimize the opportunity for loss generation and flow blockage generation?

2. What is the quantitative benefit of tip leakage flow formation delay in a rotor and tip leakage flow recovery process in a stator?

3. What is the role of inherent tip leakage unsteadiness on a rotor-stator flow field periodicity and tip leakage flow attenuation/recovery in a downstream stator blade row?

4. Based on the answers to question 1, 2, and 3, what are the required attributes (additional to those embodied in the proposed design strategy) of a compressor stage for performance enhancement?

1.4 Contributions

The key findings are summarized below:

1. Varying the rotor tip blade loading has effects on the following parameters characterizing the tip flow in a compressor stage: (i) the chordwise location at which tip leakage flow begins to develop; (ii) tip leakage flow angle distribution, hence its mismatch with the main flow; (iii) chordwise distribution of tip clearance mass flow rate, hence its total tip leakage mass flow rate; and (iv) the benefit associated with the unsteady tip leakage flow recovery in downstream stator. These characterizing parameters together determine the attendant loss associated with rotor tip leakage flow in a compressor stage environment.

2. Aft-loading rotor blade tip through shifting blade tip peak loading toward the trailing edge delays tip leakage flow formation; this not only results in a relatively less-mixed-out tip leakage flow at the rotor exit but also a reduction in the

overall tip leakage mass flow. However, the attendant changes in tip flow angle distribution is such that there is an overall increase in the flow angle mismatch between the tip flow and the main flow. The former (i.e. reduced tip leakage mass flow and relatively less mixed-out tip flow at rotor exit) would tend to mitigate the loss generation in the rotor passage while the latter would tend to incur upon a higher loss generation. These three competing effects in principle would define an optimal rotor tip blade loading distribution for minimizing tip flow loss generation within the rotor passage.

3. The disparity between the timescale defining the self-induced tip leakage unsteadiness and blade passing time introduces a tip leakage vortex phasing effect (tip leakage vortex enters the downstream stator at specific pitchwise locations for different blade passing cycles). Despite the presence of the inherent tip flow unsteadiness and the effects of rotor-stator interaction on tip flow, unsteady tip leakage flow recovery process attenuates tip leakage flow in the downstream stator on a time-averaged basis; the process yields a higher benefit for a relatively less-mixed-out tip leakage flow from aft-loading a rotor blade tip.

4. Based on the finding 2 above, the design hypothesis is revised to incorporate a constraint on tip flow angle chordwise distribution. The revised hypothesized design strategy should read as: "rotor should be tip-aft-loaded and hub-fore-loaded while stator should be hub-aft-loaded and tip-fore-loaded with tip/hub leakage flow angle distribution such that it results in no additional loss".

5. Periodicity of a compressor stage flow field is set by the two timescales, defining the tip leakage flow inherent unsteadiness and blade passing. The periodicity of a flow field can be used as a criteria to determine if and when unsteady computations have attained an equilibrium state when the flow manifests a repeating flow pattern on a temporal basis. As an example, the computed unsteady flow for a rotor-stator stage presented here has a periodicity of 11 blade passing time periods. In other words, the flow repeat at every 11 blade passing times. This is consistent with the timescales defining the tip flow inherent

unsteadiness and the blade passing

It is to be noted that findings 1 to 4 are based on computations, in which the mixing of the tip clearance flow with the main flow is incomplete; as such, the details of the mixing, including the choice of the turbulence model and the computational grid resolution, could play a role in determining both the qualitative and the quantitative aspects. However, the trend from the results based on complementary control volume analyses for complete mixing out of tip flow is in accord with that from computations.

1.5 Organization

The thesis is organized as follows. Chapter 2 provides the overall research approach, and the utilization of numerical simulations to answer the posed research questions. This is then followed by the assessment of the effect of aft-loading a rotor blade in the rotor under a steady flow approximation in Chapter 3. Beneficial and detrimental flow processes governing the overall loss reduction in the rotor are identified followed by quantification of their loss. Chapter 4 addresses characteristic of unsteady flow fields with the presence of tip leakage flow inherent unsteadiness and rotor-stator interaction to formulate the performance evaluation approach in unsteady flow fields. Chapter 5 illustrates the mechanism of tip leakage flow recovery process and the effect of tip leakage flow phasing on the recovery process; time-averaged effectiveness of the recovery process for less mixed-out tip leakage flow is quantified. Chapter 6 revisits the time-averaged loss generated from the key flow processes in the rotor based on unsteady flow fields as previously delineated in Chapter 3. The overall time-averaged loss is synthesized to demonstrate the effectiveness of the design hypothesis in a rotor-stator stage environment. Finally, all key findings based on computational work are summarized and future work is proposed in Chapter 7.

Chapter 2

Technical Approach

This chapter presents the research approach applied to answer the research questions posed in Section 1.4. It is of import that compressor flow fields be adequately modelled for assessing the performance impact of the two key mechanisms delineated in Chapter 1. Computing and modeling the flow field, steady as well as unsteady, in a rotor-stator stage are described in Section 2.1. The details of compressor geometry, computational setup, and post-processing techniques are described in Section 2.2. Evaluation of the compressor performance in a rotor-stator stage are presented in Section 2.3.

2.1 Framework of Investigation

The traceability of performance changes in a compressor stage to each of the two flow processes (namely the delay of tip leakage flow formation and the unsteady recovery of tip leakage flow in the following blade row) has to be established. As the recovery effect of tip leakage flow could be different from that of hub leakage flow as delineated in Chapter 1. Therefore, a separate assessment for a hub leakage flow in a rotor is required and the current research is limited to the benefit of tip leakage flow recovery process in a stator only. In view of this, the assessment will henceforth be on a representative embedded rotor-stator stage from a large industrial gas turbine for power generation.

Computational fluid dynamics (CFD) based on Reynolds-averaged Navier-Stokes (RANS) equations is used to compute steady and unsteady flow in compressor flow paths. Results from CFD simulations allow detailed flow field investigation in the compressor flow paths. The two main mechanisms being assessed for their impact on compressor performance are both associated with tip leakage flow but each requires different level of modelling.

As alluded to in Section 1.2, an expected consequence of aft-loading a rotor blade is the delay in tip leakage flow formation; this effect can be adequately determined with a steady flow approximated by a mixing-plane located at the intra rotor-stator axial gap. As the flow field downstream of a mixing-plane is circumferentially mixed out [15], the rotor-stator stage flow field modelled with a mixing plane approximation is not capable of assessing rotor-stator induced flow unsteadiness including the unsteady tip leakage recovery process. As such, unsteady time-accurate simulations based on Unsteady Reynolds-averaged Navier-Stokes (URANS) are used for assessing effects associated with flow unsteadiness in a rotor-stator stage. This is implemented via replacing the mixing plane with a sliding interface at the same location in the intra rotor-stator gap to allow time-accurate interactions of flow fields in the rotor and the stator. Unsteady time-accurate computational flow model of a rotor-stator stage environment would yield results that can, in principle, be used to assess the tip leakage recovery process as well as unsteady flow events with time scale different from that of blade passing.

2.2 Computational Setup and Post-processing Techniques

The compressor stage used to assess the hypothesis was taken from an embedded rear-stage compressor of a modern industrial gas turbine. Geometrical parameters and operating conditions are provided in Table 2.1. The rotor-stator blade ratio is changed to unity from its actual value to expedite the convergence rate for unsteady

Table 2.1: General characteristic of the representative compressor stage

Parameters	Value
Rotor tip to hub ratio	0.9
Rotor solidity	1.0
Rotor aspect ratio	1.4
Rotor-stator blade ratio	1
Reynolds number	$\sim 1 \times 10^6$
Inlet mach number	0.5
Rotor tip clearance size	5% span
Stator hub clearance size	1.9% span

calculations. It is noted that figures representing the geometrical compressor design in this thesis are not to scale with its actual one.

A commercial three-dimensional CFD solver, CFX 14.5, has been selected for computing flow fields of the selected compressor stage. A series of steady Reynolds-averaged Navier-Stokes (RANS) and unsteady Reynolds-averaged Navier-Stokes (URANS) computations have been performed with double precision, second-order advection schemes, and first order turbulence numerics. The k-ω Shear Stress Transport turbulence model has been employed as the turbulence model. The working fluid has been treated as an ideal gas with constant heat capacity at constant pressure. Assessments of computational solutions have been carried out by Sakulkaew to ensure the capability of CFX in computing flow fields of axial compressors [2].

The computational geometry has one upstream rotor and one downstream stator blade spanning the full annulus. The mesh resolution is 2.5 million and 2.1 million nodes for the rotor and stator, respectively. Grid density is higher in the endwall region for obtaining accurate flow features of tip leakage flow. The value of y+ on the blade surface is approximately 40. The boundary condition at the stage inlet and stage outlet have been supplied from the APNASA solver [16,17]. The boundary conditions do not have time variations for both steady and unsteady computations. The boundary condition at the stage inlet, which is specified in a stationary frame of reference, has radial variations of stagnation pressure, stagnation temperature, and flow angle. The boundary condition at the stage outlet is specified by a radial variation

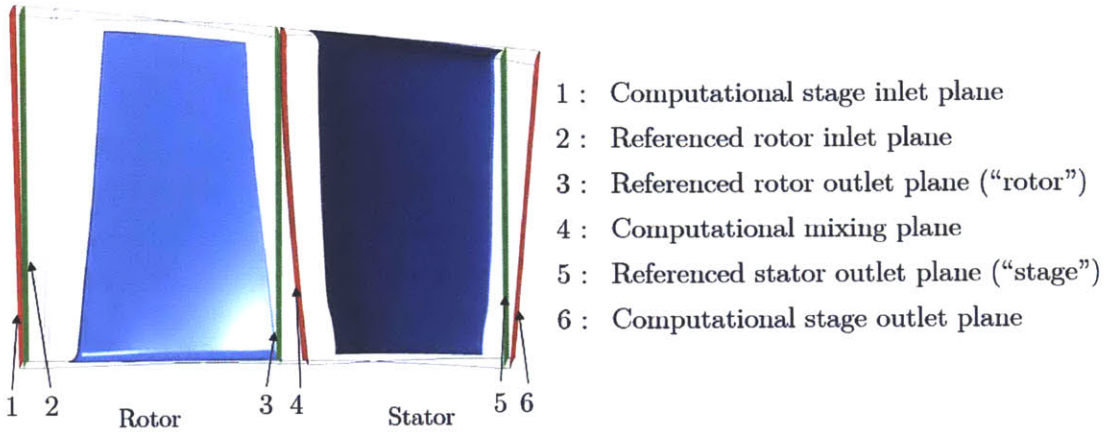

Figure 2-1: The computational geometry and the referenced locations for post-processing

of static pressure, which can be varied to obtain a desired operating condition.

CFD-Post 14.5 has been employed as a post-processing tool for this research. The actual computational stage inlet, mixing plane, stage outlet (shown as red planes in Figure 2-1) are all inclined planes; however, the reference locations for post-processing are axial planes. Location reference used in the thesis is shown in Figure 2-1 (shown as the green planes). Three main locations (rotor inlet, rotor exit, and stator) are referred to for loss accounting and pressure ratio.

2.3 Compressor Performance Evaluation and Loss Accounting Method

Overall improvement of compressor performance can be evaluated from changes in loss and pressure ratio. Stagnation pressure is averaged by a work-averaging technique, which conserves the availability of the flow field. This concept was proposed by Cumpsty and Horlock [18]. The concept of work-average pressure has been expanded by Zlatinov to accommodate time-variation in unsteady flow fields [19]. Time-averaged work-averaged pressure can be computed as shown in Equation 2.1 for unsteady flow fields.

$$P_t^{wa,ta} = \left[\frac{\int \left(T_t \rho \mathbf{u}\right)^{ta} \cdot d\mathbf{A}}{\int \left(\rho \mathbf{u} T_t / \left(P_t^{\frac{\gamma-1}{\gamma}}\right)\right)^{ta} \cdot d\mathbf{A}} \right]^{\frac{\gamma}{\gamma-1}} \tag{2.1}$$

Irreversible entropy generation (i.e. entropy generation associated with irreversible processes) is employed as a mean to quantify loss generation in computed flow fields and hence compressor performance. The irreversible entropy generation can be locally computed, allowing one to identify the loss-generating flow process. Furthermore, entropy generation in flow fields can be directly related to lost work and compressor efficiency shown in Equation 2.2.

$$\xi = \frac{\dot{W}_{lost}}{\Delta \dot{H}_{stage}} = \frac{T_{t,stator\ out} \dot{S}_{gen}}{\Delta \dot{H}_{stage}} = 1 - \eta \tag{2.2}$$

Two methods are available for computing entropy generation. The first method, which will be referred to as "entropy flux method", calculates entropy generation from the difference of entropy flux at interested planes as shown in Equation 2.3. In this method, entropy of working fluid is calculated from the equation of state of the fluid. The second method, which will be referred to as "dissipation method", calculates entropy generation from local viscous dissipation and thermal dissipation in the flow field as shown in Equation 2.4. The entropy generation from viscous dissipation and thermal dissipation are computed from Equation 2.5 and 2.6, respectively.

$$\dot{S}_{generation} = \int_{outlet} \rho s \mathbf{u} \cdot d\mathbf{A} - \int_{inlet} \rho s \mathbf{u} \cdot d\mathbf{A} \tag{2.3}$$

$$\dot{S}_{generation} = \int \left(\dot{S}'''_{viscous} + \dot{S}'''_{thermal} \right) dV \tag{2.4}$$

$$\dot{S}'''_{viscous} = \frac{1}{T}\tau_{ij}\frac{\partial u_i}{\partial x_j} \tag{2.5}$$

$$\dot{S}'''_{viscous} = \frac{k_{eff}}{T^2}\left(\frac{\partial T}{\partial x_j}\right)^2 \tag{2.6}$$

In principle, these two methods for computing entropy generation should give identical results. However, Zlatinov has assessed these two methods for computing entropy generation and has determined that the dissipation method using Equation 2.4 tends to underestimate entropy generation in the computational domain [19]. However, the trend of entropy generation in flow paths from the two methods is comparable. Therefore, in this research, the dissipation method is used for identifying flow region of high loss and flow processes responsible for loss generation. The entropy flux method will be utilized in accounting for entropy generation in compressor flow paths (e.g. rotor passage, stator passage, intra rotor-stator gap, etc) and for computing lost work in Equation 2.2.

2.4 Summary

The research approach has been developed to address the research questions posed in Chapter 1. Computational tools are applied to compute steady as well as unsteady flow fields in a rotor-stator stage environment targeting at answering the research questions. Steady compressor flow fields are used to assess loss generation associated with varying the rotor tip loading distribution. Unsteady flow fields of a rotor-stator stage environment are employed to assess the effects of tip leakage flow recovery process in stator as well as effects associated with tip leakage flow self-induced unsteadiness.

The selected compressor stage is representative of a rear-stage compressor in a modern large industrial gas turbines for power generation, where non-dimensional tip

clearance size is relatively large. CFX 14.5, has been selected as the main numerical solver for this study and CFD-Post 14.5 has been employed as a post-processing tool. A series of steady and unsteady time-accurate computations have been performed with double precision, second-order advection schemes, first order turbulence numerics, and the k-ω Shear Stress Transport turbulence.

Irreversible entropy generation is employed as a mean to quantify loss generation and compressor performance as well as to locate regions with high entropy generation rate for tracing mechanisms generating high loss in computed flow fields.

Chapter 3

Effects of Tip Blade Loading Variation under Steady Flow Approximation

Effects from the delay in tip leakage flow formation by aft-loading the rotor tip peak blade loading are assessed with computed steady flow fields with a mixing-plane approximation. Two tip aft-loaded and one tip fore-loaded rotor blades (relative to the baseline design) have been designed to elucidate the effects of aft-loading rotor blade tip. A preliminary investigation by Sakulkaew [2] suggests that tip leakage flow formation can be delayed by aft-loading a rotor blade but the benefit from tip leakage flow formation delay was not quantified. Additionally, flow separation near a rotor blade tip TE was suggested to be a competing effect possibly setting the optimum tip blade loading. These findings will be revisited and re-assessed in this chapter as well as other attendant flow effects arising from varying the rotor tip loading distribution.

3.1 Design of Fore-loaded and Aft-loaded Rotor Blades

Prior to assessing the hypothesis, delineated in Chapter 1, and its utility, the effects of tip leakage flow formation delay are first assessed. Two aft-loaded rotor blades have been designed to yield a rotor flow field, in which the tip leakage flow formation is delayed. The delay in tip leakage flow formation can be accomplished by shifting the peak of tip blade loading toward the TE. Additionally, a fore-loaded rotor blade design, in which the rotor tip peak loading is shifted toward the LE relative to the original design, has also been generated for assessing the flow effects associated with tip leakage flow forming closer to the LE. These three additional rotor blade designs would provide an adequate range of tip loading variation for defining the optimum blade tip loading if there should indeed be one.

The location of the peak blade loading is a function of the distribution of the camber blade line (i.e. incidence angle and camber angle). The changes in the camber blade line distribution of the new blade designs are shown in Figure 3-1. The incidence angle of the lessaft (but aft-loaded relative to the original design) and moreaft blade is designed to be smaller by increasing the inlet metal angle to reduce the blade loading near the LE while the blade turning is higher near the TE to provide the similar amount of overall flow turning in the tip region. In other words, the modification to the aft-loaded blades make the LE to be in closer alignment with the incoming flow relative to the baseline situation. The incidence angle of the fore blade is, on the other hand, designed to be larger by decreasing the inlet metal angle and significant flow turning occurs near the LE.

The modification process to change tip blade loading has been carried out by changing a blade camber line distribution from 80% span of the rotor blade to the blade tip. Blade loading distribution of the fore-loaded, aft-loaded, and original baseline rotor blades near the blade tip and at 75% span is shown in Figure 3-2 and 3-3, respectively. Figure 3-2 shows that the peak blade loading shifts toward the

rotor TE for the aft-loaded blade designs. Figure 3-2 and 3-3 shows that the changes in the tip blade loading would have the largest impact on the flow in the tip region but minimal impacts in the main flow region. The changes in the location of the peak blade loading for the new blades are shown in Table 3.1. Additionally, the rotor pressure ratio of the new rotor designs is managed to be similar to that of the original blade design as shown in Figure 3-4.

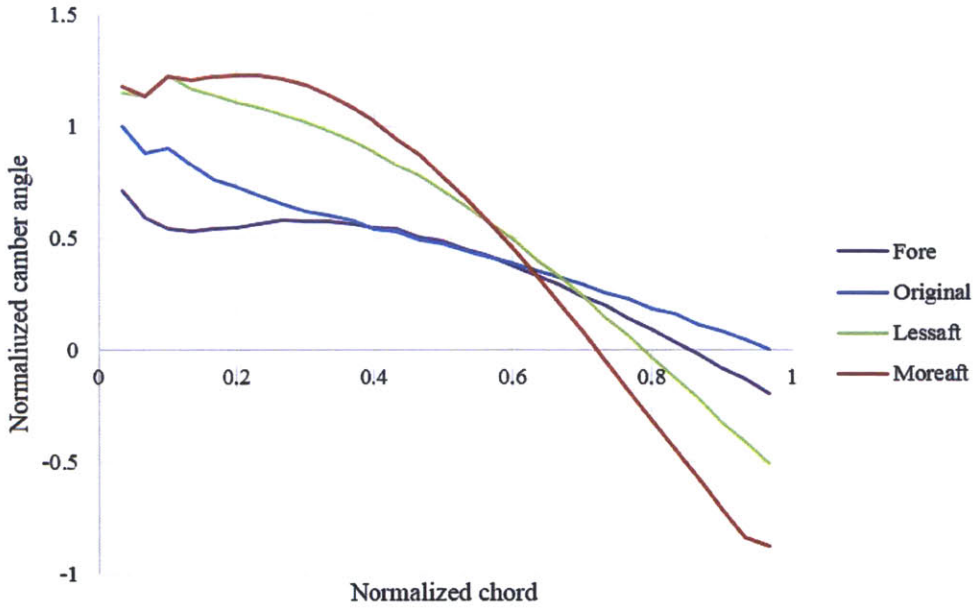

Figure 3-1: Changes in rotor blade camber line distribution near blade tip for the fore, original, lessaft, and moreaft blade

Table 3.1: Location of peak blade loading near blade tip for various blade designs

Blade design	Peak blade loading location	Shift in the peak loading location
Fore	26% chord	-6% chord
Original	32% chord	-
Lessaft	40% chord	+8% chord
Moreaft	48% chord	+16% chord

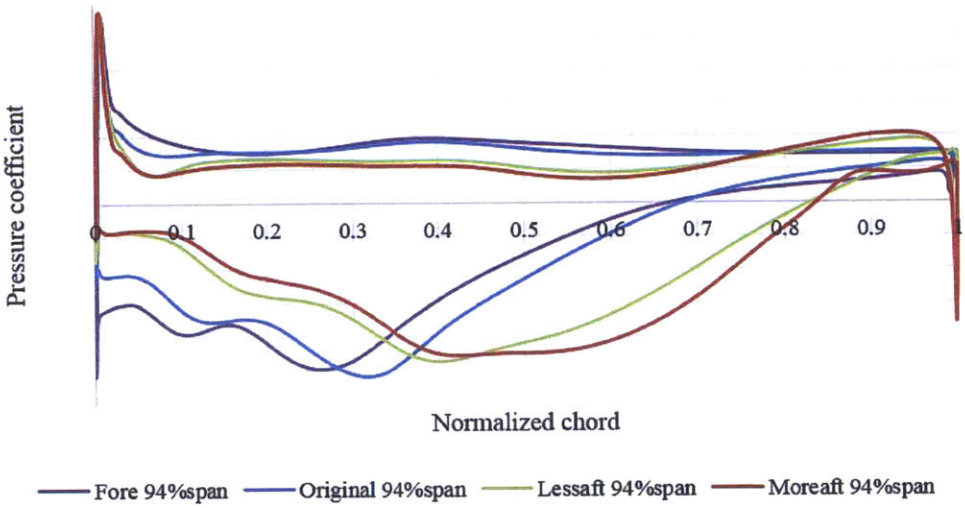

Figure 3-2: Changes in location of peak rotor blade loading distribution of the four rotor blade designs near blade tip (1% span below the tip)

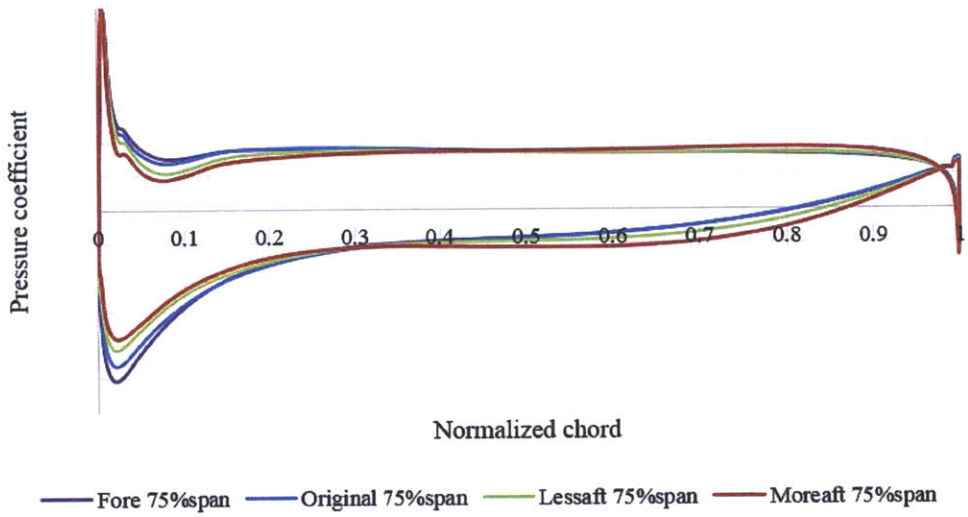

Figure 3-3: Similar rotor blade loading distribution of the four rotor blade designs at 75% span

Figure 3-4: Negligible changes in relative work-averaged rotor pressure ratio in the four rotor blade designs

3.2 Loss Reduction from Tip Leakage Flow Formation Delay

The location where tip leakage flow forms in the fore, lessaft, and moreaft blade is different from that in the original blade as the peak blade tip loading has been shifted. Distribution of tip leakage mass flow driven through tip clearance, shown in Figure 3-5, indicates that the peak of tip leakage mass flux in the fore-loaded blade appears nearer to the LE while the peak of tip leakage mass flux is shifted toward the TE for the lessaft and moreaft blade. Therefore, tip leakage flow forms closer to the LE in the fore blade and closer to the TE in the lessaft and moreaft blade. It should be noted that the integrated net tip clearance mass flow rate decreases with shifting the rotor tip loading peak toward the TE. Furthermore, formation of tip leakage flow can be tracked and visualized from irreversible local entropy generation rate proceeding downstream toward the TE. The local entropy generation rate is created in the shear layer between the tip leakage flow and the main flow during the formation of tip leakage flow. In Figure 3-6, formation of tip leakage can be seen from a region with high local entropy generation rate (indicated with a red contour) on the 20% chord

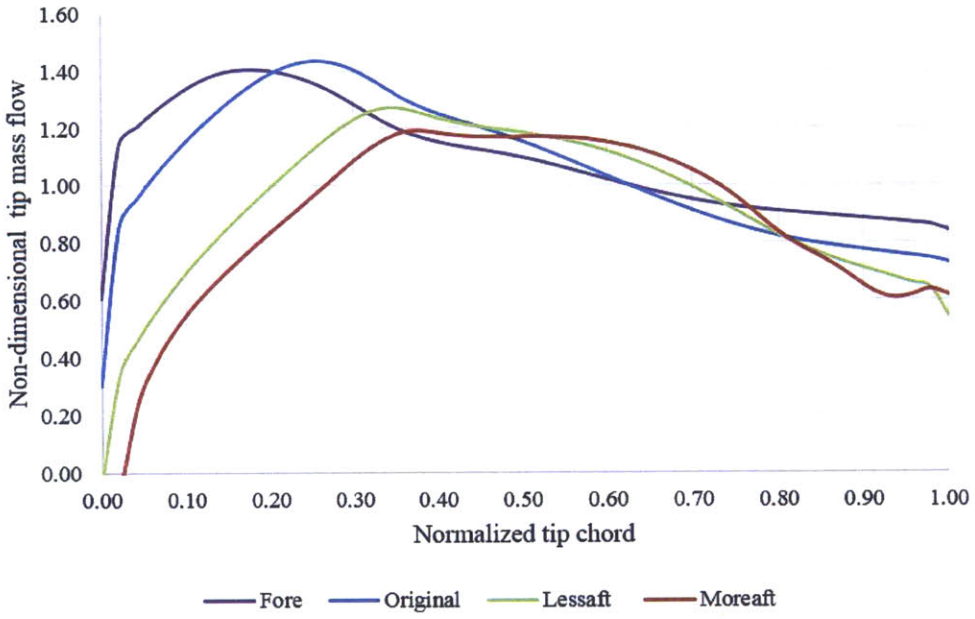

Figure 3-5: Chordwise distribution of tip leakage mass flow from various blade designs

plane in the fore blade while the formation in the original, less, and moreaft is seen on the 25%, 30%, and 35% chord plane, respectively. This indicates that the fore, lessaft, and moreaft blade have the fore-loaded/aft-loaded characteristics as desired.

To determine the extent of tip leakage flow formation delay, the location at which tip leakage flow forms needs to be quantified. The location that tip leakage flow starts to forms can be visualized by identifying a location of low static pressure or a region with high local entropy generation rate; however, such approaches are somewhat subjective. This issue can be avoided by utilizing the peak of an axial distribution of local entropy generation rate to indicate the location at which tip leakage flow formation completely forms. Figure 3-7 shows that the peak of the local entropy generation rate from the fore blade is shifted toward the LE while the peak is shifted toward the TE for the lessaft and moreaft blade. This confirms that tip leakage flow is successfully delayed in the lessaft and moreaft blade and successfully advanced toward the LE (relative to the original design) in the fore blade. The changes in tip leakage flow formation location are shown in Table 3.2.

According to the hypothesis, when tip leakage flow formation is delayed, tip leak-

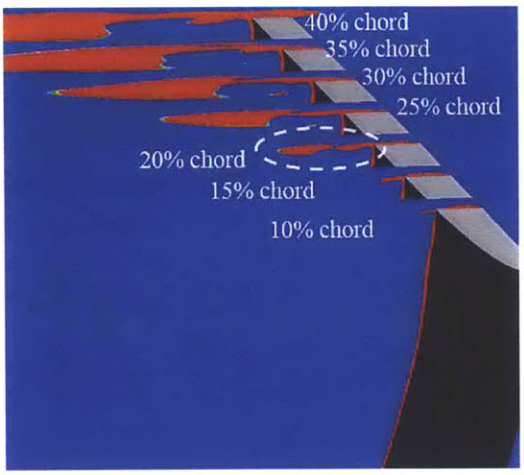

(a) Fore

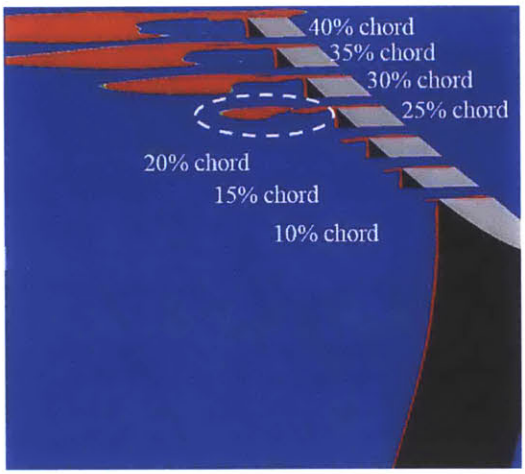

(b) Original

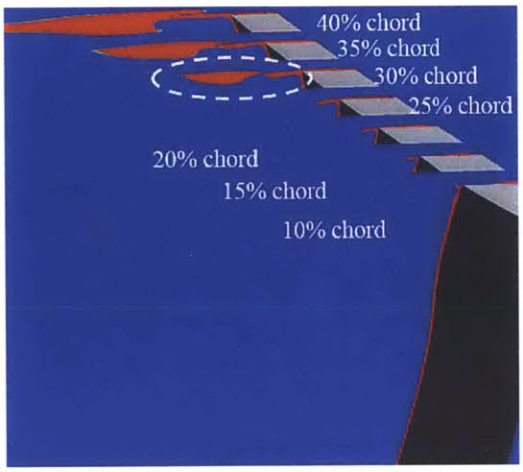

(c) Lessaft

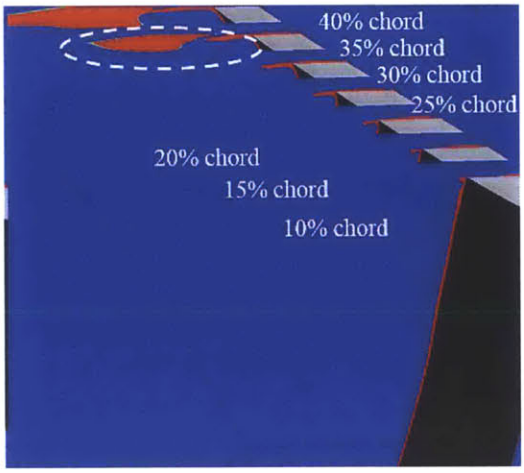

(d) Moreaft

Figure 3-6: Advance and delay in tip leakage flow formation in the four blade designs visulaized from a region with high local entropy generation rate created during formation of tip leakage flow (red region)

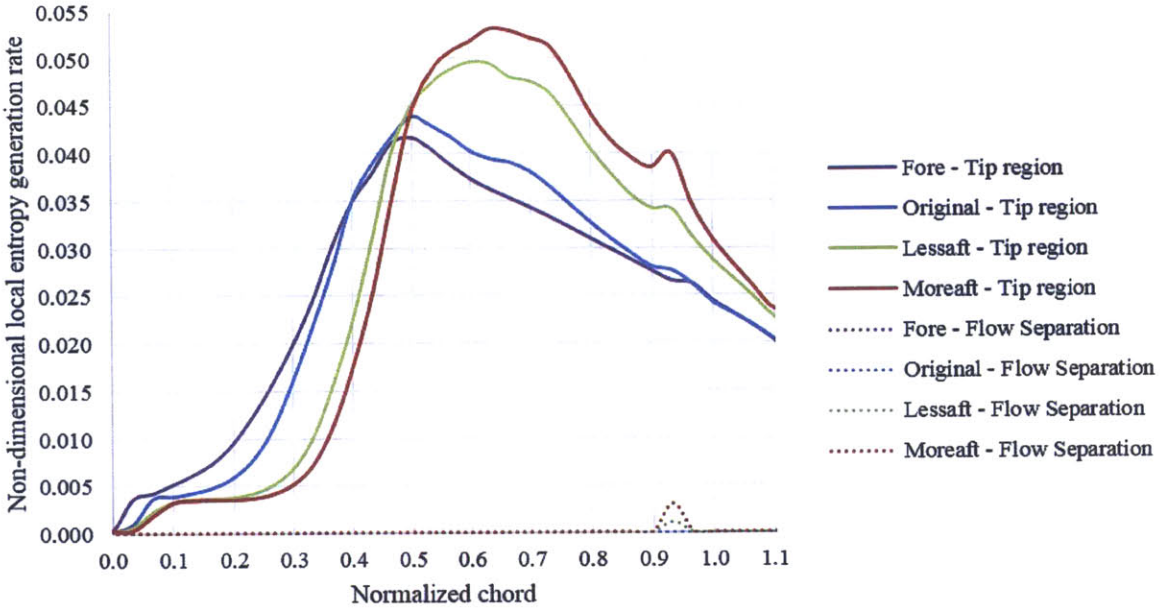

Figure 3-7: Local entropy generation rate in the tip region (75% span to 100% span) and in the flow separation bubble near the rotor tip TE

Table 3.2: Delay/advance in tip leakage flow formation location

Blade design	Shift in the location of peak local entropy generation in the tip region
Fore	-2% chord
Original	-
Lessaft	+9% chord
Moreaft	+11% chord

age flow has less time (equivalently shorter distance over which) to mix out in the rotor. Thus, such tip leakage flow would have less of an opportunity to realize its loss from its full potential. For a hypothetical case, when tip leakage flow formation is delayed, a hypothetical curve of local entropy generation rate from tip leakage flow formation and downstream development, should also shift toward the TE as shown in Figure 3-8; The distribution of local entropy generation rate for the original blade design is obtained from actual computational results while a similar distribution of local entropy generation rate for both situations has been assumed with the peak aft-shifted. As the tip leakage flow formation is delayed, the viscous loss generated in

the ideal aft-loaded blade would be smaller compared to that in the original blade. The amount of loss reduction is given by the area under the local entropy generation rate curve from the rotor exit upward to a distance of tip leakage flow formation delay (the gray area in Figure 3-8). The simplified but assumed situations are used to only elucidate the effect of tip leakage flow formation delay on loss generation within the rotor passage; the actual (quantitative) loss generation will be different from this simplified situation. However, it is difficult to separate tip leakage flow loss from other losses (e.g. boundary layer loss, rotor wake loss), thus, rendering the technique illustrated in Figure 3-8 impractical. Therefore, instead of quantifying viscous mixing loss realized by tip leakage flow, the remaining potential loss in tip leakage flow at the rotor exit is estimated instead. If tip leakage flow is allowed to mix out, remaining potential loss at the rotor exit will be small. Thus, tip leakage flow in an aft-loaded blade would be expected to retain a higher loss potential at the rotor exit due to the lower viscous mixing loss that has been realized. Thus, the difference in the loss potential between the original and various blade designs can be used to estimate the amount of viscous mixing loss generated by tip leakage flow to provide a measure on the benefit of tip leakage flow formation delay; this is given in Equation 3.1 below.

$$\mathcal{L}_{TLFdelay} = \xi_{potential,rotor\ exit,original} - \xi_{potential,rotor\ exit,aft/fore} \tag{3.1}$$

,where $\xi_{potential,rotor\ exit,aft/fore}$ and $\xi_{potential,rotor\ exit,original}$ denote potential loss at the rotor exit in an aft/fore-loaded rotor blade and the original rotor blade, respectively and $\mathcal{L}_{TLFdelay}$ denotes relative loss from the process with loss from the original blade as the reference.

A method for calculating potential mixing loss in a non-uniform flow has been proposed by Prasad [20]. The method represents a non-uniform flow with a uniform counterpart, which is in kinematic and thermal equilibrium, with conservation of mass, axial momentum, angular momentum, and energy between the uniform and non-uniform flow. Thus, potential loss is computed from the difference between en-

tropy flux from the non-uniform and uniform flow condition.

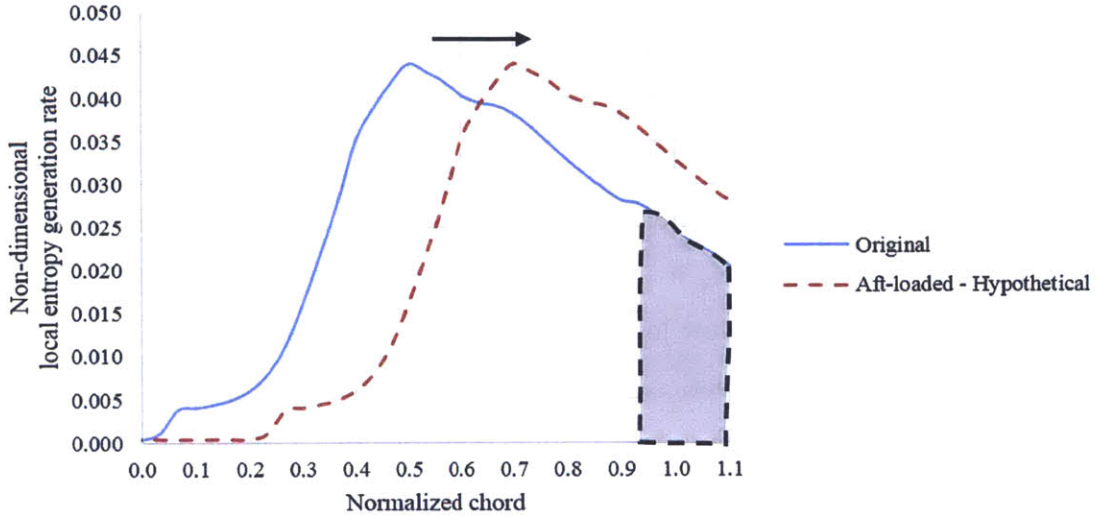

Figure 3-8: Local entropy generation rate in a hypothetical aft-loaded blade and its loss reduction (grey area)

This method allows us to separate the effect of tip leakage flow formation delay from other effects. Figure 3-9 shows relative loss benefit from the process with reference from the original blade design. The lessaft and moreaft blade gain a benefit from this tip leakage flow formation delay; on the other hand, the fore blade suffers from higher loss from this process. It can be seen that the benefit from tip leakage flow formation delay is a function of tip leakage flow formation delay distance shown in Table 3.2. The benefit from the process increases as a rotor blade is more aft-loaded, in accord with the hypothesis.

It has to be noted that the mixing process of tip leakage flow is incomplete and the choice of a turbulence model and the numeric (such as undesirable artificial numerical diffusivity, etc.) could play a role on the details of the mixing process involving the tip flow and the main flow. Although the mesh resolution is high (2.5 million nodes), this might not be adequate to represent the structure of tip leakage flow. Additionally, the current mesh provides high grid resolution in the rotor wake region but lower grid resolution in the midpassage region where the tip leakage flow is. This would yield a relatively more numerically diffusive computed flow field in the tip region. Thus, an artificially higher mixing rate of tip leakage flow in the rotor could be introduced by

the numerically diffusive flow, leading to lower estimated benefit of tip leakage flow formation delay.

In summary, tip leakage flow formation can be successfully delayed or advanced as desired by appropriately tailoring the rotor tip loading distribution. Computational results suggests that aft-loading the rotor tip would yield a lower loss from the tip leakage flow formation delay while fore-loading the rotor tip would yield a higher loss. We will next proceed to determine what other attendant loss sources associated with aft-loading the rotor tip.

Figure 3-9: Relative loss benefit of tip leakage flow formation delay

3.3 Loss Generation from Changes in Tip Flow Angle Mismatch and Tip Leakage Mass Flow

Preliminary work conducted by Sakulkaew [2] indicated that an additional detrimental flow process resulting from aft-loading the rotor tip is flow separation on the rotor blade tip SS. Therefore, we use the present computed results to determine whether loss from such flow separation is significant and can outweigh the potential benefit from aft-loading the rotor tip.

As shown in Figure 3-10, the computed flow fields show, for both the lessaft and

moreaft blade, the existence of flow separation bubble on the blade tip SS; however, flow separation is absent in the fore and original blade. Loss from flow separation can be quantified by integrating local entropy generation rate over the extent of flow separation bubble shown in Figure 3-10. Entropy generation rate from flow separation bubble in the lessaft and moreaft blade is shown separately in Figure 3-7. Although flow separation is a complex flow feature and might not be predicted accurately with RANS simulations [21], the order of loss from flow separation is negligible compared with loss generated in the midchord region as shown in Figure 3-7. This would suggest that we should focus on the cause of the higher computed entropy generation rate in the midchord region.

Additional loss generation in the midchord region shown as the difference between the computed local entropy generation rate and the hypothetical counterpart in Figure 3-11 needs to be separated from loss reduction from tip leakage formation delay. The hypothetical aft-loaded blades are assumed to have similar tip leakage flow structure and the same amount of tip leakage flow as that in the original blade, resulting in identical but aft-shifted local entropy generation rate curves as shown in Figure 3-8. Thus, if there should be no additional loss mechanism generated in this hypothetical aft-loaded blade, mixed-out loss at the rotor exit of the original and the hypothetical aft-loaded blade should be identical. On the other hand, if there are other flow processes generating additional loss as seen from actual computed local entropy generation curves of the new blade designs in Figure 3-11, the mixed-out loss at the rotor exit could be different. Therefore, the difference of mixed-out loss can be used to quantify the loss generated from new flow processes. Loss generated from new flow processes can be computed from Equation 3.2.

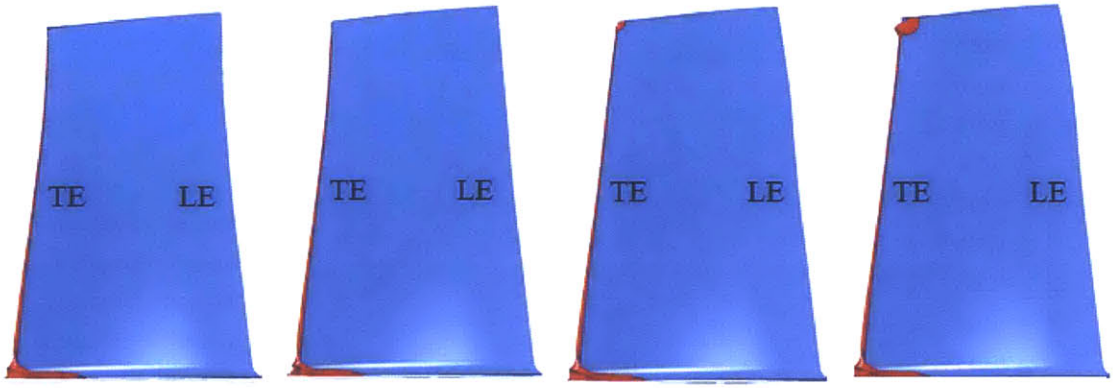

(a) Fore (b) Original (c) Lessaft (d) Moreaft

Figure 3-10: Flow separation bubble (red surface) on rotor blade tip SS near TE

$$\begin{aligned}\mathcal{L}_{midchord} &= (\xi_{rotor\ exit,aft/fore} + \xi_{potential,rotor\ exit,aft/fore}) \\ &\quad - (\xi_{rotor\ exit,original} + \xi_{potential,rotor\ exit,original}) \\ &= \xi_{mixed-out,rotor\ exit,aft/fore} - \xi_{mixed-out,rotor\ exit,original}\end{aligned} \tag{3.2}$$

,where $\xi_{mixed-out,rotor\ exit,aft/fore}$ and $\xi_{mixed-out,rotor\ exit,original}$ denote mixed-out loss at the rotor exit in an aft/fore-loaded rotor blade and the original rotor blade, respectively and $\mathcal{L}_{midchord}$ denotes relative mixed-out loss in the midchord region with loss from the original blade as the reference.

This equation only provides the upper bound of loss from this additional flow process as it may still be developing/evolving at the rotor exit. Loss generated in the midchord region quantified with Equation 3.2 is shown in Figure 3-12 with the highest loss for the moreaft blade and a relatively lower loss for the fore blade. This suggests that there are other flow effects that change in response to aft-loading rotor tip to yield a higher entropy generation rate in the midchord region and thus a higher mixed-out loss; this change in flow effect can potentially outweigh the benefit arising from the delay in tip flow formation if not managed appropriately.

Changes in tip flow angles are observed in the aft-loaded blades as shown in

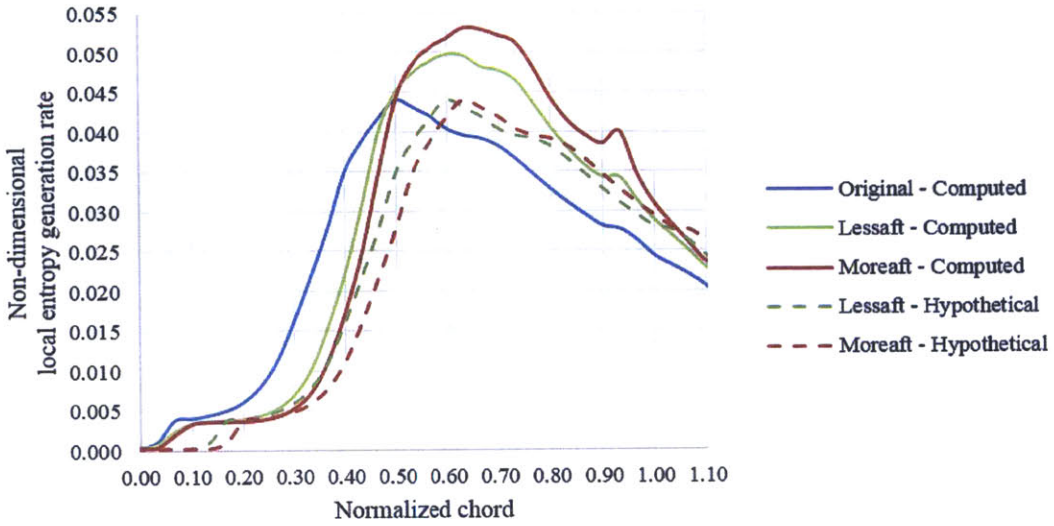

Figure 3-11: Discrepancy between hypothetical and computed local entropy generation rate in the aft-loaded blades

Figure 3-13. It can be seen that tip leakage flow angle at approximately 70% chord is higher for the aft-loaded blade designs with representative velocity vector pointing in more toward to the upstream direction. As flow angle of the main flow is essentially unaltered, flow angle mismatch between the tip flow and the main flow is changed shown Figure 3-14. Figure 3-14 shows that tip flow angle mismatch in the lessaft and moreaft blade is lower than that in the original blade from the LE up to approximately 55% chord but higher from 55% chord to 85% chord. The opposite trend can be seen from the fore blade. The maximum flow angle difference in the original blade is approximately 80 degree while the maximum flow angle mismatch in the moreaft blade is 85 degree. It appears that the region with higher flow angle mismatch in the lessaft and moreaft blade corresponds to the region with higher local entropy generation rate shown in Figure 3-7. Although local entropy generation rate cannot be used to represent the mixed-out loss, it suggests a possibility that larger flow angle mismatch could affect the total mixed-out loss. To assess the effect from the higher flow angle mismatch on loss generation, a control volume analysis is formulated and carried out; the results from this control volume analysis are then use to interpret the computed results.

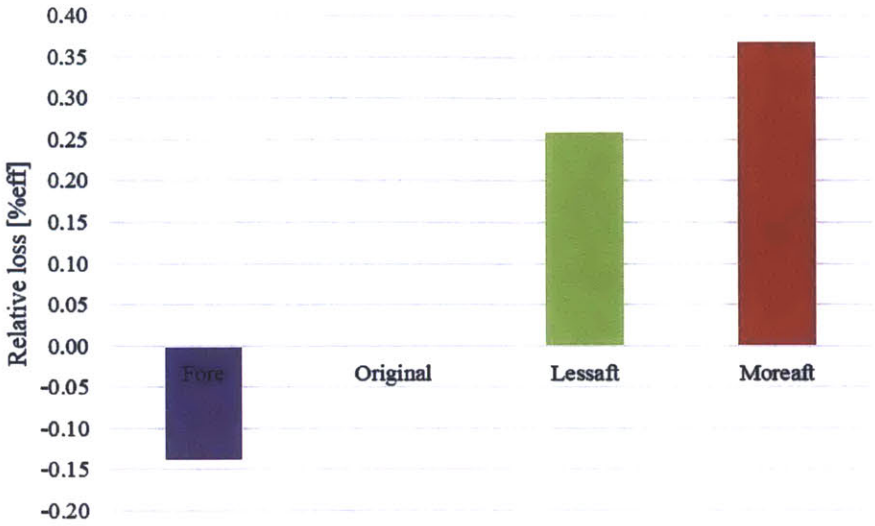

Figure 3-12: Relative loss benefit in the midchord region

The changes in the tip flow angle are not the only factor controlling loss from tip leakage flow mixing loss. The tip leakage mass flow driven across the tip clearance also changes in the aft-loaded blades. Tip leakage mass flow is lowest in the moreaft blade and highest in the fore blade as shown in Figure 3-15. It can be seen from Figure 3-15 that tip leakage mass flow decreases as a rotor blade is aft-loaded. Therefore, tip leakage flow mixed-out loss is controlled by flow angle mismatch between the main flow and the tip flow, and tip leakage mass flow. The increasing flow angle mismatch should generate higher mixed-out loss while a decrease in tip leakage mass flow would reduce mixed-out loss generation. These two effects act as competing effects and the sensitivity of mixed-out loss to these two flow effects must be assessed.

To quantify the overall effects from increasing tip flow angle and decreasing tip mass flow, tip leakage flow mixed-out loss is approximated with a model from Young and Wilcox [22]. The model uses a control volume method to compute irreversible entropy generation from mixing between tip leakage flow and the main flow. Tip leakage flow is treated as a small injected flow into the main flow in this model. Tip leakage mixed-out loss based on Young and Wilcox is computed from Equation 3.3.

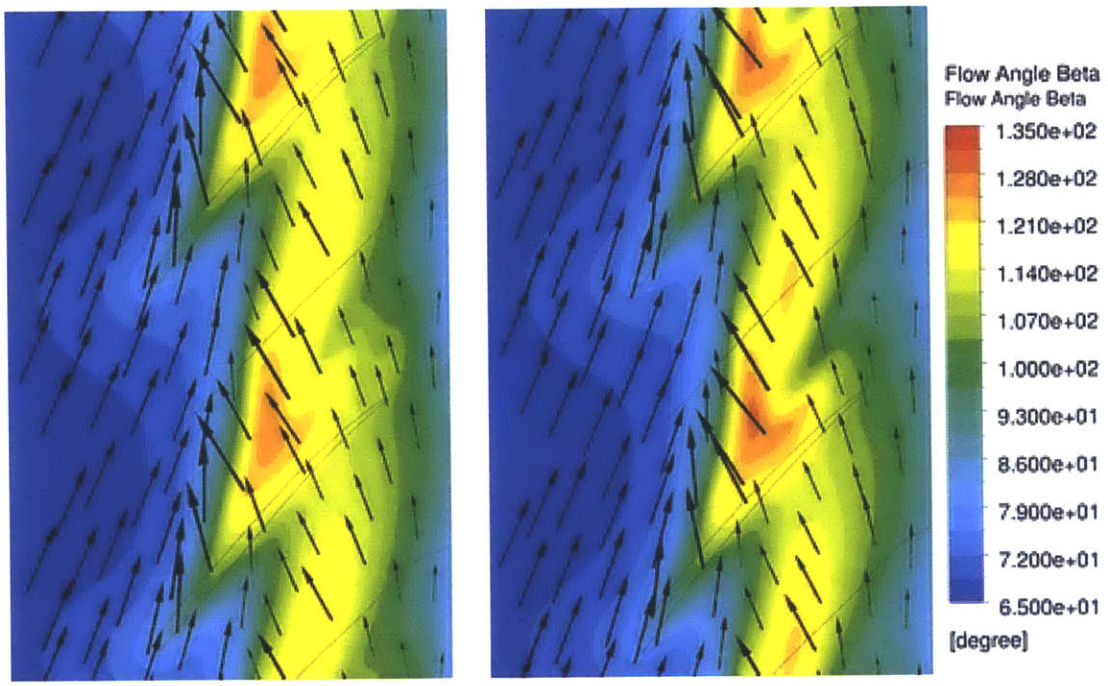

(a) Fore

(b) Original

(c) Lessaft

(d) Moreaft

Figure 3-13: Contours of flow angle and representative velocity vectors at the mid tip gap (97.5% span) indicating higher tip leakage flow angle in the aft-loaded blade designs at approximately 70% chord

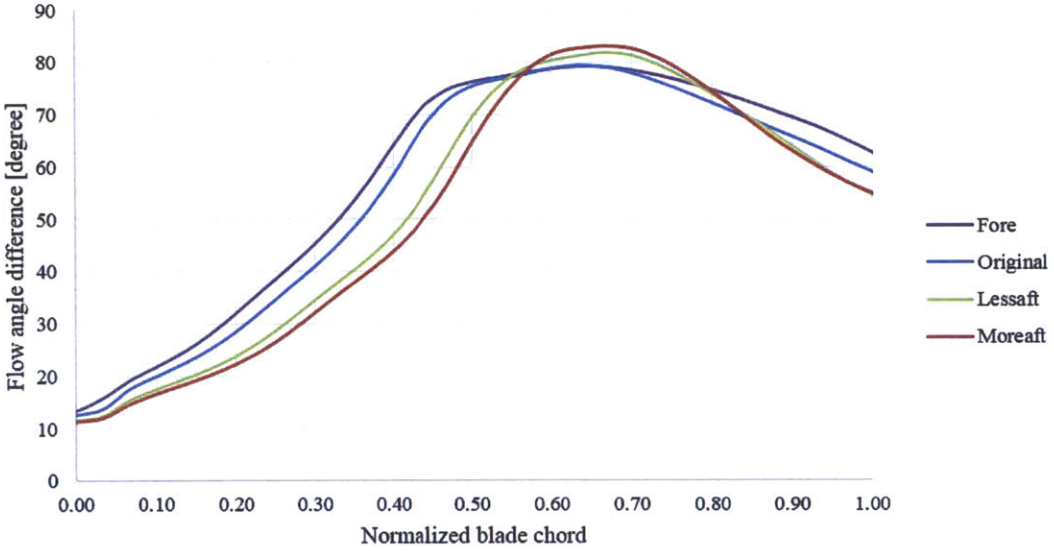

Figure 3-14: Flow angle mismatch between the main flow (at 80% span) and the tip flow (at mid tip gap)

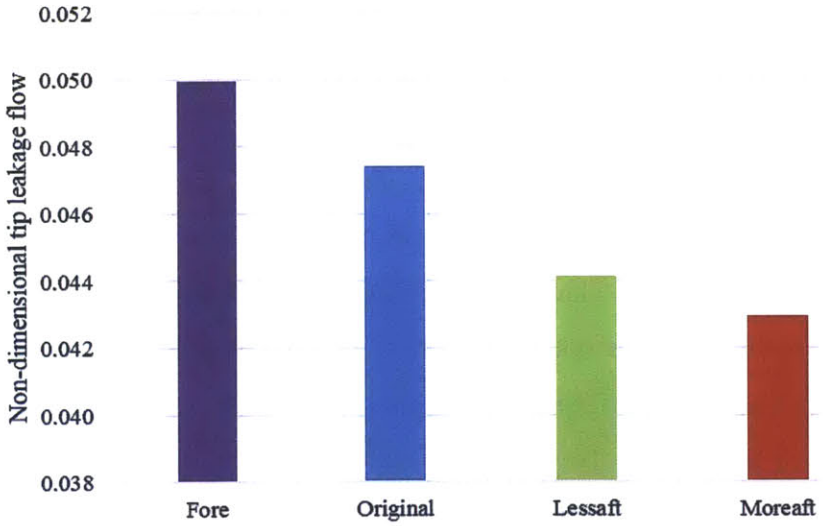

Figure 3-15: Changes in total tip leakage mass flow in the four rotor blade designs

$$Ts_{irr} = \frac{1}{\dot{m}_{main}} \left[\int \frac{(u_{blade\,ss} - u_{TLF}\cos\Delta\beta)^2 + u_{TLF}\sin\Delta\beta^2}{2} \right] (g\rho u_{TLF}\sin\Delta\beta dc_{blade}) \tag{3.3}$$

,where $\dot{m}_{main}$ denotes mass flow rate in the main blade passage, $u_{blade\,ss}$ the main flow velocity on the rotor blade SS, u_{TLF} the velocity of tip leakage flow driven through tip clerance, $\Delta\beta$ the flow angle mismatch between the main flow and the tip leakage flow, g the rotor tip clearance size, and c_{blade} the rotor tip chord.

A preliminary sensitivity assessment can be performed by varying tip leakage mass flow and the flow angle mismatch. Figure 3-16 shows a result from the preliminary assessment with velocity ratio of the tip leakage flow to the main flow of 0.8. For small changes in flow angle difference and tip leakage mass flow, it can be approximated that loss changes from 1% decrease in tip leakage mass flow is equivalent to that from 0.7 degree reduction in flow angle difference. This result implies a rather substantial impact of the flow angle difference in the tip leakage flow mixing process. The sensitivity computed with Young and Wilcox's model is found to be comparable with a result from Zlatinov in a situation where the axial turbine purge flow mixing loss is not generated from swirl velocity difference between the purge flow and the main flow [19].

The total mixed-out loss from tip leakage flow can be computed from Young and Wilcox's model by discretizing tip clearance into small chordwise sections followed by integrating the total loss along the tip chord. The input parameters for Young and Wilcox's model has been taken from the computed flow fields. Total tip leakage flow mixed-out loss is highest for the moreaft blade and lowest for the fore blade as shown in Figure 3-17a. The trend is identical with mixed-out loss computed from computational results at the rotor exit shown in Figure 3-17b. This suggests that the reduction in tip leakage mass flow has a smaller impact on loss generation than the increase in tip leakage flow angle, and the aft-loaded blades have higher loss mainly from the increase in the maximum tip flow angle.

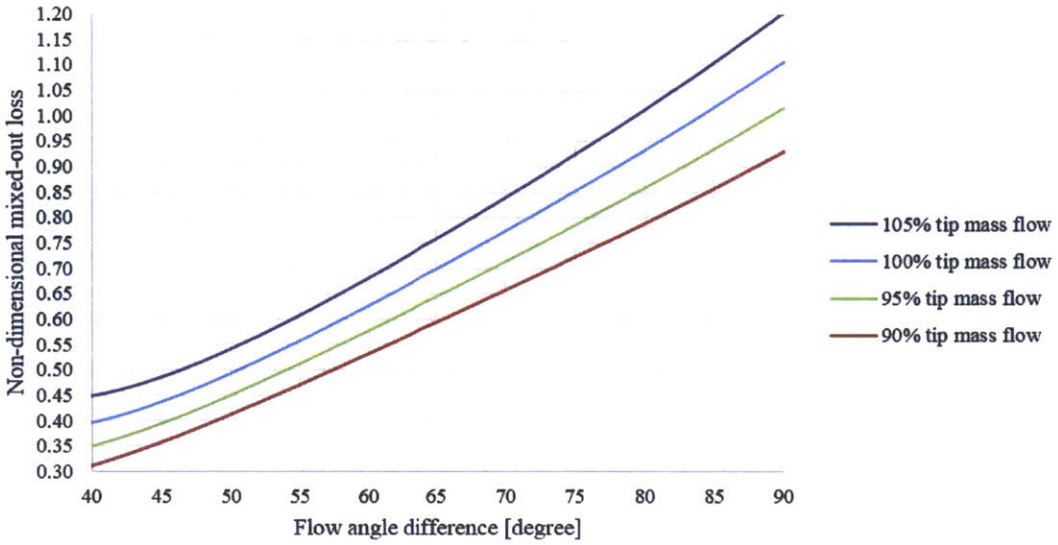

Figure 3-16: Sensitivity of Young and Wilcox's control volume model on injected mass flow and flow angle mismatch

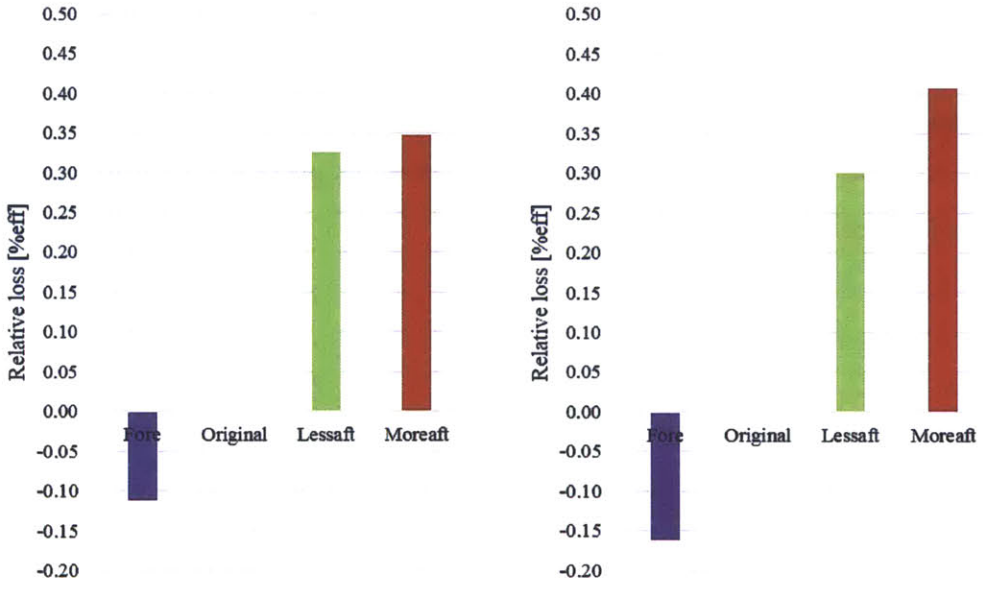

(a) Young and Wilcox's control volume method

(b) Computed results

Figure 3-17: Tip leakage flow mixed-out loss from the control volume method and computed results

In order to mitigate the additional mixing loss associated with tip flow angle mismatch with the main flow, we propose a design strategy such that tip leakage flow angle distribution of an aft-loaded blade has to be managed in a manner that its detrimental impact does not outweigh the benefit from the delay in tip leakage flow formation and the decrease in tip leakage mass flow. Assuming the variation of density and velocity on the rotor blade SS in a chordwise direction to be negligible, the mixed-out loss from tip leakage flow can be approximated as a function of tip leakage flow velocity, flow angle mismatch, and tip clearance size. Mixed-out loss from tip leakage flow can be rewritten as Equation 3.4 and the term $(f(u_{TLF}(x), \Delta\beta(x)))$ will be referred to as mixing function.

$$Ts_{irr} = C \cdot g \int f(u_{TLF}(x), \Delta\beta(x)) dc_{blade} \tag{3.4}$$

At constant tip clearance size, the additional mixed-out loss can be eliminated or minimized if tip leakage flow velocity distribution and tip flow angle mismatch distribution are shifted toward the TE with distance $\Delta x_{TLF\,delay}$ simultaneously while retaining their distribution profile as shown in Equation 3.5. This provides us a feasible method to aft-load a rotor blade tip without generating additional mixing loss from tip leakage flow.

$$Ts_{irr} = C \cdot g \int f(u_{TLF}(x - \Delta x_{TLF\,delay}), \Delta\beta(x - \Delta x_{TLF\,delay})) dc_{blade} \tag{3.5}$$

Maintaining the mixing function $(f(u_{TLF}(x), \Delta\beta(x)))$ in Equation 3.4 constant is feasible and can be shown from a situation where tip clearance size varies. With the constant mixing function in Equation 3.4 and 3.5, tip leakage flow mixed-out loss increases linearly with increasing tip clearance size. Additional computations have been performed to support this estimation. Figure 3-18 shows similarity of tip leakage flow velocity distribution for three tip clearance sizes ranging from 3.3% to 5% span. As tip clearance size increases, the velocity distribution retains its

profile and only shifts toward the TE. The change in flow angle mismatch distribution behaves in a similar manner to the tip leakage flow velocity distribution as shown in Figure 3-19. Based on the unaltered tip leakage flow velocity distribution and tip leakage flow angle mismatch distribution, Figure 3-20 shows that tip leakage flow mixed-out loss computed from computational results and Young and Wilcox's model increases linearly with increasing tip clearance size. This result confirms that the mixing function can be maintained constant and additional loss from tip leakage flow angle mismatch can be prevented if tip leakage flow angle distribution is shifted toward TE in a similar manner to tip leakage flow velocity distribution.

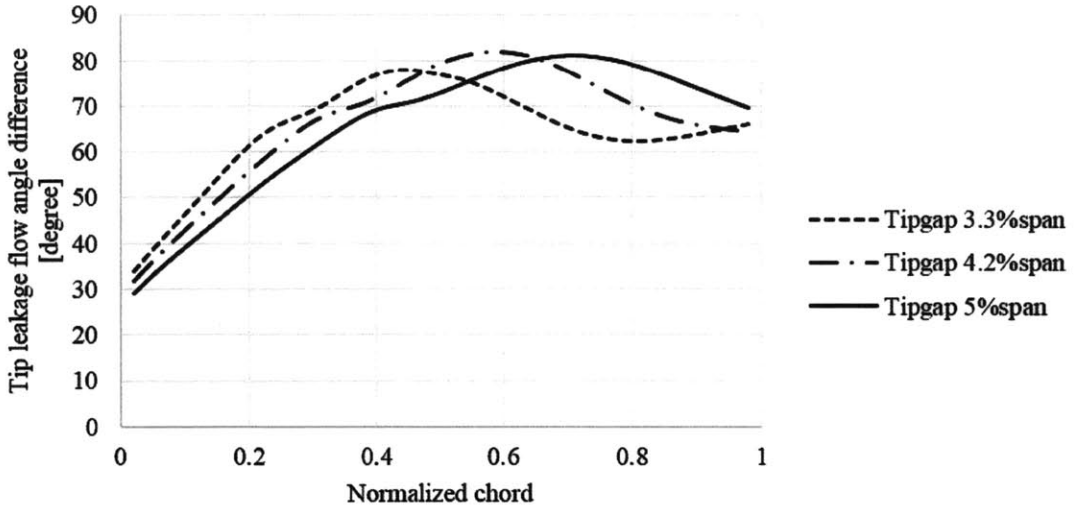

Figure 3-18: Similarity of chordwise distribution of tip leakage flow angle mismatch at three tip clearance sizes

In summary, computational results suggest that competing effect setting up the optimum rotor blade loading distribution is not flow separation but rather changes in tip and main flow angle mismatch and changes in tip leakage mass flow. The maximum flow angle difference between the main flow and the tip leakage flow in the lessaft and moreaft blade is found to be higher than that in the original blade while tip leakage mass flow decreases in the aft-loaded blades. These two effects are competing effects governing the changes in tip loss as the tip loading is being changed. Mixed-out loss associated with the two effects computed from Young and Wilcox's model indicates that loss from flow angle difference dominates loss from a reduction of tip

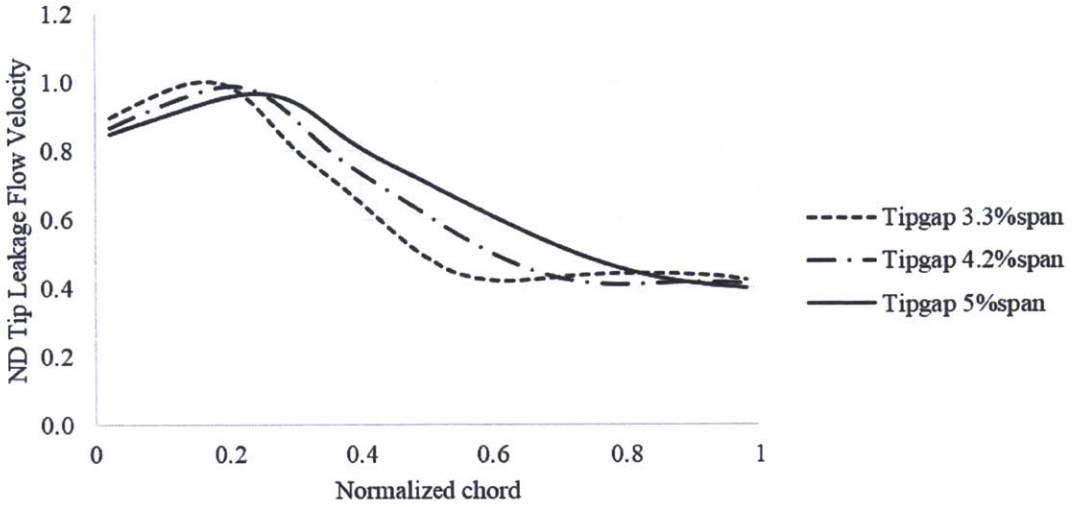

Figure 3-19: Similarity of chordwise distribution of tip leakage flow velocity at three tip clearance sizes

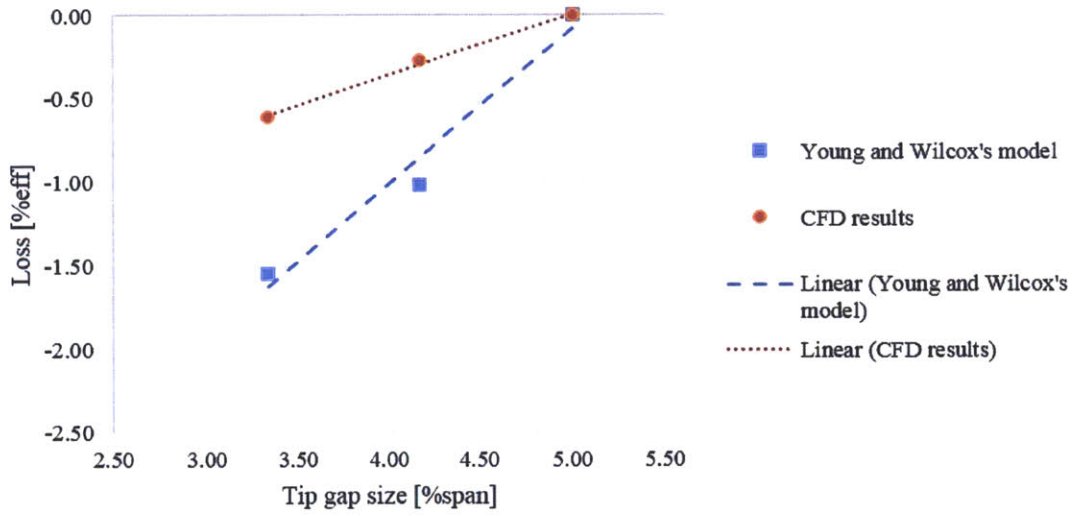

Figure 3-20: Linear mixed-out tip leakage flow loss at three tip clearance sizes

leakage mass flow, resulting in higher overall rotor tip loss. The loss estimated from the control volume analysis (Young and Wilcox's model) is also in agreement with that from computed flow fields. Loss from tip leakage flow angle difference appears to be manageable if tip leakage flow angle distribution and tip leakage flow velocity distribution are unaltered and shifted downstream in a similar manner. Therefore, the hypothesis needs to be modified to incorporate an additional constraint that tip flow angle distribution must be managed appropriately for an aft-loaded blade to yield an overall benefit.

3.4 Overall Effects of Tip Blade Loading Variation in a Rotor

Three key flow effects associated with variations in rotor tip loading, namely, less mixed-out tip leakage flow due to delay in tip leakage flow formation, changes in tip leakage mass flow, and changes in a distribution of tip leakage flow angle, play a role in setting loss generation within the rotor passage. Loss from tip leakage flow formation delay reduces as a rotor blade is more aft-loaded. Although tip leakage mass flow decreases for the aft-loaded blades, loss from tip flow angle mismatch (between tip flow and main flow) increases as a rotor blade is aft-loaded more aggressively. Thus, the change in loss (relative to a baseline design) from rotor tip loading changes can be written as Equation 3.6.

$$\begin{aligned} \mathcal{L}_{rotor} &= \xi_{rotor\ exit,fore/aft-loaded} - \xi_{rotor\ exit,original} \\ &= \mathcal{L}_{TLF\ delay} + \mathcal{L}_{TLF\ flow\ angle\ mismatch\ and\ mass\ flow} \end{aligned} \tag{3.6}$$

,where $\xi_{rotor\ exit,aft/fore}$ and $\xi_{rotor\ exit,original}$ denote loss at the rotor exit in an aft/fore-loaded rotor blade and the original rotor blade, respectively and $\mathcal{L}_{rotor}$ denotes relative total loss in the rotor with loss from the original blade as the reference. Loss in the rotor ($\mathcal{L}_{rotor}$) is also a summation of loss from tip leakage flow formation

delay process ($\mathcal{L}_{TLF\ delay}$) and loss from changes in tip leakage flow angle mismatch and changes in total tip leakage mass flow ($\mathcal{L}_{TLF\ flow\ angle\ mismatch\ and\ mass\ flow}$), which was called as $\mathcal{L}_{midchord}$ in Equation 3.2.

The trend in the change in the overall loss due to aft-loading rotor tip, shown in Figure 3-21, indicates that the benefit of tip leakage flow formation delay and a reduction in tip leakage mass flow is outweighed by loss from flow angle mismatch. The lessaft and moreaft blade have higher loss generation in the rotor while the fore blade has a similar loss generation to that of the original blade. As such, the results presented here contradict the hypothesis delineated in Chapter 1.

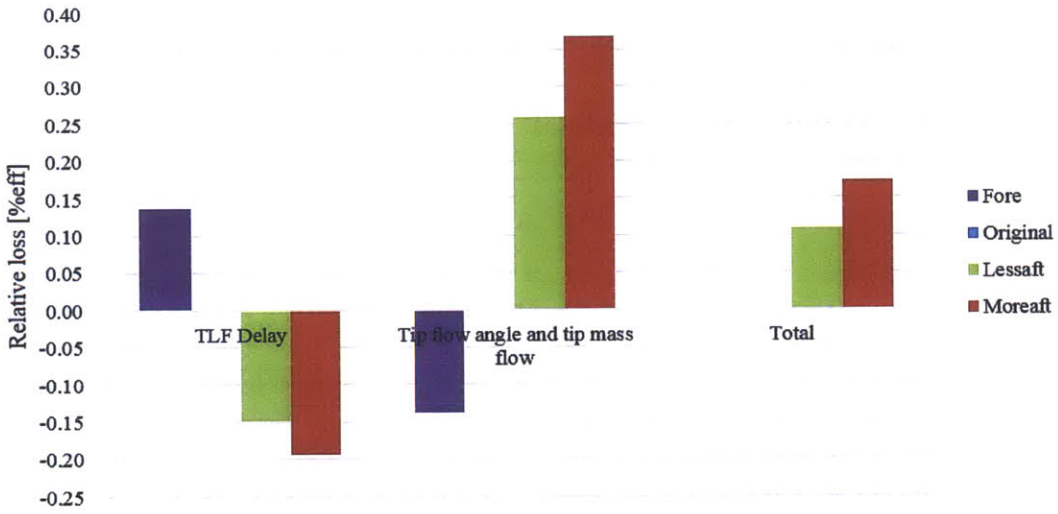

Figure 3-21: Overall computed loss in a rotor environment in steady flow fields

In view of the above analysis of the computational results, the originally stated hypothesis needs to be modified to include the effect of tip flow angle mismatch with the main flow. Thus, an additional constraint must be added into the original hypothesis and the hypothesis for performance improvement in a stage environment has to be revised as follows:

"Rotor tip and stator hub should be aft-loaded with tip/hub leakage flow angle distribution managed to retain its distribution but aft-shifted accordingly so that there is a net benefit while rotor hub and stator tip should be fore-loaded".

As previously noted, the flow field is likely to be overly diffusive from artificial

numerical dissipation so that the benefit of the tip leakage flow formation delay computed from the current computational results is considered to be a lower bound of the actual process. Furthermore, if loss from flow angle difference can be reduced by 50% of its original amount, the benefit from tip leakage flow formation delay would begin to yield a net overall benefit in the rotor. By appropriately managing the tip flow angle distribution, the overall loss reduction benefit in the rotor from the moreaft blade could potentially lead to an enhancement of 0.20% efficiency or higher.

3.5 Summary

Three additional rotor blade designs, one fore-loaded and two aft-loaded blade designs, provide an adequate range of tip loading variation for defining the optimum blade tip. The new rotor blades are modified from the original blade in such a way that the impact on the flow in the tip region is substantial but minimal in the main flow region; additionally, the rotor pressure ratio of the new rotor designs is managed to be similar to that of the original blade design. The fore, lessaft, and moreaft blade are confirmed to have the fore-loaded/aft-loaded characteristics. Three main flow processes, namely, delay in tip leakage flow formation, changes in tip leakage flow angle mismatch, and changes in tip leakage mass flow are found to govern the overall loss in the rotor passage.

Aft-loading a rotor blade also results in larger tip leakage flow angle mismatch with the main flow and lower tip leakage mass flow in the aft-loaded blades. Loss increase from flow angle difference outweighs the loss reduction from a decrease in tip leakage mass flow and delay in tip leakage flow formation, resulting in higher overall rotor tip loss for the aft-loaded blade designs. Thus, an additional constraint must be added into the original hypothesis and the hypothesis for performance improvement in a stage environment has to be revised as follows: "rotor tip and stator hub should be aft-loaded with tip/hub leakage flow angle distribution managed to retain its distribution but aft-shifted accordingly so that there is a net benefit while rotor hub and stator tip should be fore-loaded".

It has to be noted that the mixing process of tip leakage flow is incomplete and the choice of a turbulence model and the numeric could play a role on the details of the mixing process involving the tip flow and the main flow. Although the mesh resolution is high, this might not be adequate to represent the structure of tip leakage flow. Thus, an artificially higher mixing rate of tip leakage flow in a rotor could be introduced by the numerically diffusive flow, leading to lower estimated benefit of tip leakage flow formation delay.

Chapter 4

Characteristic of Unsteady Rotor-Stator Flow Field

Chapter 3 has assessed the effects of aft-loading a rotor blade tip on loss generation. The assessment has been performed with steady flow fields; however, the actual compressor flow field is unsteady and the unsteady flow mechanism described in Section 2.1 could play a role, leading to a change in the quantitative impact of aft-loading a rotor blade. The assessment in unsteady flow fields must be carried out based on a flow field that has reached an equilibrium state. The unsteady flow and performance also needs to be collected and averaged over a proper time period. In order to meet these requirements, the behavior of unsteady flow fields will be interrogated in depth in this chapter. Specifically, the role of tip flow inherent unsteadiness [6] with a timescale distinct from that of blade passing would have on: (i) tip leakage flow interacting with the downstream stator [10]; and (ii) the periodicity of rotor-stator unsteady flow fields.

4.1 Frequency of the Inherent Unsteadiness in Tip Leakage Flow

As noted in Chapter 2, tip leakage flow is inherently unsteady. Bae et al. conducted an experiment in a compressor rotor cascade to identify a natural frequency mode in tip leakage flow core [6]. Their experiment suggested that the time scale associated with tip leakage flow scales with the through flow time in a rotor passage. The reduced frequency of tip leakage flow computed from Equation 4.1 was estimated to be approximately 0.75.

$$F_c^+ = \frac{fc}{u_\infty} \tag{4.1}$$

, where F^+ denotes reduced frequency, f the tip leakage flow frequency, c the rotor blade chord, and u_∞ the upstream flow velocity.

To identify the frequency of tip leakage flow in the current unsteady computational flow fields, numerical probes are installed at 95% span in the core of tip leakage flow. Unsteadiness in tip leakage flow inducing variations of pressure in the tip leakage flow core is monitored to identify the frequency of unsteady tip leakage flow. Pressure variations observed from the probes in time domain are converted into frequency domain using Fast-Fourier Transform (FFT).

Frequency of tip leakage flow is found to exist at 0.45 blade passing frequency (BPF) without any changes from 25% chord to 125% chord as shown in Figure 4-1. The constant value of frequency in tip leakage flow unsteadiness is somewhat similar to the computational results found by Zhang et al. [9]. Reduced frequency of tip leakage flow in the current experiment is 0.55, which is of the order of that shown in Figure 4-2, ranging from 0.6 to 0.8. Additionally, there have been other works [4,8,23] that indicate the existence of tip leakage vortex unsteadiness at a reduced frequency in accord with the present result shown in Figure 4-2.

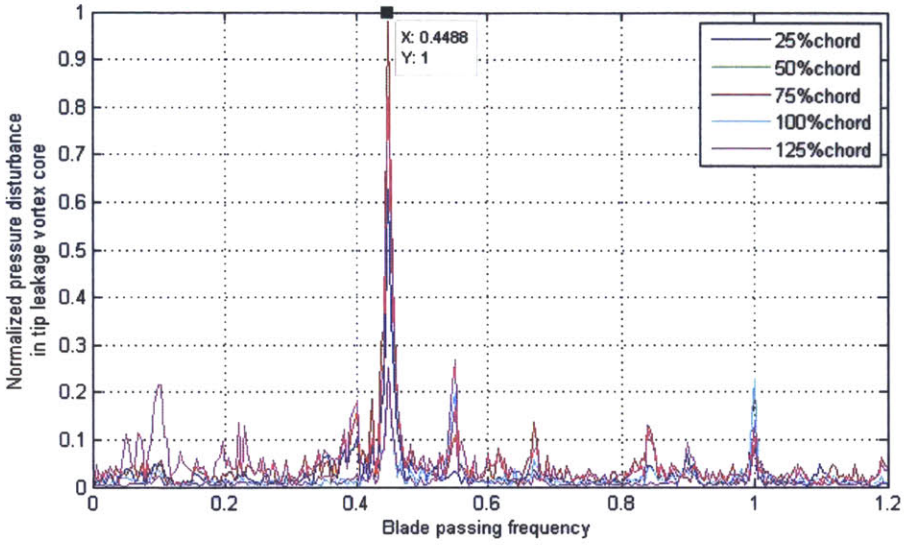

Figure 4-1: Pressure variation in tip leakage flow core in frequency domain obtained from current numerical simulations

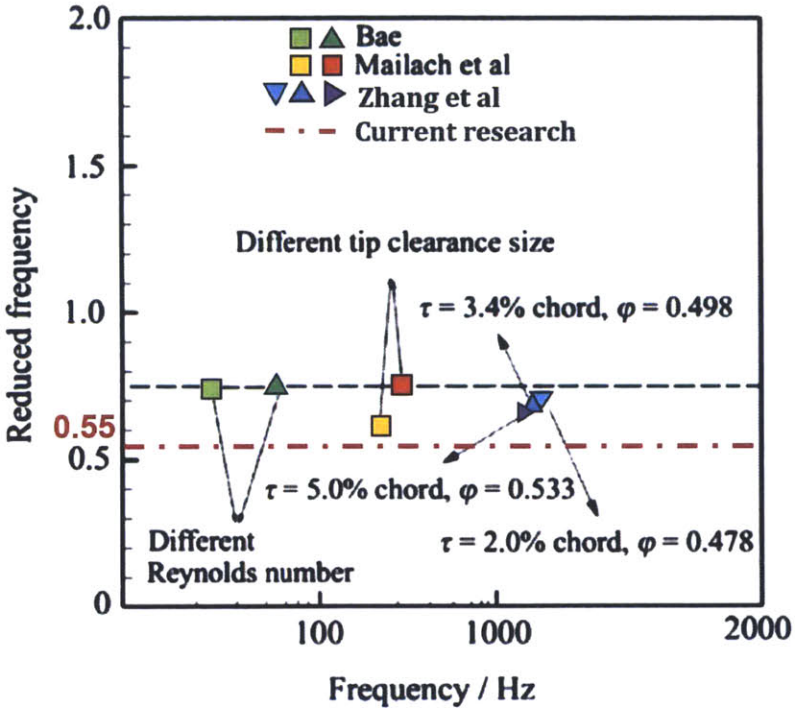

Figure 4-2: Reduced frequency of tip leakage flow compared with previous research (adapted from [4])

4.2 Tip Leakage Flow Phasing Effect and Periodicity of Unsteady Rotor-stator Flow Fields

Tip leakage flow in a rotor-stator environment is governed by two timescales: one associated with its own unsteadiness described in Section 4.1 and the other with the rotor-stator interaction. The additional timescale from blade passing affects the formation of tip leakage flow and its trajectory (pathline) in a rotor-stator environment. Figure 4-3 shows two possible trajectories of tip leakage flow. It is noted that the trajectories of tip leakage flow is shown with respect to the local frame of reference in the rotor and the stator. In Figure 4-3, tip leakage flow forms on the SS of a rotor blade and moves downstream toward the stator. As the period of tip leakage flow is 2.2 times of blade passing period, the relative position between the rotor and the stator is different for each cycle of tip leakage flow. This causes the trajectory of tip leakage vortex in the stator frame of reference to be different for each cycle of tip leakage flow (i.e., tip leakage flow phasing) as shown in Figure 4-4 for four different cycles. It can be seen that tip leakage flow can enter the stator at various locations, for example, on the stator PS, on the stator SS, in the middle of the stator passage, and at the LE. The effects of tip leakage flow recovery quantified by Valkov were assessed without the tip leakage flow phasing effect. Therefore, the effects of tip leakage flow phasing on the tip leakage recovery process need to be assessed.

A similar flow effect has been observed by Nolan et al. [24] in a transonic axial compressor. They observed wake phasing between an upstream inlet guide vane and a downstream rotor. Furthermore, the location at which wake enters a downstream rotor can be determined from the ratio of total wake convection time (including time scale for vortex shedding) to rotor passing time. This phase-locked location can be shown to be a function of blade spacing, rotor blade pitch flow coefficient, and shock wave interface angle. The key difference in behavior between tip leakage flow phasing and wake phasing is the interaction between two blade rows. In wake

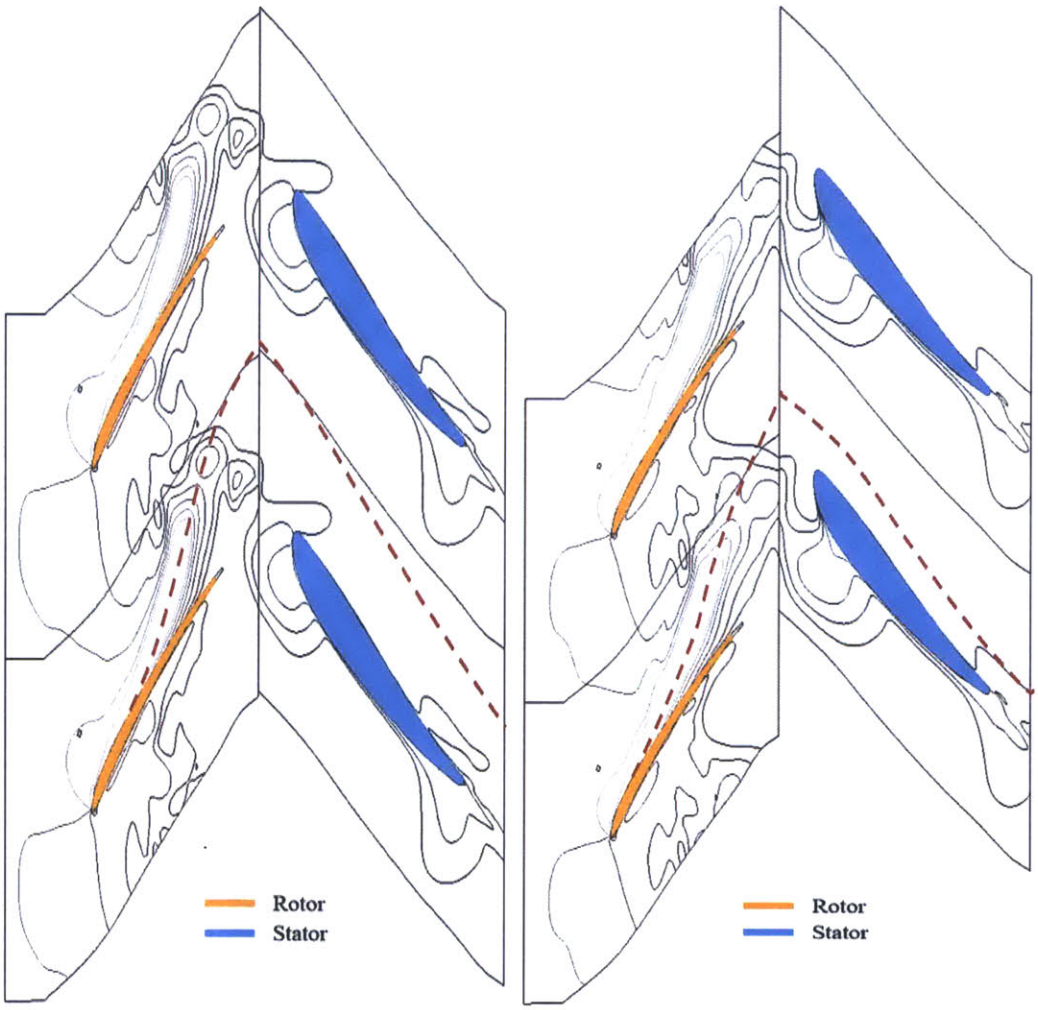

(a) t_0 (b) t_0 + 1 tip leakage flow period

Figure 4-3: Variation of tip leakage flow trajectory (red dashed line) displayed on a pressure contour in rotor and stator due to discrepancy of tip leakage flow and blade passing period)

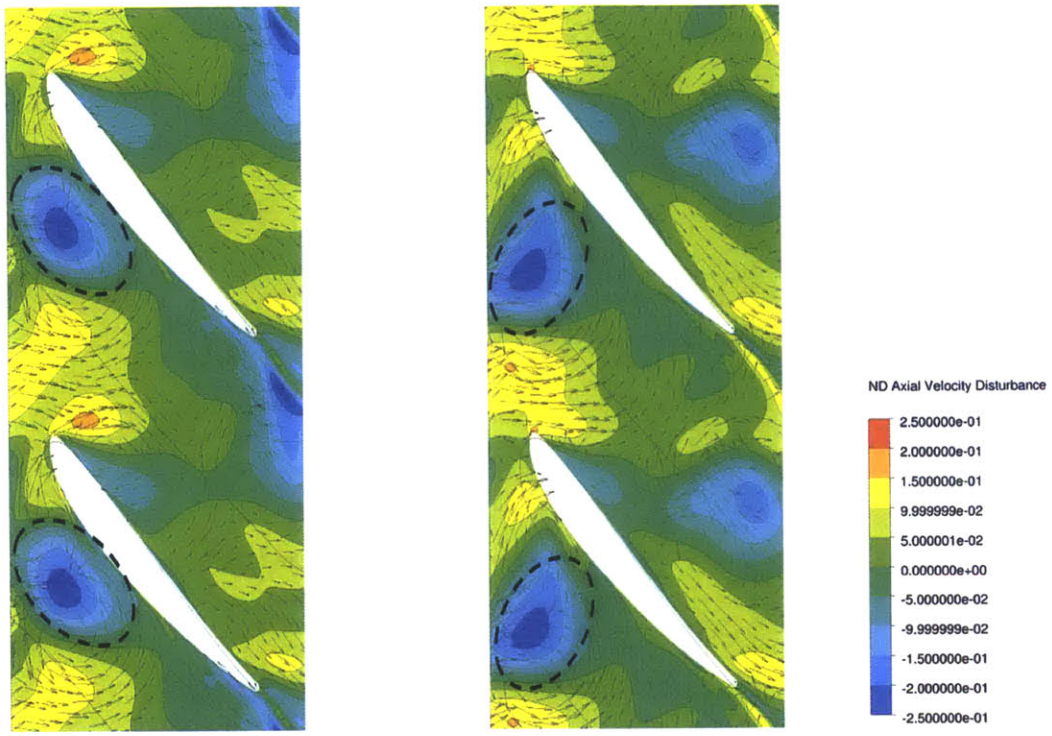

(a) near the stator blade SS

(b) at the middle of the stator passage

(c) near the stator blade PS

(d) at the stator blade LE

Figure 4-4: Possible locations at which tip leakage vortex (blue region in the dashed circle) enters a downstream stator from tip leakage flow phasing effect

phasing, vortex shedding in the wake is induced by the shock wave interaction from a downstream rotor and a reference location can be defined for the analysis in this situation. On the other hand, the formation of tip leakage flow is self-induced rather than forced-induced; a similar approach to obtain a phase-locked behavior cannot be used. However, there is a possibility to alter the tip leakage flow phasing effect to have a phase-locked behavior. This possibility will be revisited at the end of this chapter.

Not only does the rotor-stator interaction have an impact on the trajectory of tip leakage flow in the stator, it also has upstream effects on the formation of tip leakage flow in a rotor. Hwang et al. conducted a numerical experiment and showed that the structure of tip leakage flow was identical for all blade passage when the computational domain was that of an isolated rotor [10]. In other words, tip leakage flow would have identical flow structure at corresponding instants of each cycle of variation in tip vortex unsteadiness when the rotor-stator interaction is not present. However, for a compressor stage with a downstream stator blade row, their numerical results showed that structure of tip leakage flow was different in the adjacent blade passages for a compressor with a rotor and a stator. The current results show a similar finding to that of Hwang et al. as shown in Figure 4-5. The structure of tip leakage flow taken from four distinct cycles of tip leakage flow is different. This reflects the upstream influence from the rotor-stator interaction on the formation/development of tip leakage flow in a rotor.

From the above, one would expect the unsteady computed flow field to not have a time periodicity corresponding to the blade passing time due to an additional time scale associated with the tip vortex inherent unsteadiness. The time periodicity is needed to determine the time-average metrics and flow characteristics from the computed unsteady solution. Periodicity of unsteady flow field is governed by different time scales of various sources of flow unsteadiness in the flow field as well as the varying degree of spatial extent of their influence. The periodicity of flow field in the midspan will be determined first, followed by that in the tip region. In the midspan region, the only source of unsteadiness is from the rotor wake, which forms at the

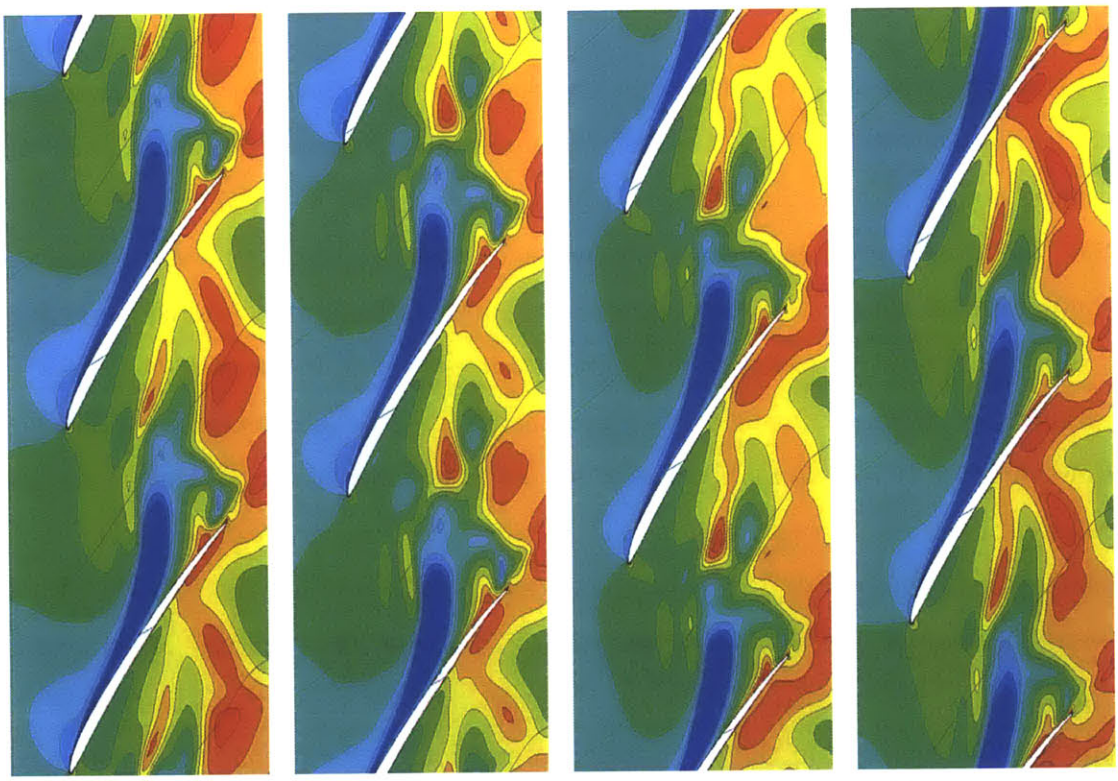

(a) t_0

(b) t_0 + 1 tip leakage flow cycle

(c) t_0 + 2 tip leakage flow cycle

(d) t_0 + 3 tip leakage flow cycle

Figure 4-5: Variations of structure of tip leakage flow (visualized from instantaneous stagnation pressure) affected by upstream effects of the rotor-stator interaction

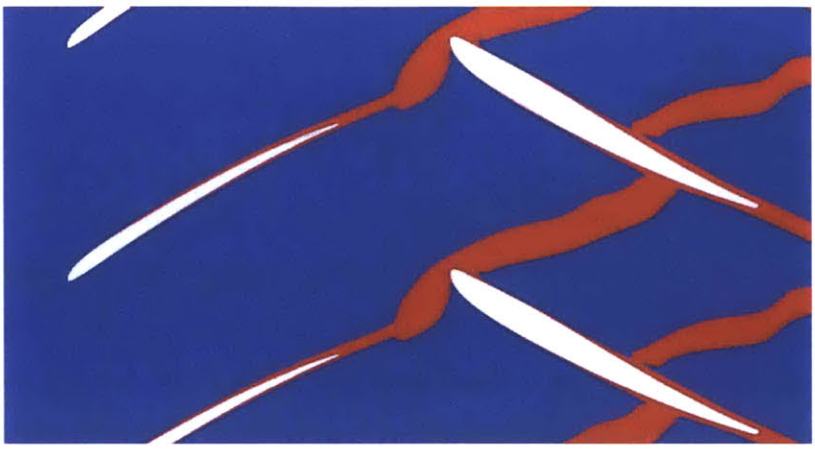

(a) t_0

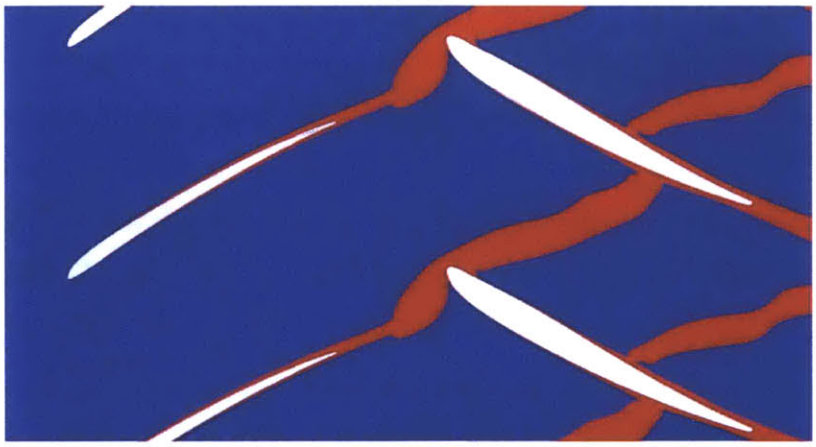

(b) t_0 + 1 blade passing period

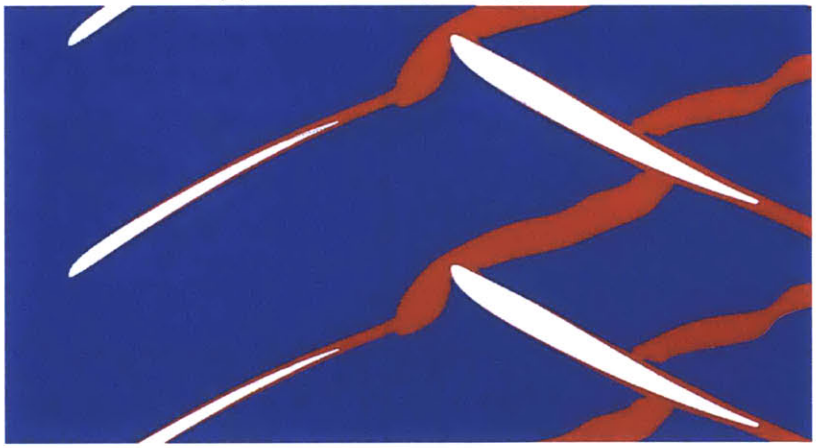

(c) t_0 + 2 blade passing period

Figure 4-6: Similar structure of rotor wake (red region) exhibiting periodicity of flow field in the midspan region

rotor TE and enters the stator. The influence from tip leakage flow can be considered negligible in the midspan region. Therefore, timescale that controls the periodicity is from the rotor-stator interaction only and the periodicity of the flow field is found every 1 blade passing period. Figure 4-6 shows similar flow fields in the midspan region from three instantaneous results with 1 blade passing period apart.

Flow field in the tip region is more complicated as there are several sources of unsteadiness. Flow separation at blade tip SS could be one source of unsteadiness in the tip region besides the tip leakage flow and the rotor-stator interaction. Flow separation bubble size is found to vary with time and the frequency of the flow separation bubble is determined as shown in Figure 4-7. In Figure 4-7, there are four main frequency modes; two frequency modes at 1 BPF and 0.45 BPF are the rotor-stator interaction and tip leakage flow unsteadiness, respectively, as previously delineated. The frequency mode at 0.55 BPF is induced by the interaction between the rotor-stator interaction and tip leakage flow unsteadiness as the frequency is at 0.55 BPF (1 BPF-0.45 BPF). Therefore, frequency of flow separation bubble can be identified to exist at 0.90 BPF. Probes installed in the tip region away from the trailing edge do not pick up the characteristic frequency of flow separation. Therefore, the effects of flow separation is locally confined near the blade tip TE and does not affect the flow field in the tip region.

From the above we may thus infer that the two main sources of unsteadiness in the tip region consist of one due to tip leakage flow unsteadiness and the other due to the rotor-stator interaction. The global periodicity of the flow field can be found from the total time period that the cycles of the two interactions require to begin and to complete at the same time. In other words, at the end of the global periodicity cycle, the relative rotor-stator position has to return to its original position and tip leakage flow has to form in the same manner as that at the beginning of the global cycle.

This periodicity timescale can be generally computed from Equation 4.2 :

$$t_{periodicity} = (t_{period} \cdot n_{cycle})_{tip\ leakage\ flow} = (t_{period} \cdot n_{cycle})_{blade\ passing} \qquad (4.2)$$

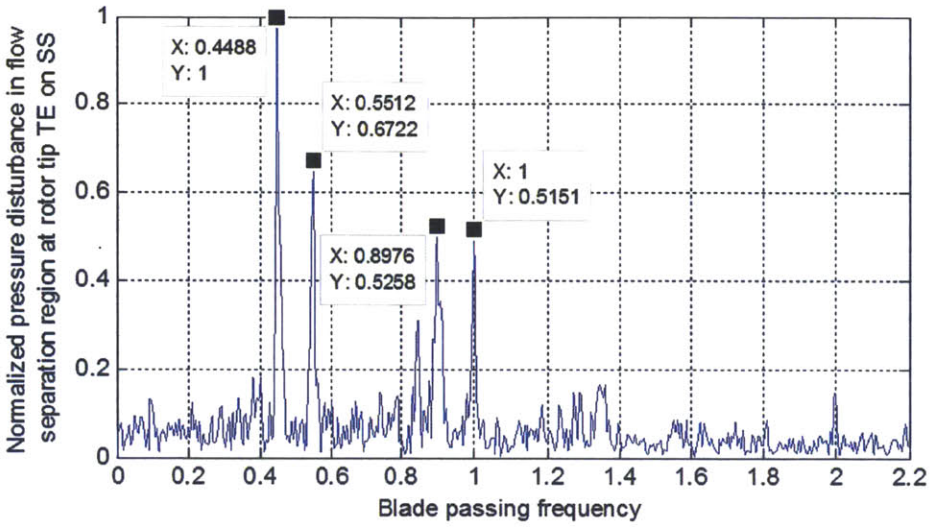

Figure 4-7: Frequency of flow separation bubble detected at the rotor blade tip

,where t_{period} and n_{cycle} denotes the period and the number of cycle of the each flow process. The global periodicity of the unsteady flow flow ($t_{periodicty}$) is found when the number of cycle of the two interactions are integer to reflect a full cycle of the interactions. The periodicity of the flow field is found to be 11 blade passing periods for tip leakage flow unsteadiness with a characteristic time of 2.2 blade passing periods as shown in Equation 4.3.

$$t_{periodicity} = (2.2\, t_{blade\,passing} \cdot 5)_{tip\,leakage\,flow} = (1\, t_{blade\,passing} \cdot 11)_{blade\,passing} \qquad (4.3)$$

Flow fields in the tip region representing similar structure of tip leakage flow from 11 blade passing periods apart shown in Figure 4-8 confirms the determined periodicity. Furthermore, temporal variation in corrected mass flow and stage pressure ratio over 110 blade passing periods is plotted every 11 blade passing periods in Figure 4-9 to reflect this determined periodicity of the flow field. Therefore, the current unsteady flow fields can be demonstrated to have attained an equilibrium and time-averaging of the unsteady flow fields needs to be performed over a time period that is a multiple of 11 blade passing periods.

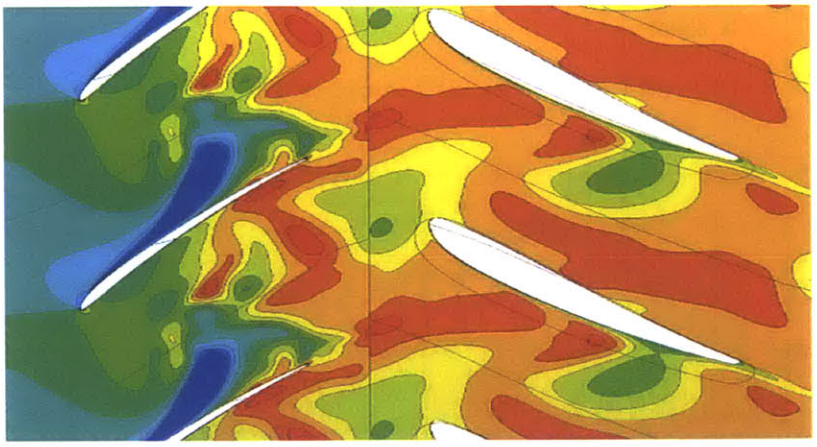

(a) t_0

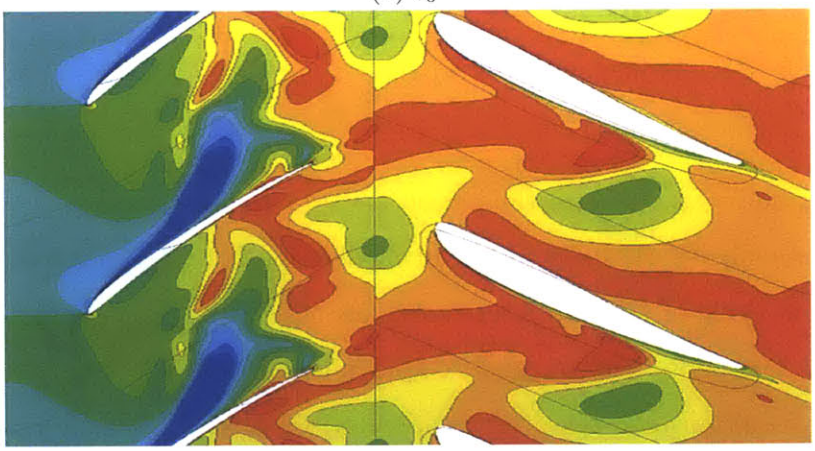

(b) t_0 + 11 blade passing periods

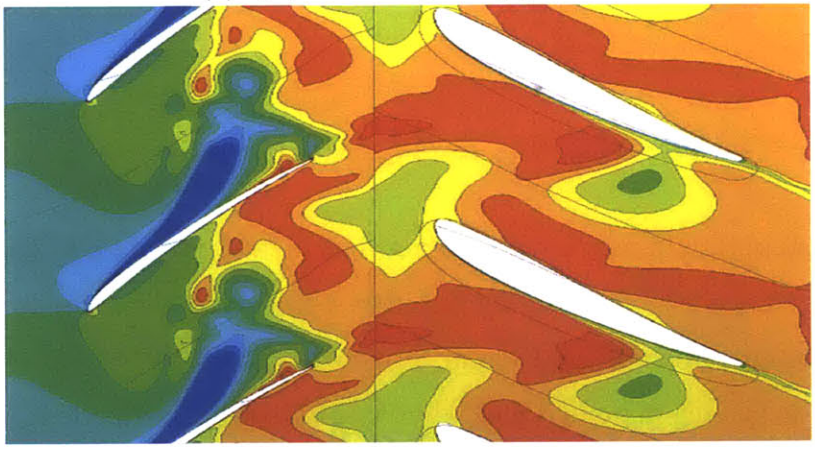

(c) t_0 + 22 blade passing periods

Figure 4-8: Similar structure of tip leakage flow (visualized from instantaneous stagnation pressure) exhibiting periodicity of flow field in the tip region

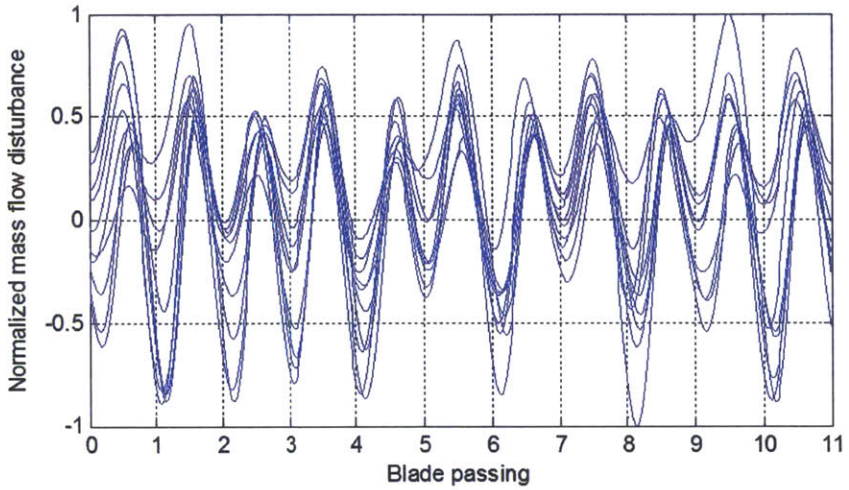

(a) Corrected mass flow disturbance

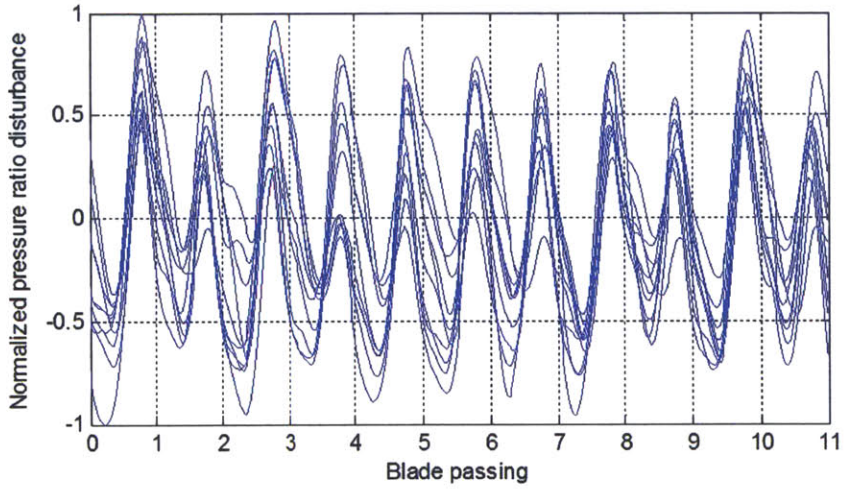

(b) Stage pressure ratio disturbance

Figure 4-9: Periodicity behavior of the global unsteady flow field observed from corrected mass flow and pressure ratio over 110 blade passing periods (10 global periods)

Equation 4.2 also sheds some light on a possible strategy to obtain a phase-locked behavior for tip leakage flow. To attain the phase-locked behavior, we expect the formation of tip leakage flow to be identical every cycle; thus, tip leakage flow moves into the stator at the same location for every cycle. This could be done by altering the blade passing period in Equation 4.2 to be identical as the period of tip leakage flow. To attain the phase-locked behavior in the current flow field, the new blade passing period needs to be 2.2 times of the original value, which allows the tip leakage flow cycle and blade passing cycle to complete at the same time. The blade passing period could be increased by changing the rotor-stator blade ratio to be 2.2 (i.e. the rotor blade takes longer time to complete its cycle). The advantage of the phase-locked behavior of tip leakage flow is that tip leakage flow recovery process will occur in a similar manner for every tip leakage flow cycle; therefore, if we can arrange tip leakage flow in such a way that it enters the downstream at the proper location, the process will always be effective, leading to its higher effectiveness on a time-averaged basis. However, the phase-locked behavior will also create a resonance in the tip leakage flow, which could introduce detrimental aeromechnaical issues. As such, this strategy to obtain the phase-locked behavior may yield operability issues that outweigh the benefits.

4.3 Summary

The behavior of unsteady flow fields is interrogated to ensure that investigated computed unsteady flow fields have reached an equilibrium state and time-averaged can be properly evaluated. Frequency of tip leakage flow is found to exist at 0.45 blade passing frequency. As the period of tip leakage flow is 2.2 times of blade passing period, the relative position between the rotor and the stator is different for each cycle of tip leakage flow. This causes tip leakage flow to enter the stator at various locations for each cycle of tip leakage flow (i.e., tip leakage flow phasing).

We propose that the global periodicity of the flow field, especially in the tip region, can be found from the total time period that the cycles of the two interactions (e.g. tip

leakage flow and blade passage) require to begin and to complete at the same time. The periodicity of the flow field is found to be 11 blade passing periods based on tip leakage flow unsteadiness with a characteristic time of 2.2 blade passing periods. Therefore, the current unsteady flow fields can be demonstrated to have attain an equilibrium and time-averaging of the unsteady flow fields needs to be performed over a time period that is a multiple of 11 blade passing periods. The impact of tip leakage flow phasing effect on tip leakage flow recovery process will be addressed in the next chapter.

Chapter 5

Unsteady Tip Leakage Recovery Process

The unsteady tip leakage flow recovery process, described in Chapter 1, is an essential component of the design hypothesis as it reduces the opportunity for the less-mixed tip leakage flow to generate loss in the downstream stator. However, in light of the tip leakage flow phasing effect presented in Chapter 4, the tip recovery process in the stator will be re-assessed here for its impact on potential benefit.

5.1 Mechanisms of Unsteady Tip Leakage Flow Recovery Process

The mechanism of wake recovery will be first delineated as a background for the tip leakage flow recovery. Smith first proposed a model for explaining wake recovery [5]. The core of wake has low velocity and can be represented as a region of velocity deficit. In unsteady flow fields, velocity disturbance is defined to be the difference between the instantaneous velocity and the time-averaged velocity. Thus, the velocity deficit in the wake core can be represented as a region of negative velocity disturbance. In a stator, the rotor wake core acts as a negative jet toward the PS of a stator blade

with the largest velocity deficit at the center of the core. The motion of rotor wake is depicted in Figure 5-1. Due to higher velocity on the SS of a stator blade and lower velocity on the PS, a contour of wake fluid is stretched as the wake fluid moves downstream. The length and width of the fluid contour at the stator exit increases and decreases, respectively. For an inviscid incompressible flow in a two-dimensional flow, Kelvin's theorem requires that circulation of any fluid contour remains constant in time. A fluid contour can be drawn around the edge and the core of the rotor wake to explain the velocity disturbance change according to the theorem. Velocity disturbance at the edge of rotor wake is zero and the circulation of the wake is from the velocity disturbance in the core. As the length of the wake increases at a downstream location, the velocity disturbance in the wake core has to decrease to preserve the circulation on the fluid contour line. Therefore, a stretching of rotor wake through a stator blade row attenuates the velocity disturbances in the wake and thus reducing the potential loss generation in the wake.

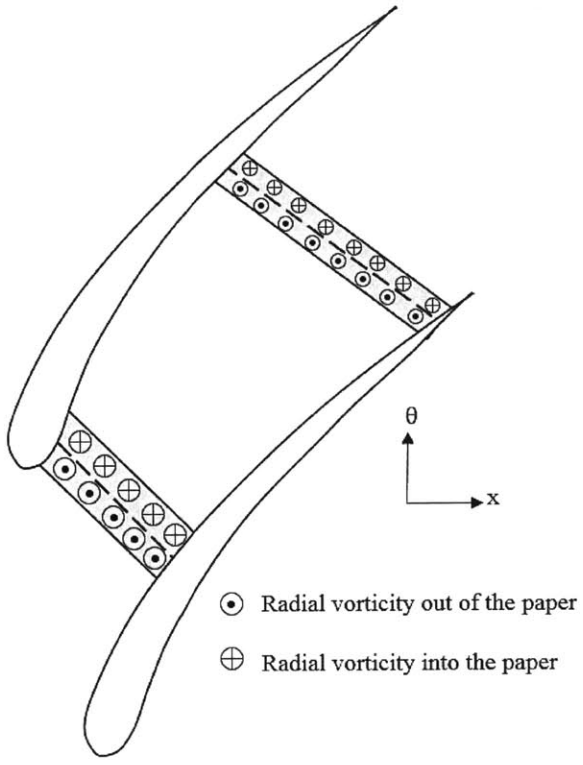

Figure 5-1: Progression of structure and velocity disturbance of rotor wake in a stator [5]

Van Zante et al. utilized the concept proposed by Smith and developed a model for quantifying the inviscid and viscous effects during the wake recovery process [11]. Their experiment indicated that wake recovery process is primarily governed by an inviscid behavior (wake stretching) and viscous mixing is of secondary importance. Their model also showed good agreement with the experimental results. Additionally, Navier-Stokes computations were performed to assess the experimental data and the model. The computational results supported the findings from the model and the experimental data. Suggestions for stage designs of compressors from the results are reduction of axial spacing between blade rows to reduce viscous mixing loss before rotor wake enters a downstream blade row and fore-loading a stator to attenuate the rotor wake as soon as possible to mitigate viscous dissipation of wake.

The effects of the unsteady tip leakage flow attenuation process in a representative stator passage downstream of a rotor were assessed by Valkov (Valkov, 1997). In a stator frame of reference, the core of rotor tip leakage flow has axial velocity disturbance directed toward the PS of the stator blade, which is analogous to that of rotor wake. However, the velocity deficit in the tip leakage flow core has a three-dimensional structure that is somewhat different from the two-dimensional wake flow situation. In other words, not only tip leakage flow has axial velocity deficit, it also has tangential velocity disturbance in the core as shown in Figure 5-2. This excess tangential velocity also acts as a jet toward the PS of a stator blade. The axial velocity disturbance can be attenuated through tip leakage flow stretching in a similar manner as the wake stretching through a stator passage. As such, the opportunity for the tip leakage flow to realize its potential loss through viscous mixing is reduced by the process.

The attenuation of the excess tangential velocity disturbance can be explained through the attenuation of the related streamwise vorticity in tip leakage flow. As excess tangential velocity is largest in the core of tip leakage flow, this velocity profile introduces two layers of streamwise vorticity pointing in the upstream and downstream direction. In a stator, flow decelerates and experiences a static pressure rise, similar to flow in a diffuser. A fluid contour is shortened and widened as shown in Fig-

ure 5-3 as tip leakage flow convects downstream in a stator. Therefore, streamwise vorticity in tip leakage flow decreases as area of the tip leakage flow fluid contour increases according to Kelvin's theorem. Excess tangential velocity disturbance is attenuated as streamwise vorticity decreases. In summary, in an inviscid flow, the attenuation of axial and tangential velocity disturbance is governed by the reversible recovery process; hence, no entropy is generated during the process.

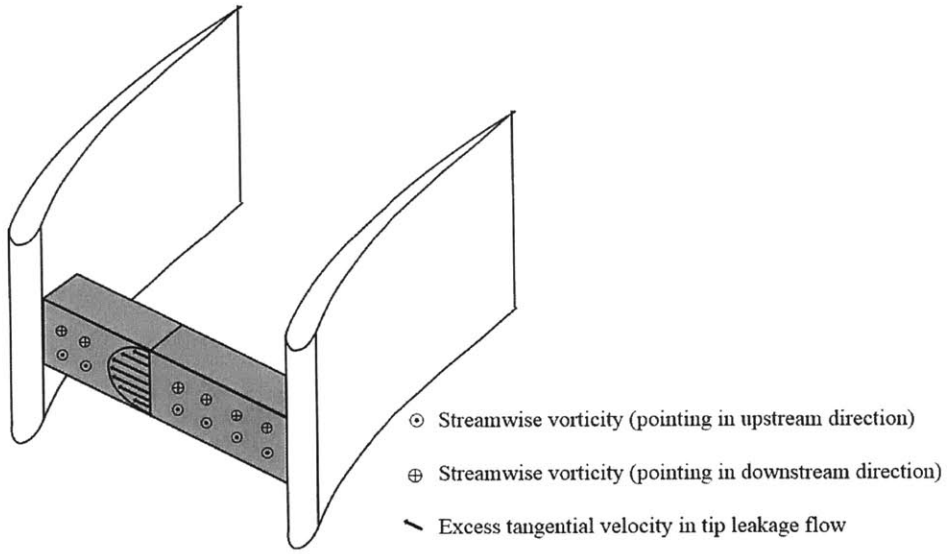

Figure 5-2: Distribution of excess tangential velocity disturbance and two layers of streamwise vorticity in tip leakage flow

For ease of reference, the benefit of the recovery process is described again. Computational experiments in an isolated stator was used by Valkov to assess the benefit of the process. The inlet boundary condition of the stator was based on the computational results of Khalid [13] for an isolated rotor with a tip clearance of 2.5% span. Valkov found that the tip leakage recovery process yields an efficiency gain of 0.1% compared to a situation where tip leakage flow is mixed-out at the stator inlet. Furthermore, he performed a sensitivity study to investigate the situation that tip leakage flow is less mixed-out through reducing an axial rotor-stator gap by 30% chord; the recovery process for the relatively less mixed-out tip leakage flow results in an additional efficiency benefit of 0.1% to yield a net 0.20% efficiency gain. It is noted that the performance benefit of tip leakage recovery process has been demonstrated assuming a time-averaged representation of the rotor tip leakage flow.

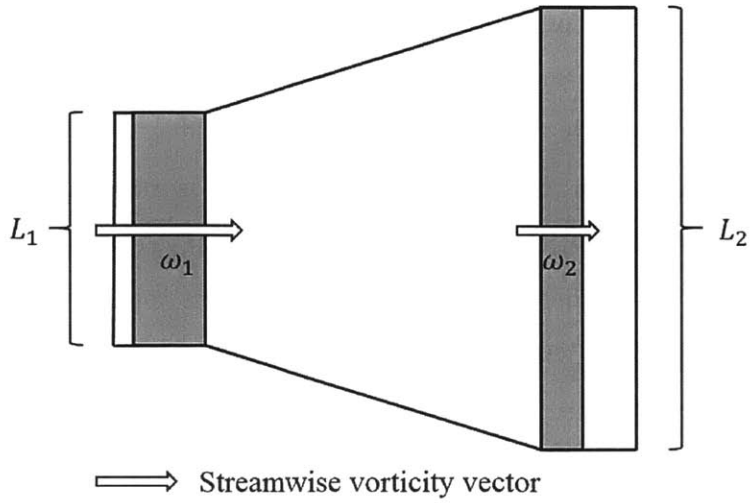

Figure 5-3: Stretching of tip leakage flow and attenuation of streamwise vorticity in a diffuser

5.2 Qualitative Effects of Unsteady Tip Leakage Flow Recovery Process

As noted above, Valkov neglected the inherent unsteadiness in the tip leakage flow; this is equivalent to utilizing the inlet boundary condition of a stator from a steady-state flow field of an isolated rotor with tip leakage flow. However, the results of Chapter 4 show that the tip leakage flow is locally unsteady characterized with a time scale different from the blade passing time. As such, the location at which tip leakage flow enters the stator differs in each tip leakage flow cycle. This flow effect is referred to as tip leakage flow phasing and has been described in Chapter 4; thus, the attenuation process could be different for each tip leakage flow cycle. The impact of tip leakage phasing on tip leakage flow recovery process in the downstream will be assessed next.

We first present a situation where tip leakage enters a stator passage in the middle of the passage. In this situation, the behavior of tip leakage flow during the attenuation process is similar to that found in Valkov's work. Tip leakage flow entering a stator is stretched due to the velocity difference on the PS and the SS in

the stator passage as shown in Figure 5-4. Velocity disturbance in Figure 5-4 is computed from the difference between velocity from instantaneous unsteady flow fields and time-average of unsteady flow fields. As tip leakage flow is stretched in the passage, velocity disturbance in the core of tip leakage flow is attenuated, resulting in a reduction in potential loss of tip leakage flow to mix out. Additionally, tip leakage flow entering stator at the middle of the passage migrates toward the PS of a stator blade from the effect of the jet-like velocity disturbance pointing toward the PS of a stator blade.

The evolution of streamwise vorticity in tip leakage flow is shown in Figure 5-5. The tip leakage vortex is visualized as contour of disturbance streamwise vorticity on axial planes at approximately 0, 20, 40, 60, 80, and 100% stator chord at various time instants corresponding to the same tip leakage vortex. Disturbance streamwise vorticity is computed from the difference between vorticity from instantaneous and time-averaged unsteady flow fields and projected in the time-averaged streamwise direction. In Figure 5-5, two layers of streamwise vorticity pointing in the upstream and downstream direction are observed and the disturbance streamwise vorticity decreases as tip leakage moves further downstream. This is the effect from tip leakage vortex stretching as seen in Figure 5-4. Therefore, the reduction of disturbance streamwise vorticity results in an attenuation of the non-uniformity in the tip leakage flow core.

The next case to be discussed is when tip leakage flow enters the stator in the proximity of stator blade PS with the tip leakage flow core located at approximated 0.2 stator pitch from the PS. Figure 5-6 shows the trajectory of tip leakage flow in the stator passage and the direction of velocity disturbance. Tip leakage flow is stretched and the velocity disturbance is attenuated from the stretching effect of tip leakage flow. The evolution of streamwise vorticity is seen to decrease as tip leakage flow moves downstream as shown in Figure 5-7. An additional flow effect seen in this case is when tip leakage flow reaches the PS of the stator blade, it moves radially inward to the main flow region as shown in Figure 5-7f. In summary, both axial velocity deficit and streamwise vorticity in the core of tip leakage flow are recovered when tip leakage flow enters the stator in the proximity of the stator blade PS.

Lastly, we present the tip leakage flow recovery in a situation where the tip leakage flow enters the stator passage in the proximity of stator blade SS with the tip leakage flow core located at approximate 0.2 stator pitch from the stator blade SS. In this situation, the behavior of tip leakage flow in the stator passage is different due to the direction of velocity disturbance. Figure 5-8 shows that the direction of the velocity disturbance is in the upstream direction. This is contrary to the direction of the velocity disturbance in the previous two situations where it directs toward the PS of the stator blade. The magnitude of the axial velocity disturbance in this situation does not diminish as tip leakage flow evolves in the stator passage; this observation can be explained from Kelvin's theorem shown in Figure 5-9. In the previous two cases, in which axial velocity disturbance is attenuated, the direction of the stretching axis and velocity disturbance is parallel. Thus, when a fluid contour is stretched, velocity disturbance must decrease to maintain the circulation of the fluid contour. However, in the current situation, the direction of the stretching axis and the velocity disturbance is perpendicular. Thus, when a fluid contour is stretched in its main axis, the width of the fluid contour decreases, causing the velocity disturbance to be amplified. The direction of velocity disturbance changes when tip leakage flow accelerates over the LE of the stator blade as shown in Figure 5-10; large velocity gradient near LE in the passage causes tip leakage flow to turn and change its direction. This effect is a new finding and is a result of the tip leakage flow phasing effect. However, the attenuation of streamwise vorticity still occurs in a similar manner to the previous cases.

5.3 Time-averaged Quantitative Benefit of Unsteady Tip Leakage Flow Recovery Process

In general, tip leakage flow recovery process has been qualitatively demonstrated to be capable of attenuating non-uniformity of tip leakage flow (axial velocity and

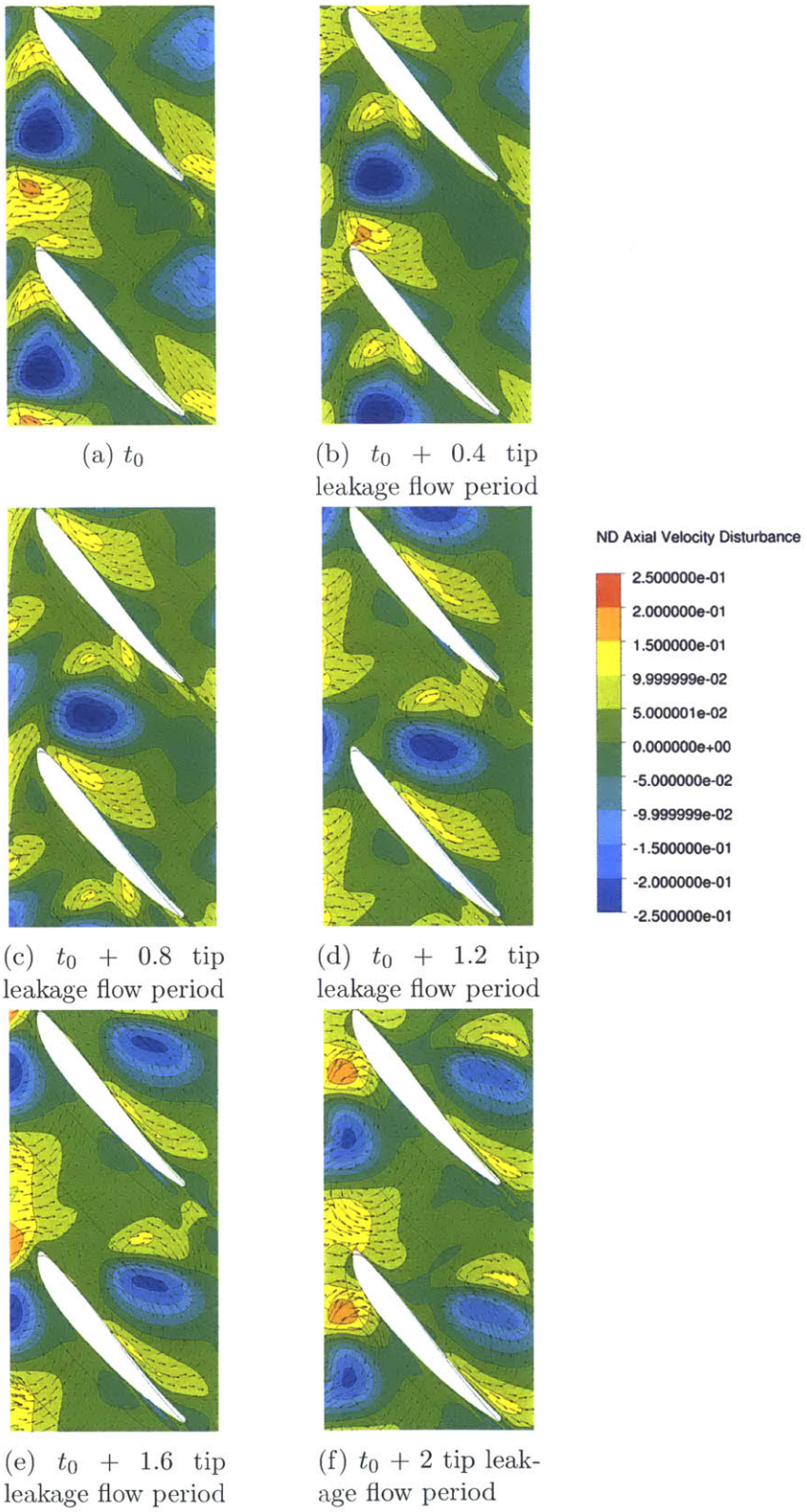

(a) t_0

(b) t_0 + 0.4 tip leakage flow period

(c) t_0 + 0.8 tip leakage flow period

(d) t_0 + 1.2 tip leakage flow period

(e) t_0 + 1.6 tip leakage flow period

(f) t_0 + 2 tip leakage flow period

Figure 5-4: Recovery of axial velocity disturbance when tip leakage flow (blue region) enters a stator at the middle of the stator passage

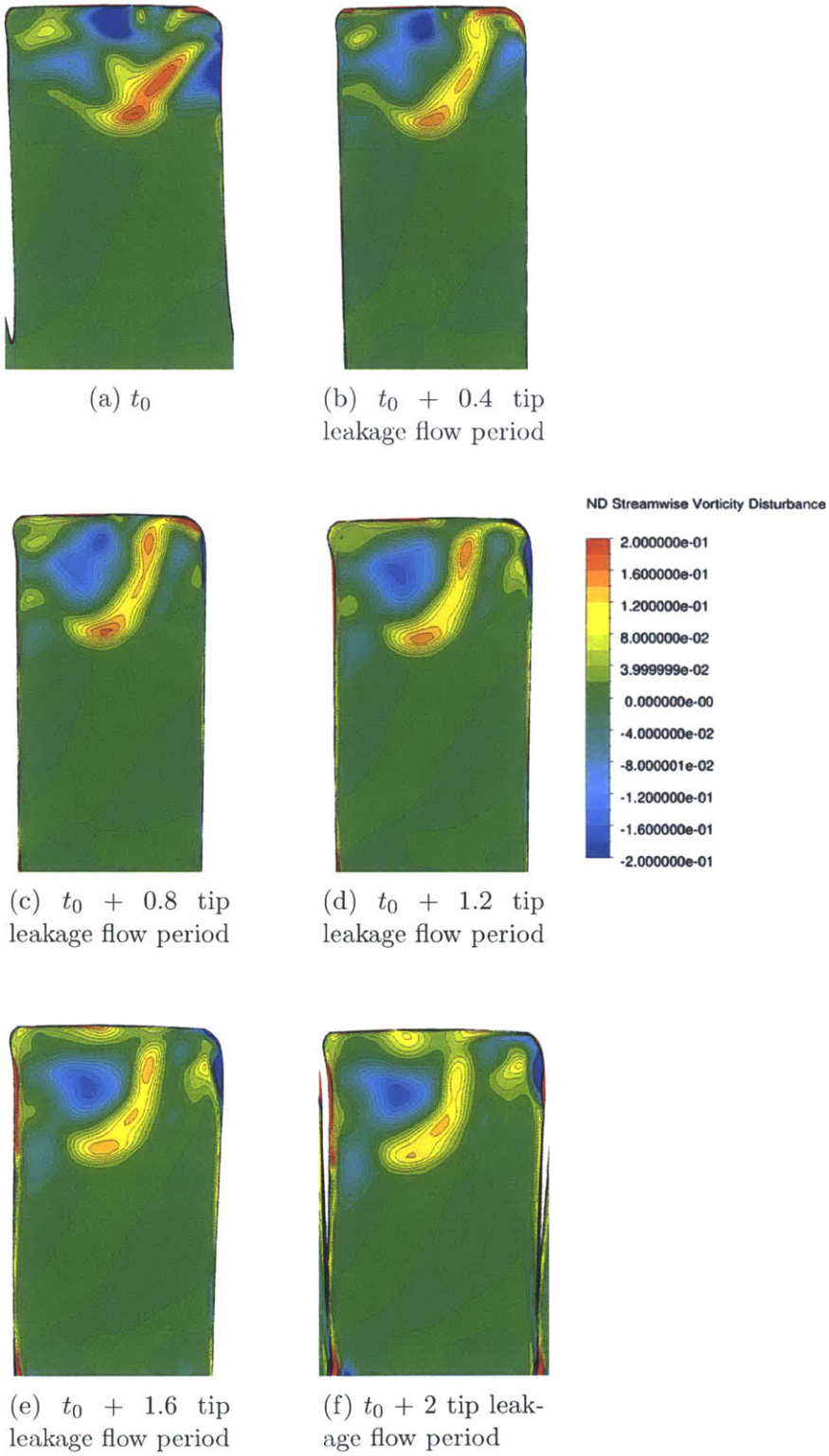

(a) t_0

(b) t_0 + 0.4 tip leakage flow period

(c) t_0 + 0.8 tip leakage flow period

(d) t_0 + 1.2 tip leakage flow period

(e) t_0 + 1.6 tip leakage flow period

(f) t_0 + 2 tip leakage flow period

Figure 5-5: Recovery of streamwise vorticity disturbance when tip leakage flow (red and blue region) enters a stator at the middle of the stator passage

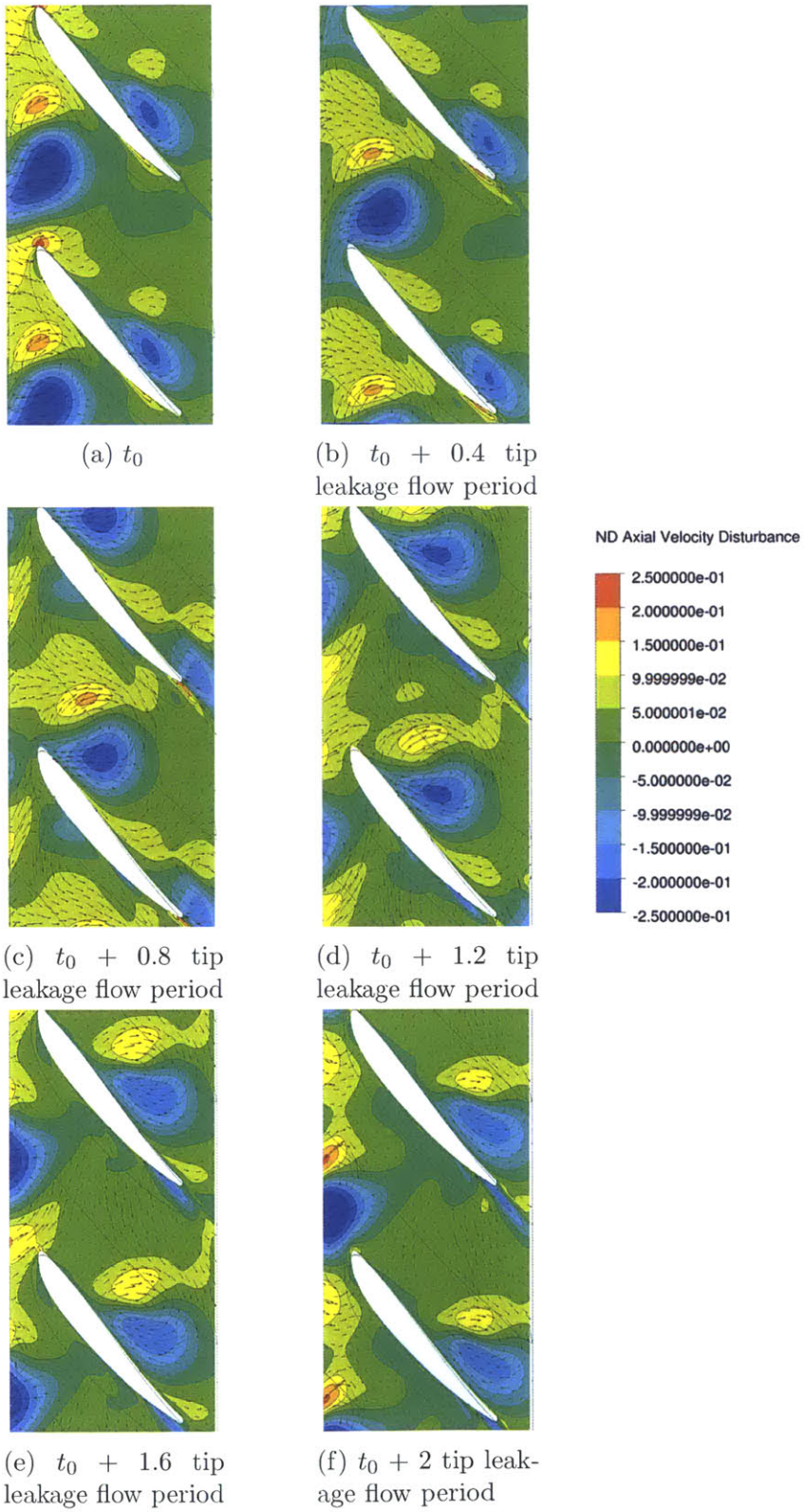

(a) t_0

(b) t_0 + 0.4 tip leakage flow period

(c) t_0 + 0.8 tip leakage flow period

(d) t_0 + 1.2 tip leakage flow period

(e) t_0 + 1.6 tip leakage flow period

(f) t_0 + 2 tip leakage flow period

Figure 5-6: Recovery of axial velocity disturbance when tip leakage (blue region) flow enters the stator in the proximity of the stator blade PS

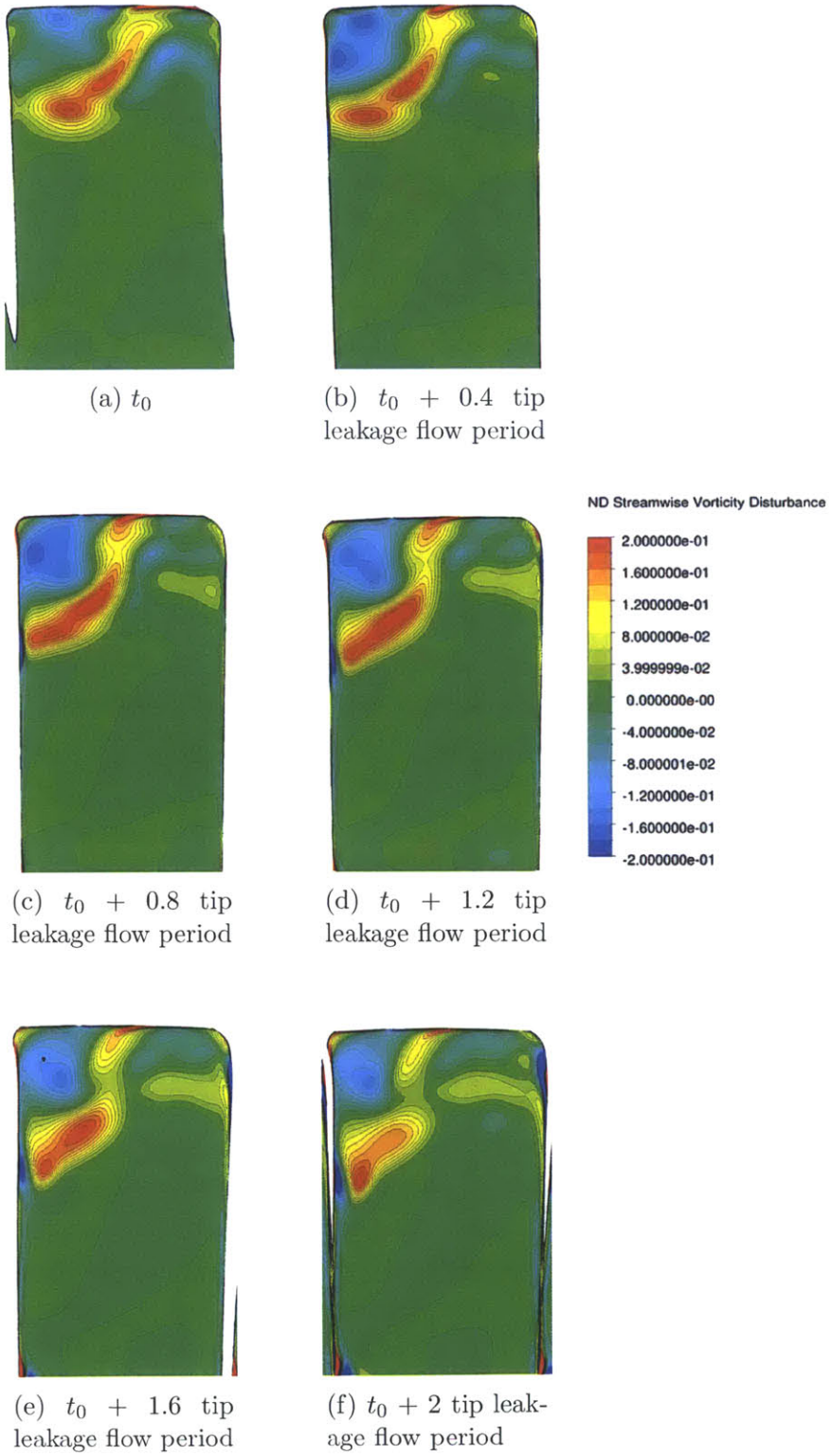

(a) t_0

(b) t_0 + 0.4 tip leakage flow period

(c) t_0 + 0.8 tip leakage flow period

(d) t_0 + 1.2 tip leakage flow period

(e) t_0 + 1.6 tip leakage flow period

(f) t_0 + 2 tip leakage flow period

Figure 5-7: Recovery of streamwise vorticity disturbance when tip leakage flow (red and blue region) enters the stator in the proximity of the stator blade PS

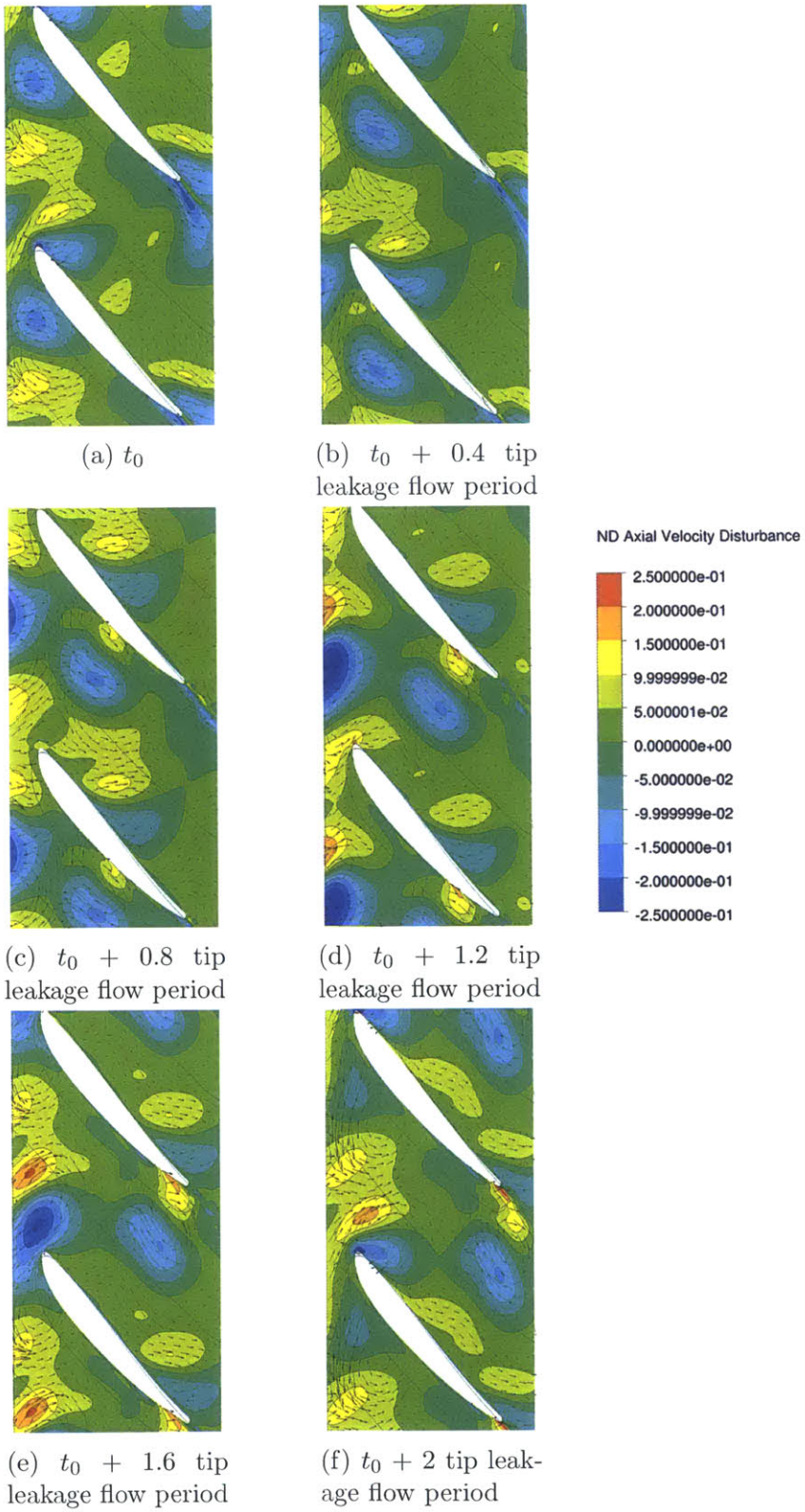

(a) t_0

(b) t_0 + 0.4 tip leakage flow period

(c) t_0 + 0.8 tip leakage flow period

(d) t_0 + 1.2 tip leakage flow period

(e) t_0 + 1.6 tip leakage flow period

(f) t_0 + 2 tip leakage flow period

Figure 5-8: Recovery of axial velocity disturbance when tip leakage flow (blue region) enters the stator in the proximity of the stator blade SS

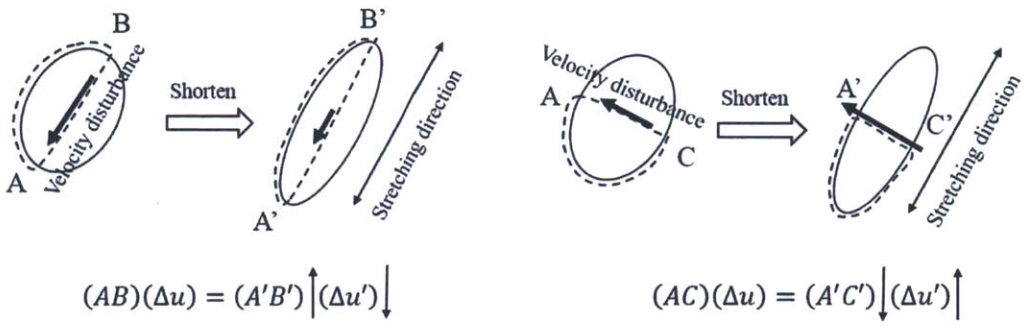

(a) Effective attenuation

(b) Ineffective attenuation

Figure 5-9: Ineffectiveness of tip leakage recovery process due to lack of alignment in direction of velocity disturbance and of stretching of fluid contour

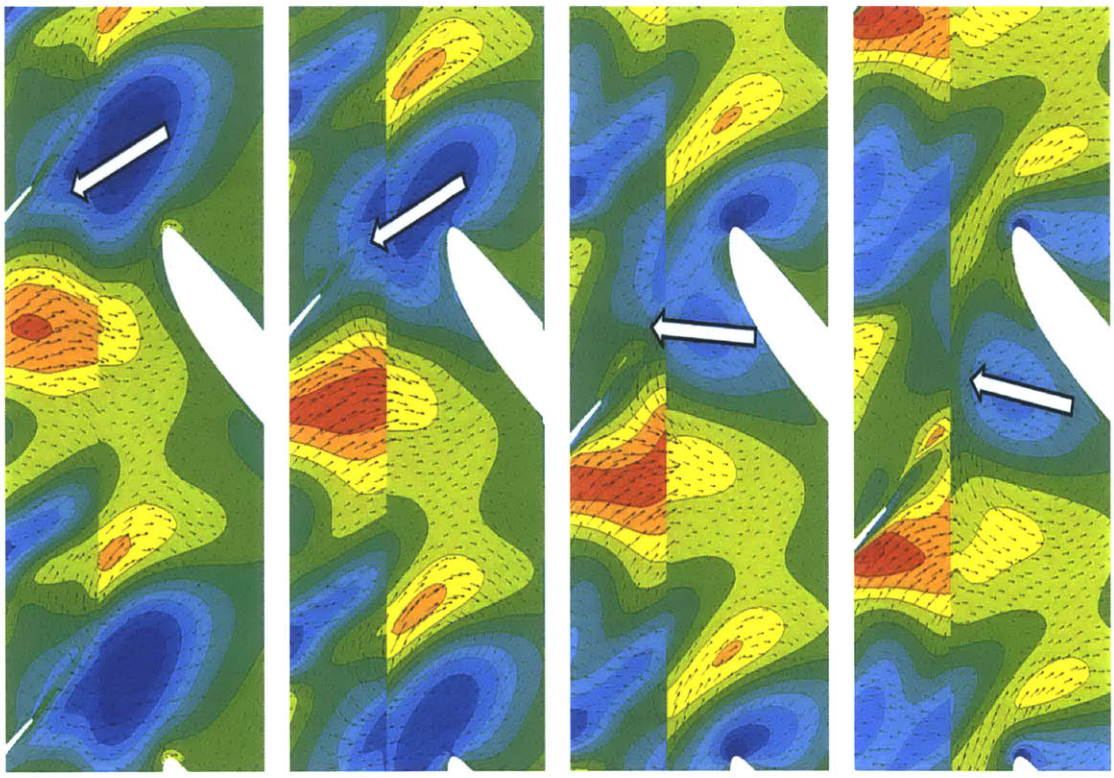

(a) t_0

(b) t_0 + 0.2 tip leakage flow period

(c) t_0 + 0.4 tip leakage flow period

(d) t_0 + 0.6 tip leakage flow period

Figure 5-10: Change in the direction of velocity disturbance in tip leakage flow at the stator LE on the SS

streamwise vorticity disturbance), despite the presence of tip leakage flow phasing effect. Thus, the quantitative benefit of the process need to be assessed on a time-averaged basis. To evaluate the benefit of the recovery process, we compare the recovery effect from two situations. The baseline situation corresponds to the absence of tip leakage flow recovery, such as, that in steady flow fields computed using a mixing-plane approximation. The mixing-plane located in the intra rotor-stator axial gap eliminates non-uniformity in the circumferential direction of the flow passing from the rotor to the stator. Thus, tip leakage flow is circumferentially mixed-out with no recovery opportunity. The second situation is found in unsteady flow fields computed using a sliding plane located in the intra rotor-stator axial gap. The sliding plane allows time-accurate interactions of flow field between the rotor and the stator. Thus, tip leakage flow is not mixed-out and can be recovered in the stator as described in Section 5.2.

Although the tip leakage flow recovery process can attenuate the non-uniformity in the tip leakage flow, some non-uniformity still exists in tip leakage flow at the stator exit. Therefore, we need to account for this remaining potential loss in tip leakage flow at the stator exit. The potential loss will be computed with the method delineated in Chapter 3 and loss generation in the stator can be calculated from Equation 5.1.

$$\mathcal{L}_{stator} = [(\xi_{stator\ exit} - \xi_{rotor\ exit}) + \xi_{stator\ exit,potential}]_{aft/fore} - [(\xi_{stator\ exit} - \xi_{rotor\ exit}) + \xi_{stator\ exit,potential}]_{original} \quad (5.1)$$

To evaluate the benefit of tip leakage flow recovery in unsteady flow fields with less mixed-out tip leakage flow, the loss in the stator computed from computational results for the four blade designs is shown in Table 5.1 for both the mixing-plane steady flow fields and unsteady flow fields. The losses in Table 5.1 are shown relative to the baseline loss associated with steady flow computed from the original blade design. Loss in the stator increases with aft-loading the rotor blade tip and a relatively less mixed-out tip flow at the rotor exit. However, the loss increasing rate for the aft-

Table 5.1: The benefit of tip leakage recovery process relative to steady flow fields

Blade design	Relative total stator loss in steady flow fields [% efficiency]	Relative total stator loss in unsteady flow fields [% efficiency]	Loss reduction [% efficiency]
Fore	-0.02	-0.28	0.25
Original	0.00	-0.27	0.27
Lessaft	-0.18	-0.20	0.38
Moreaft	-0.20	-0.18	0.38

loaded blades in unsteady flow field is smaller due to the benefit of the tip leakage recovery process. The benefit of the tip leakage recovery process can be computed from the difference between the stator loss in steady and unsteady flow fields. The benefits of the process increases as a rotor blade is more aft-loaded. This result is in agreement with the finding of Valkov.

Despite the higher benefit of the tip leakage recovery process for the aft-loaded blades, these benefits are a comparison with a situation that tip leakage flow is not recovered but assumed mixed-out before the stator inlet. In actual flow fields of the original and the aft-loaded blades, tip leakage recovery process always occurs; therefore, another evaluation is carried out for unsteady flow fields. Table 5.2 shows the potential mixing loss in tip leakage flow at the rotor exit and the total stator loss in unsteady flow fields. The total stator loss increases with increasing potential loss at the rotor exit for the four blade designs. If the tip leakage flow recovery process is capable of recovering all potential loss before viscous mixing takes place, the total stator loss will be similar for all of the blade designs. However, tip leakage flow recovery process is not capable of completely attenuating the non-uniformity in tip leakage flow so that part of the potential loss is realized by viscous mixing. The potential loss reduction from the process can be indicated by the difference between potential loss at the rotor exit and the total stator loss. From Table 5.2, the loss reduction is only approximately 35% of the additional potential loss for the aft-loaded blades. Therefore, this computational result suggests the tip leakage flow recovery process is not capable of fully recovering the less mixed-out tip leakage flow

Table 5.2: The benefit of tip leakage recovery process relative to unsteady flow fields

Blade design	Relative potential loss at rotor exit [% efficiency]	Relative total stator loss [% efficiency]	Loss reduction [% efficiency]
Fore	-0.06	-0.01	0.05
Original	0.00	-0.00	0.00
Lessaft	0.09	0.06	0.03
Moreaft	0.14	0.09	0.05

in the aft-loaded blades so that the potential loss in the less-mixed tip leakage flow is eventually realized from viscous mixing. The ineffectiveness the recovery process implies a negligible overall loss reduction.

The computed ineffectiveness of the recovery process is unexpected. Work from Van Zante et al. found that an inviscid interaction plays a significant role in wake recovery while viscous mixing is of secondary importance [11]. As such, our finding that viscous mixing is a dominant process contradicts with the previous finding. To assess the discrepancy, our current flow fields have been investigated.

One plausible cause of the high mixing loss is due to numerical diffusion associated with the computational mesh. The computational mesh has been designed and optimized for steady flow fields. Thus, grid density is high at the rotor TE and the stator LE; however, the grid density is lower in the middle of the flow passage, where tip leakage flow core exists. The low grid density could possibly introduces excessive numerical diffusion in the tip leakage flow core. Furthermore, the low grid density in the main passage of a rotor and a stator causes poor grid matching at the sliding interface. When tip leakage flow passes through a region with low grid density, the structure of tip leakage flow diffuses out, thus generating unintended loss. Therefore, inadequate grid density in the tip region of the current computations might lead to excessive numerical diffusion, thus overestimating the mixing loss in the flow field and the computed ineffectiveness of the recovery process. This "artificial" ineffectiveness would result in a computed benefit from aft-loading rotor tip that is much smaller than the situation of a flow devoid of unavoidable numerical diffusion.

Next chapter will synthesize the results of Chapter 4 and 5 to assess the hypothesis in light of the flaw associated with the excessive numerical dissipation due to the lack of grid resolution of low-order numeric.

5.4 Summary

The unsteady tip leakage flow recovery process in the stator has been re-assessed here for its impact on potential benefit, in light of the tip leakage flow phasing effect presented in Chapter 4. For a situation where tip leakage enters a stator passage in the middle of the passage and near the proximity of the stator blade PS, the recovery process occurs in a manner that has been described in previous research; tip leakage flow is stretched in the passage and velocity disturbance in the core of tip leakage flow is attenuated. Disturbance streamwise vorticity also decreases as tip leakage moves further downstream and the reduction of disturbance streamwise vorticity results in an attenuation of the non-uniformity in the tip leakage flow core. However, when tip leakage flow enters the stator passage in the proximity of the stator blade SS, the axial velocity disturbance is not attenuated due to the misalignment of the direction of velocity disturbance and the stretching direction.

The quantitative benefit of the process is first assessed on a time-averaged basis to compare to a baseline situation where tip leakage flow recovery is absent. The benefit of the process increases as a rotor blade is more aft-loaded. However, tip leakage flow recovery process is not capable of completely attenuating the tip leakage flow. The loss reduction is only approximately 35% of the additional potential loss for the aft-loaded blades so that the potential loss in the less-mixed tip leakage flow is eventually realized through viscous mixing. It has to be noted that inadequate grid resolution and poor grid matching in the tip region is likely to cause excessive numerical diffusion and lower benefit of the recovery process.

Chapter 6

Effects of Rotor Tip Blade Loading Variation in Unsteady Flow Field of a Rotor-Stator Compressor Stage

Effects of rotor tip blade loading variation in unsteady rotor flow fields are attributed to three main flow processes, namely, tip leakage flow formation delay, changes in tip flow angle mismatch, and changes in tip leakage mass flow. A method for categorizing loss in the rotor from tip leakage flow formation delay and the other two flow effects described in Chapter 4 will be used to quantify the time-averaged effects on performance changes in this chapter. For a rotor-stator stage, the effect from tip leakage flow recovery in the stator, which is assessed and presented in Chapter 5, is included as well so that the overall impact on stage performance changes from the synthesizing these four flow effects can be determined.

6.1 Loss Generation in a Rotor Unsteady Flow Field

As previously alluded in Chapter 3 that loss generation associated with rotor tip clearance flow is determined by tip leakage flow formation delay (set by location of rotor tip peak loading), tip leakage mass flow, and tip leakage flow angle mismatch with main flow. The effect of aft-loading a rotor blade is now investigated in unsteady flow fields. Here we will not be concerned with details of the unsteady flow in the rotor passage but we will instead focus on the attendant changes in time-averaged unsteady flow fields.

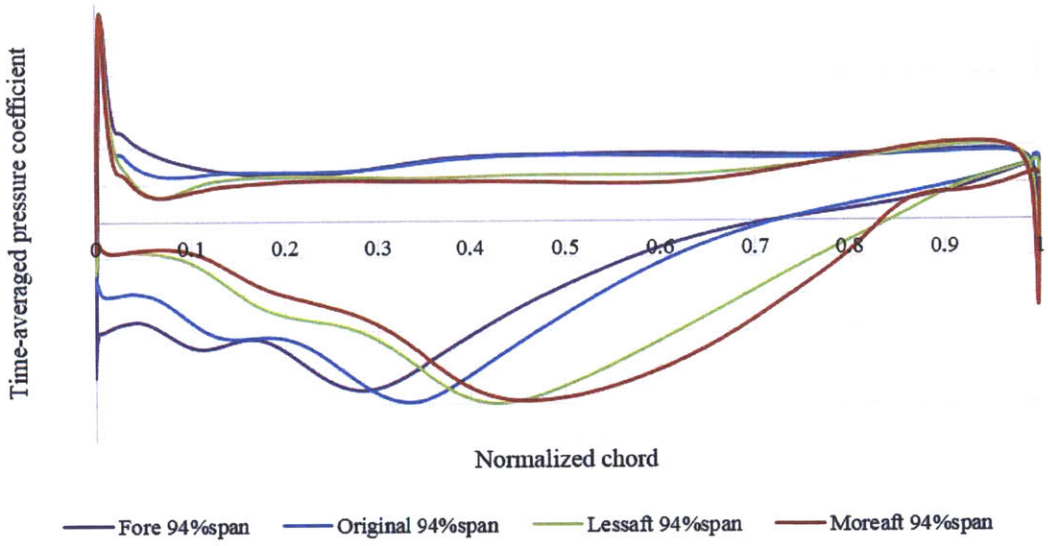

Figure 6-1: Time-averaged blade loading distribution of aft-loaded, fore-loaded, and original rotor blades near blade tip (1% span below the tip)

The formation of tip leakage flow is first assessed to confirm the delay in tip leakage flow formation in unsteady rotor-stage flow. As tip leakage flow is driven through tip clearance, tip blade loading of a rotor blade needs to be investigated. Time-averaged rotor blade loading near the blade tip is shown in Figure 6-1. The rotor blade designs studied in this chapter are the ones shown in Chapter 3. For ease of reference, the fore blade is fore-loaded compared the baseline rotor blade. The lessaft and moreaft

blade are aft-loaded compared to the baseline rotor blade and the moreaft blade is the most aft-loaded rotor blade. The peak of tip blade loading is shifted toward the TE for the aft-loaded blades, creating a condition favorable for delay in the tip leakage flow formation. Furthermore, the time-averaged blade loading profiles in unsteady flow fields are similar to those in steady flow fields. The distribution of time-averaged tip leakage mass flow rate shown in Figure 6-2 indicates that tip leakage flow forms closer to the TE in the aft-loaded blades.

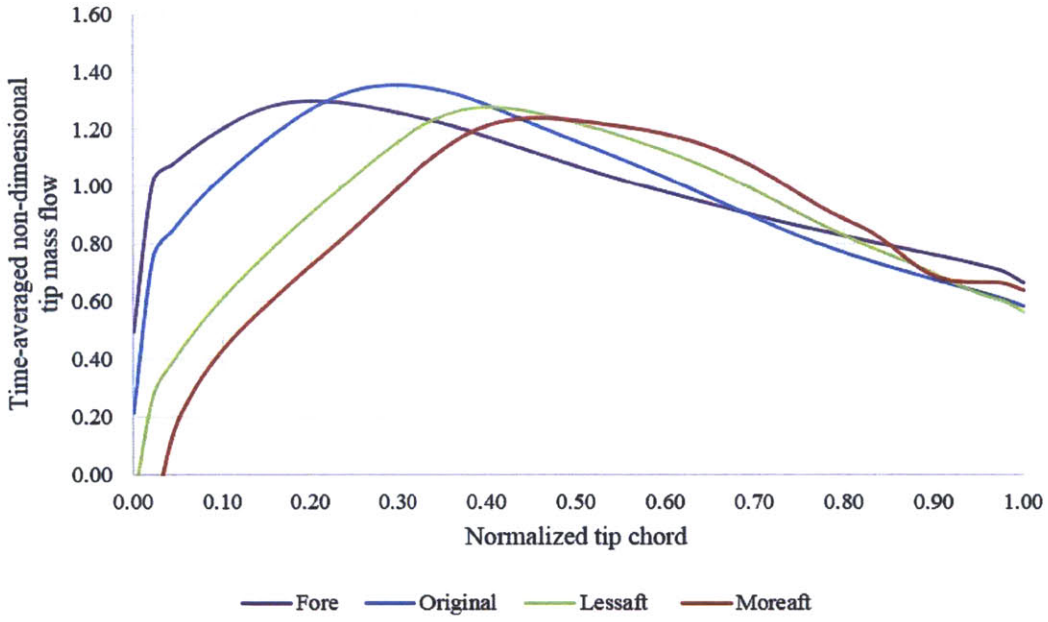

Figure 6-2: Time-averaged tip leakage mass flow distribution from various blade designs

The formation of tip leakage flow in unsteady flow fields can also be identified from local entropy generation rate (as was done for steady flow fields in Chapter 3). Figure 6-3 shows time-averaged local entropy generation rate distribution in the rotor. The peak of the entropy generation rate is shifted toward the TE for the aft-loaded blades and shifted toward the LE for the fore-loaded blade. This confirms that the formation of tip leakage flow is successfully delayed or advanced as expected in unsteady flow fields. The location of the maximum local entropy generation rate is shown in Table 6.1 to provide an estimation of the extent of tip leakage flow formation delay.

As tip leakage flow formation is successfully delayed, we can use the method

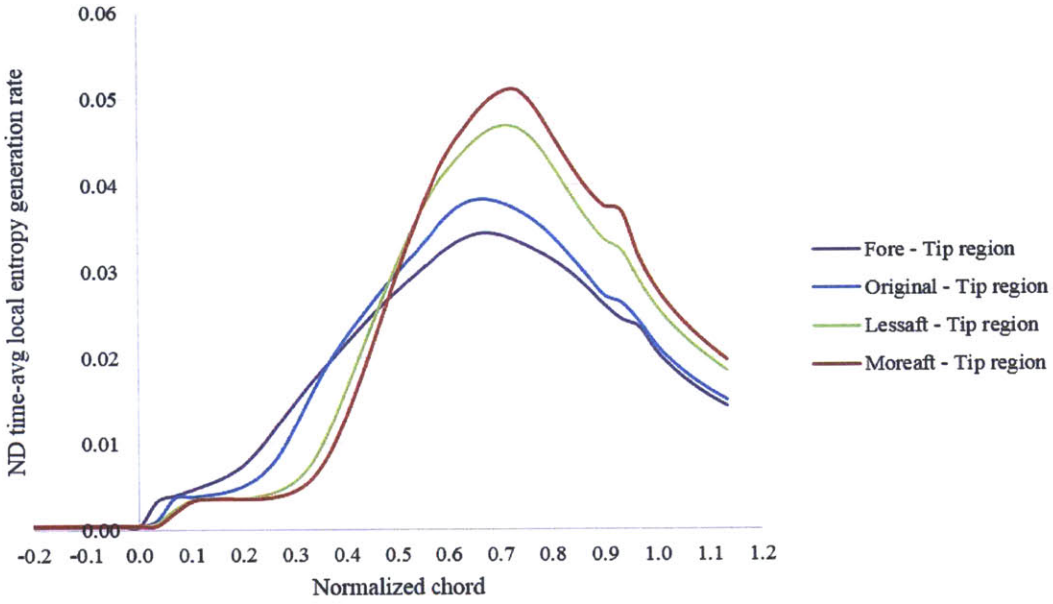

Figure 6-3: Time-averaged local entropy generation rate in the tip region (75% span to 100% span)

Table 6.1: Delay/advance in tip leakage flow formation location in unsteady flow fields

Blade design	Shift in the location of peak local entropy generation in the tip region
Fore	-2% chord
Original	-
Lessaft	+4% chord
Moreaft	+6% chord

presented in Chapter 3 to quantify the effects on performance changes from tip leakage flow formation delay. The benefit from tip leakage flow formation delay is shown in Figure 6-4. The benefit increases as the rotor blade is more aft-loaded and becomes negative for the fore blade. The lessaft and moreaft blade yield a benefit from this process and the fore blade incurs a performance penalty from the process. This finding is similar to the previous finding from the steady flow fields.

One effect from aft-loading a rotor blade is changes in tip flow angle. This effect has been evaluated in a steady flow field and will not be explained in details again for conciseness. The distribution of time-averaged tip flow angle differences along a rotor blade is shown in Figure 6-5. The flow angle difference is larger at approximate 70% chord for the lessaft and moreaft as noted earlier in Chapter 3. This higher flow angle mismatch in the aft-loaded blades, upon mixing out of the tip leakage flow, would generate higher loss on a time-averaged basis. On the other hand, the time-averaged total tip leakage mass flow driven through tip clearance decreases as a rotor blade is more aft-loaded as shown in Figure 6-6 and the reduction of tip leakage mass flow would result in the lower loss generation. The overall mixed-out loss governed by these two competing flow processes is higher for the aft-loaded blades as shown in Figure 6-7. As such, the result indicates that additional loss is dominated by the changes in the flow angle mismatch as was previously found in steady flow fields.

As we have articulated earlier the mixing process is not complete so that the details of the mixing process could play a key role, especially on the tip leakage flow formation delay. For a numerically computed unsteady flow field, the artificial viscosity (due to temporal and spatial discretization details) would thus add an additional degree of uncertainty to the quantitative value of computed loss. Therefore, the results should be interpreted and inferred in the light of these uncertainties. With the loss generation now consistently categorized, we can now revisit and reassess the hypothesis stated in Chapter 1.

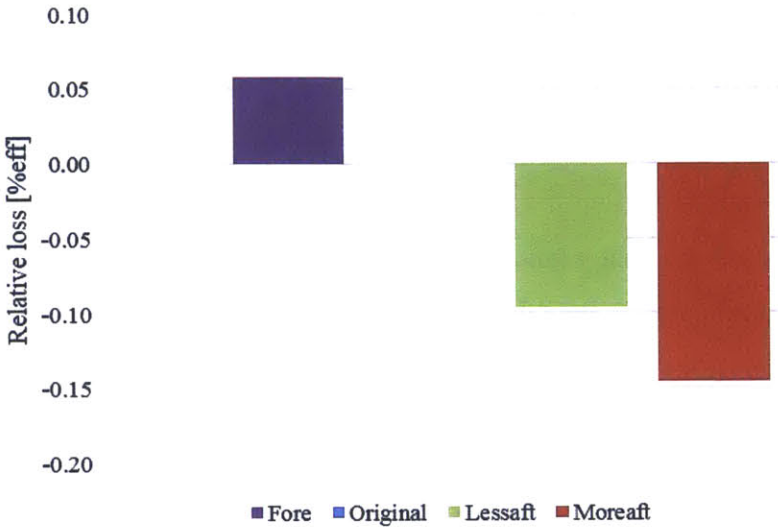

Figure 6-4: Time-averaged effect from tip leakage flow formation delay in unsteady flow fields

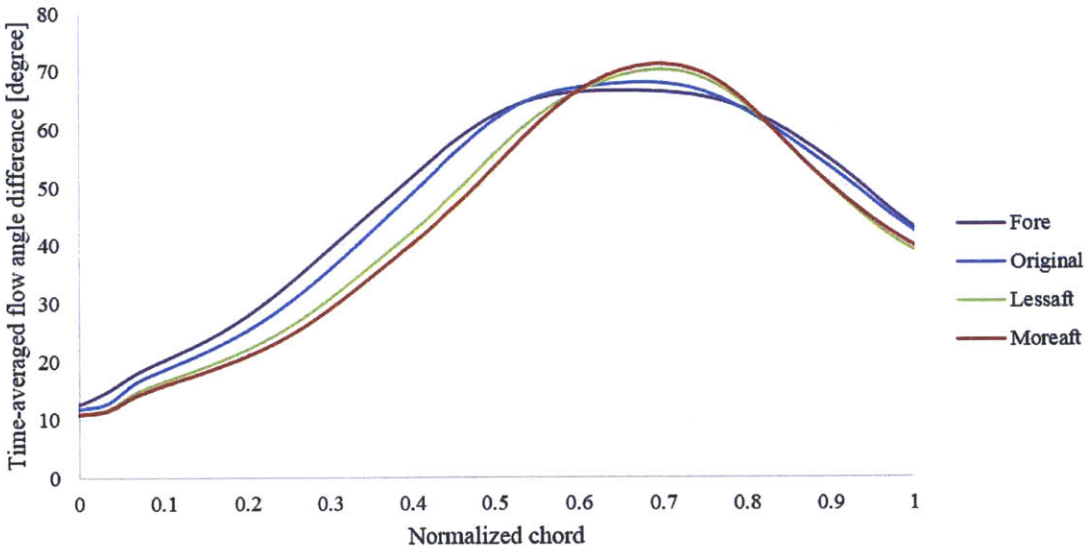

Figure 6-5: Time-averaged flow angle difference between the main flow (80% span) and the tip flow (the middle of tip clearance)

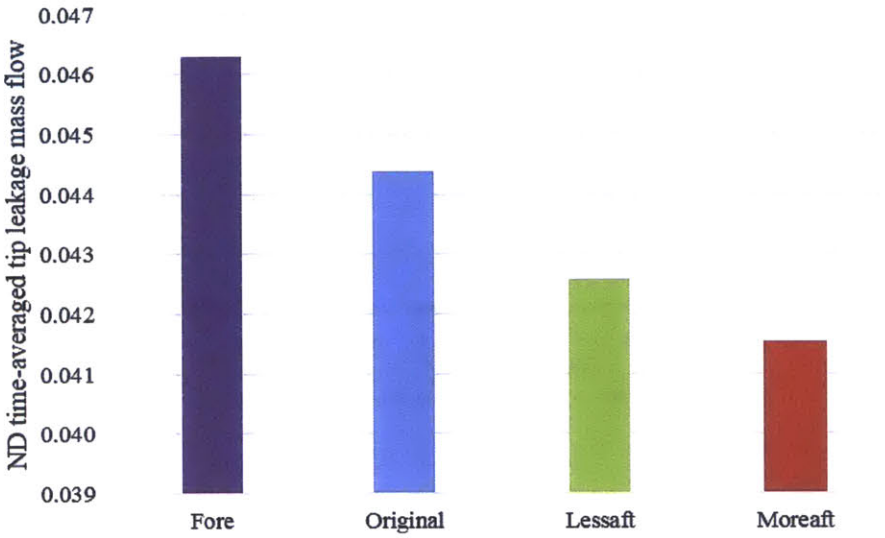

Figure 6-6: Changes in time-averaged tip leakage mass flow in the four rotor blade designs

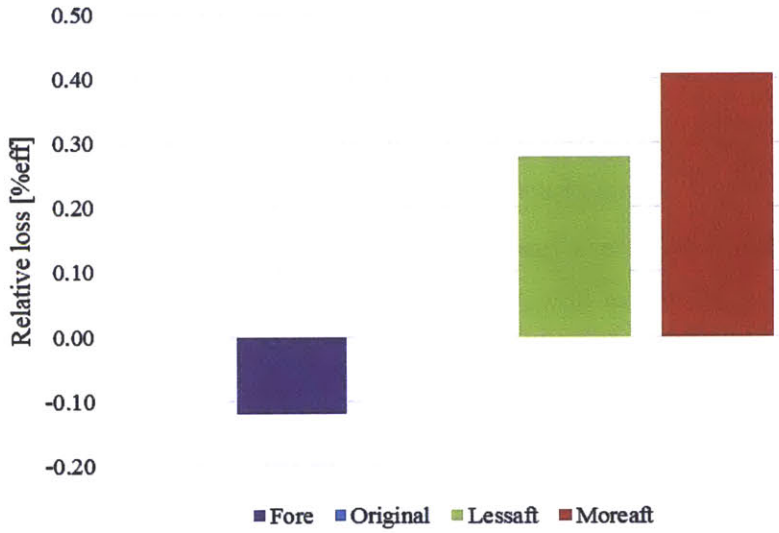

Figure 6-7: Time-averaged effect of changes in tip leakage angle mismatch and changes in total tip leakage mass flow in unsteady flow fields

6.2 Overall Effects of Rotor Tip Blade Loading Variation in a Rotor-Stator Stage Environment

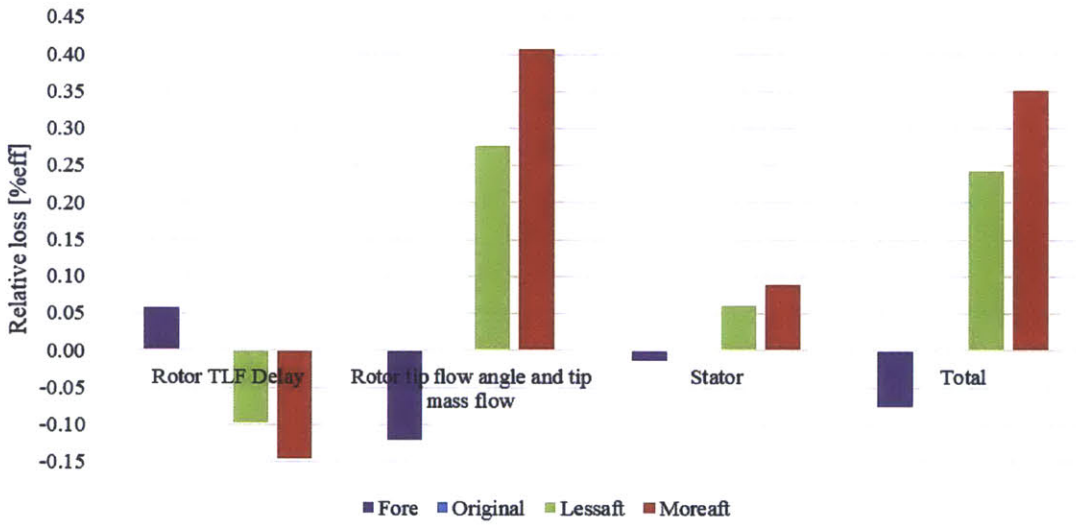

Figure 6-8: Time-averaged overall computed loss in a stage environment from the key flow effects in unsteady flow field

To assess the overall effects of rotor tip blade aft-loading in a stage environment, loss generated in the rotor (consisting of that associated with the delay in tip leakage flow formation, changes in tip flow angle mismatch with main flow, and changes in tip leakage mass flow) and the stator (essentially associated with tip leakage flow recovery process) have to be appropriately synthesized to give the overall stage loss. Loss generation in the stator with an incoming rotor tip leakage vortex has already been assessed in Chapter 5. The overall loss in a stage environment shown in Figure 6-8 is computed from the four main flow effects based on Equation 6.1.

$$\mathcal{L}_{stage} = \mathcal{L}_{TLF\ delay} + \mathcal{L}_{TLF\ flow\ angle\ mismatch\ and\ mass\ flow} + \mathcal{L}_{stator} \tag{6.1}$$

From Equation 6.1, we can separate losses into two categories. The first category is tip leakage flow mixed-out loss (consisting of that associated with changes in tip flow angle mismatch and changes in tip leakage mass flow) and tip leakage flow recovery, which increases as a rotor blade is more aft-loaded. The second category is loss from tip leakage flow formation delay, which decreases as a rotor blade is more aft-loaded. From Figure 6-8, the loss reduction from tip leakage flow formation delay is overwhelmed by loss from the tip leakage flow mixed-out loss in the aft-loaded blades. Furthermore, performance penalty from stator loss is smaller than that from tip leakage flow angle mismatch. Therefore, it is suggested that an aft-loaded rotor must be designed in such a way that tip leakage flow angle distribution does not generate the additional loss from tip flow angle mismatch. The potential of this design alternative has been demonstrated from a situation, in which tip clearance size varies as shown in Chapter 3. As noted the current computational flow field is likely to be overly-diffusive, actual loss reduction in the tip leakage flow formation delay is anticipated to be higher and loss generation during the tip leakage recovery process is anticipated to be smaller. Thus, the benefit computed from the computational results should be regarded as the lower bound for the overall benefit from the design hypothesis.

6.3 Summary

Effects of rotor tip blade loading variation in unsteady rotor-stator flow fields are attributed to four main flow processes, namely, tip leakage flow formation delay, changes in tip flow angle mismatch, changes in tip leakage mass flow, and unsteady tip leakage flow recovery in a downstream stator. Loss from these flow processes is quantified on a time-averaged basis with a method proposed in Chapter 3. These effects and the attendant trend are similar to those found in Chapter 3. As such, the hypothesis proposed by Sakulkaew needs to be revised. The revised hypothesis suggests that rotor blade should be tip-aft-loaded and hub-fore-loaded and stator blade should be hub-aft-loaded and tip-fore-loaded while tip and hub leakage flow angle distribution

should be designed with negligibly additional loss generation. The suggested maximum benefit from the hypothesis inferred from unsteady computational results is 0.15% efficiency improvement at design point, which could be higher if a rotor blade can further be aft-loaded with the proposed constraint.

Chapter 7

Summary and Future Work

This chapter summarizes the objectives of the research and the research approach utilized to answer the research questions. It also includes the key research findings and recommendations for the future work.

7.1 Objectives and Approach

The overall goal of the research is to assess the compressor design strategy proposed by Sakulkaew [2] and to determine if the design guideline can indeed yield a compressor performance improvement as postulated; and if it does not, what additional constraints or attributes need be incorporated. The proposed design strategy suggests that rotor should be tip-aft-loaded and hub-fore-loaded while stator should be hub-aft-loaded and tip-fore-loaded. To provide an adequate range of tip loading variation, additional two aft-loaded rotor blade designs and one fore-loaded rotor blade design are generated.

The representative compressor stage is taken from a rear-stage industrial compressor with an upstream rotor and a downstream stator. Steady compressor flow fields are used to assess loss generation (irreversible entropy generation) associated with varying the rotor tip loading distribution. Unsteady flow fields of a rotor-stator stage environment are employed to assess the effects of tip leakage flow recovery process in

stator as well as effects associated with tip leakage flow self-induced unsteadiness.

7.2 Key Findings

The key findings of this research provide understanding of changes in flow processes in response to variation of rotor tip blade loading in a rotor-stator stage environment. These findings are enumerated below:

1. Varying the rotor tip blade loading has effects on the following parameters characterizing the tip flow in a compressor stage: (i) the chordwise location at which tip leakage flow begins to develop; (ii) tip leakage flow angle distribution, hence its mismatch with the main flow; (iii) chordwise distribution of tip clearance mass flow rate, hence its total tip leakage mass flow rate; and (iv) the benefit associated with the unsteady tip leakage flow recovery in downstream stator. These characterizing parameters together determine the attendant loss associated with rotor tip leakage flow in a compressor stage environment.

2. Aft-loading rotor blade tip through shifting blade tip peak loading toward the trailing edge delays tip leakage flow formation; this not only results in a relatively less-mixed-out tip leakage flow at the rotor exit but also a reduction in the overall tip leakage mass flow. However, the attendant changes in tip flow angle distribution is such that there is an overall increase in the flow angle mismatch between the tip flow and the main flow. The former (i.e. reduced tip leakage mass flow and relatively less mixed-out tip flow at rotor exit) would tend to mitigate the loss generation in the rotor passage while the latter would tend to incur upon a higher loss generation. These three competing effects in principle would define an optimal rotor tip blade loading distribution for minimizing tip flow loss generation within the rotor passage.

3. The disparity between the timescale defining the self-induced tip leakage unsteadiness and blade passing time introduces a tip leakage vortex phasing effect (tip leakage vortex enters the downstream stator at specific pitchwise locations

for different blade passing cycles). Despite the presence of the inherent tip flow unsteadiness and the effects of rotor-stator interaction on tip flow, unsteady tip leakage flow recovery process attenuates tip leakage flow in the downstream stator on a time-averaged basis; the process yields a higher benefit for a relatively less-mixed-out tip leakage flow from aft-loading a rotor blade tip.

4. Based on the finding 2 above, the design hypothesis is revised to incorporate a constraint on tip flow angle chordwise distribution. The revised hypothesized design strategy should read as: "rotor should be tip-aft-loaded and hub-fore-loaded while stator should be hub-aft-loaded and tip-fore-loaded with tip/hub leakage flow angle distribution such that it results in no additional loss".

5. Periodicity of a compressor stage flow field is set by the two timescales, defining the tip leakage flow inherent unsteadiness and blade passing. The periodicity of a flow field can be used as a criteria to determine if and when unsteady computations have attained an equilibrium state when the flow manifests a repeating flow pattern on a temporal basis. As an example, the computed unsteady flow for a rotor-stator stage presented here has a periodicity of 11 blade passing time periods. In other words, the flow repeat at every 11 blade passing times. This is consistent with the timescales defining the tip flow inherent unsteadiness and the blade passing

It is to be noted that findings 1 to 4 are based on computations, in which the mixing of the tip clearance flow with the main flow is incomplete; as such, the details of the mixing, including the choice of the turbulence model, could play a role in determining both the qualitative and the quantitative aspects. However, the trend from the results based on complementary control volume analyses for complete mixing out of tip flow is in accord with that from computations.

7.3 Future Work

The current work suggests an additional constraint in the original design hypothesis, based on results presented in Chapter 3 and 6. The constraint requires that changes in tip leakage flow angle mismatch must not result in additional loss that outweighs the potentially realizable benefit from aft-loading the rotor tip. As such, future work needs to develop a technique to design an aft-loaded blade with such constraint. It is proposed that this could be achieved via an optimization blade design tool.

One of the key underlying mechanisms of the design hypothesis is tip/hub leakage flow recovery. Due to some differences in their unsteady recovery mechanisms, the recovery process could differ and this aspect also needs to be assessed.

The uncertainties introduced by the computational tool and computational mesh need to be remedied. If future work is to be performed via computational experiments, a rigorous grid convergence study has to be carried out in order to prevent artificial numerical diffusion as much as feasible. The convergence study has to be assessed based on unsteady flow fields, consisting of both spatial and temporal resolutions. This would then be followed by formulating a proper high-resolution grid design and efficient computational research framework.

It is proposed that experimental and computational work be carried out in a two-stage compressor (i.e. rotor-stator-rotor-stator). designed based on the revised hypothesis to assess: (i) compressor performance enhancement at off-design operating conditions, , (ii) compressor capability to retain its high performance for changes in operating conditions from the design operating condition, and (iii) compressor performance robustness to variations in tip/hub clearance.

Bibliography

[1] M. Inoue and M. Furukawa. Physics of Tip Clearance Flow in Turbomachinery. In *Volume 2: Symposia and General Papers, Parts A and B*, pages 777–789. ASME, 2002.

[2] S. Sakulkaew. *Effects of Rotor Tip Clearance on an Embedded Compressor Stage Performance.* Master's thesis, Massachusetts Institute of Technology, 2012.

[3] D. C. Wisler. Loss Reduction in Axial-Flow Compressors Through Low-Speed Model Testing. *Journal of Engineering for Gas Turbines and Power*, 107(2):354–363, 1985.

[4] H. Zhang, X. Deng, J. Chen, and W. Huang. Unsteady Tip Clearance Flow in an Isolated Axial Compressor Rotor. *Journal of Thermal Science*, 14(3):211–219, September 2005.

[5] L. H. Smith. Wake Dispersion in Turbomachines. *Journal of Basic Engineering*, 88(3):688–690, 1966.

[6] J. Bae, K. S. Breuer, and C. S. Tan. Periodic Unsteadiness of Compressor Tip Clearance Vortex. In *Volume 6: Turbo Expo 2004*, pages 457–465. ASME, 2004.

[7] X. Deng, H. Zhang, J. Chen, and W. Huang. Unsteady Tip Clearance Flow in a Low-Speed Axial Compressor Rotor With Upstream and Downstream Stators. In *Volume 6: Turbo Expo 2005, Parts A and B*, pages 1371–1381. ASME, 2005.

[8] R. Taghavi-Zenouz and S. Eslami. Numerical simulation of unsteady tip clearance flow in an isolated axial compressor rotor blades row. *Proceedings of the*

Institution of Mechanical Engineers, Part C: Journal of Mechanical Engineering Science, 226(1):82–93, September 2011.

[9] H. Zhang, X. Deng, F. Lin, J. Chen, and W. Huang. A Study on the Mechanism of Tip Leakage Flow Unsteadiness in an Isolated Compressor Rotor. In *Volume 6: Turbomachinery, Parts A and B*, volume 2006, pages 435–445. ASME, 2006.

[10] Y. Hwang, S. Kang, and S. Lee. Numerical Study on Unsteadiness of Tip Clearance Flow Induced by Downstream Stator Row in Axial Compressor. In *Volume 7: Turbomachinery, Parts A, B, and C*, pages 2553–2560. ASME, 2010.

[11] D. E. Van Zante, J. J. Adamczyk, A. J. Strazisar, and T. H. Okiishi. Wake Recovery Performance Benefit in a High-Speed Axial Compressor. *Journal of Turbomachinery*, 124(2):275–284, 2002.

[12] T. V. Valkov. *The Effect of Upstream Rotor Vortical Disturbances on the Time-average Performance of Axial Compressor Stators.* PhD thesis, Massachusetts Institute of Technology, 1997.

[13] S. A. Khalid. *The Effects of Tip Clearnace on Axial Compressor Pressure Rise.* PhD thesis, Massachusetts Institute of Technology, 1995.

[14] E. M. Greitzer, C. S. Tan, and M. B. Graf. *Internal Flow.* Cambridge University Press, Cambridge, 2004.

[15] ANSYS Inc. *ANSYS CFX-Solver Modeling Guide*, 14.0 edition, 2011.

[16] J. Adamczyk. Aerodynamic Analysis of Multistage Turbomachinery Flows in Support of Aerodynamic Design. *Journal of Turbomachinery*, 122(2):189–217, 2000.

[17] S. Kulkarni. *Development of a Methodology to Estimate Aero-Performance and Aero-Operability Limits of a Multistage Axial Flow Compressor for Use in Preliminary Design.* Master's thesis, Case Western Reserve University, 2011.

[18] N. A. Cumpsty and J. H. Horlock. Averaging Non-Uniform Flow for a Purpose. In *Volume 6: Turbo Expo 2005, Parts A and B*, pages 1–14. ASME, 2005.

[19] M. B. Zlatinov. *Secondary Air Interaction with Main Flow in Axial Turbines.* Master's thesis, Massachusetts Institute of Technology, 2011.

[20] A. Prasad. Calculation of the Mixed-Out State in Turbomachine Flows. *Journal of Turbomachinery*, 127(3):564–572, 2005.

[21] G. Iaccarino, A. Ooi, P. A. Durbin, and M. Behnia. Reynolds averaged simulation of unsteady separated flow. *International Journal of Heat and Fluid Flow*, 24(2):147–156, April 2003.

[22] J. B. Young and R. C. Wilcock. Modeling the Air-Cooled Gas Turbine: Part 2-Coolant Flows and Losses. *Journal of Turbomachinery*, 124(2):214–221, 2002.

[23] R. Mailach, H. Sauer, and K. Vogeler. The Periodical Interaction of the Tip Clearance Flow in the Blade Rows of Axial Compressors. In *Volume 1: Aircraft Engine; Marine; Turbomachinery; Microturbines and Small Turbomachinery*, page V001T03A004. ASME, June 2001.

[24] S. P. R. Nolan, B. B. Botros, C. S. Tan, J. J. Adamczyk, E. M. Greitzer, and S. E. Gorrell. Effects of Upstream Wake Phasing on Transonic Axial Compressor Performance. *Journal of Turbomachinery*, 133(2):021010, 2011.